A STATISTICAL APPROACH TOWARDS THE RESPONSE OF DUNE SYSTEMS TO TIDAL INLET PROCESSES

Author: A.J. Dekker

Master Thesis Civil Engineering and Management

Water Engineering and Management

UNIVERSITY OF TWENTE.

A statistical approach towards the response of dune systems to tidal inlet processes

A.J. Dekker

MSc Thesis in Civil Engineering and Management

Enschede, 06 July 2017

To presented on 14 July 2017 in Enschede

University of Twente

Faculty of Engineering Technology

Department of Water Engineering of Management

PO Box 217

7500 AE Enschede

Graduation committee:

Prof. dr. S.J.M.H. Hulscher (head of the committee)

F. Galiforni Silva, MSc (daily supervisor)

Dr. K.M. Wijnberg

UNIVERSITY
OF TWENTE.

Abstract

Tidal inlets are complex systems that have an unknown influence on adjacent dune systems. The objective of this research is to assess which tidal inlet processes are important for dune development. A statistical approach, namely categorical regression, is used to assess which processes are significant.

For this research, 45 tidal inlets and its adjacent dune systems were selected from western Europe, the contiguous United States, Brazil, Africa and Australia. These inlets were characterized based on the hydrodynamic forcing, the migratory behaviour and the number of channels, whereas the adjacent dune systems were characterized by the overall dune development, the vegetation cover, the extent of the active part of the dune system, the maximum observed dune height, the climate type and the wind regime.

The data set is analysed using CATREG, an algorithm for regression of categorical variables. This algorithm quantifies the categorical data and then does a linear regression. The output of this model gives which variables are significant for responses in the dune system. The responses were the overall development of the dune system, the extent of the active part, the vegetation cover and the maximum dune height.

The overall development of a dune system near a tidal inlet seems to be affected by the hydrodynamic forcing and the migration of the inlet. Furthermore, the dune height seems to be affected by the climate and the vegetation cover. The vegetation cover itself is affected by the wind, the climate and the migration style of the inlet.

The migration of a tidal inlet is the only accessed inlet-process that significantly influences the nearby dune systems. The other significant processes, such as the hydrodynamics and wind, are also present near straight coasts. However, the morphology, topography and geometry near the tidal inlet may influence the local hydrodynamics and wind conditions, so the exact influence of those processes may be different than on straight coasts.

As a conclusion, the migration of inlets is the most direct factor leading to dune systems behaving differently near tidal inlet than on straight coasts. Other processes, such as waves, are also present near straight coasts, but they may be influenced by the morphology of the tidal inlet. Although the statistical test has large uncertainties involved (e.g. high unexplained variability), this research gives some insight in the important processes in an around dune systems near tidal inlets.

Preface

This thesis is written as final part of the specialization Water Engineering and Management (WEM) of the master Civil Engineering and Management at Twente University, The Netherlands. This research has been conducted at the chair group Marine and Fluvial Systems of the Twente Water Centre, Enschede, The Netherlands. This research is about the response of dune systems on tidal inlet processes.

I would like to thank Filipe Galiforni Silva for his support and feedback during the process. I am also very grateful to Kathelijne Wijnberg and Suzanne Hulscher for their feedback. Furthermore, my fellow graduate students were a big support during the research and writing process. They kept me sharp and sometimes provided well-needed distractions.

Bert Dekker

Enschede, July 2017

Content

1. Introduction

This chapter describes the background of the research. Secondly, the knowledge gap is described. The study area of this research is presented followed by the research questions. To conclude the outline of this thesis is presented.

1.1. Background

Large parts of the coasts in the world are protected by coastal dunes, which are wind-driven accumulations of sand. Dune development is reliant on the supply of sediment to the backshore, which is dependent on the wind, the beach geometry and the sediment characteristics (Bauer & Davidson-Arnott, 2003). The proximity of the land-sea interface leads to the fact that the morphological aspects of dunes are influenced by marine processes. The waves and tides are responsible for the supply of sediment to the beach. When the sediment is on the beach, it can be picked up by the wind and transported to the backshore. Wave attack can also lead to erosion and the formation of blowouts (Hesp, 2002). The beach-dune system is therefore a dynamic system with many processes going on and interacting with each other (Houser & Ellis, 2013; Sherman & Bauer, 1993).

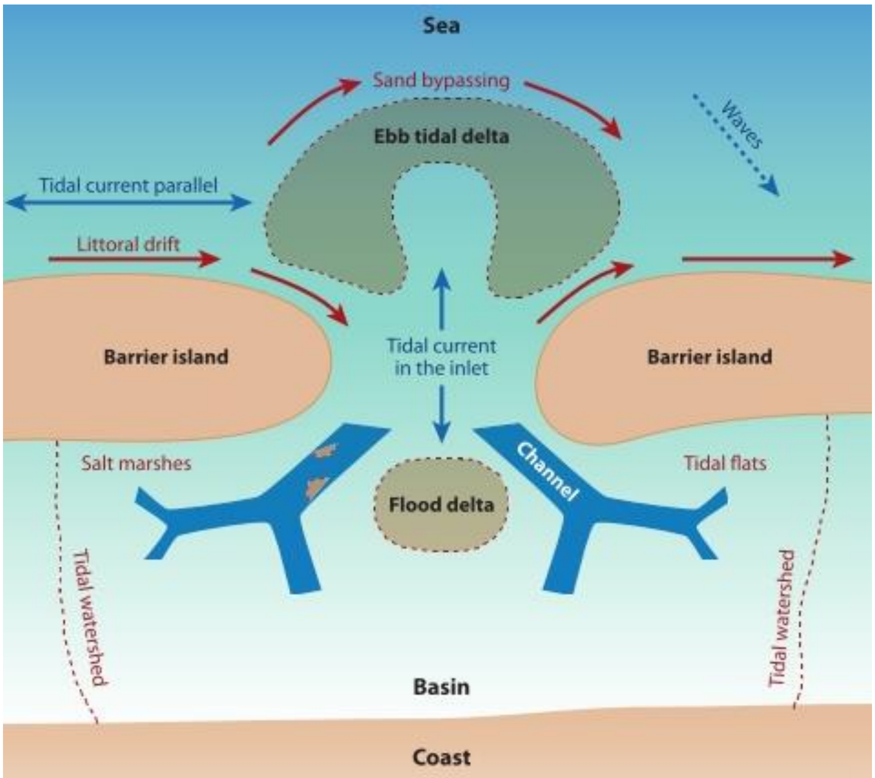

Figure 1: components in a tidal inlet system (de Swart & Zimmerman, 2009)

Most studies on beach-dune systems have considered systems with a straight coast, away from inlets (Hesp, 2012; Sherman & Bauer, 1993). Tidal inlets are short narrow waterways that connect a basin in the form of a bay or lagoon to the open ocean or sea. The side where the inlet connects to the open ocean or sea is called the seaward side. The side where the inlet connects to the bay or lagoon is called the landward side. A tidal inlet system can be divided into multiple components (Figure 1): the ebb-tidal delta, the flood delta, the tidal channels, the channel networks, the tidal bars and the intertidal zone. If multiple inlets connect the same basin to the same sea, barrier islands are formed (e.g. The Wadden). The hydrodynamic forces (waves and tides) are the drivers for morphological development of the tidal inlet system. The sediment fluxes near tidal inlets are significantly different from fluxes on straight coasts (FitzGerald, 1996), which will most probably have an influence on the dune systems near tidal inlets.

Storm surges and other extreme events can have a huge influence on dune systems near tidal inlets too (Houser, Hapke, & Hamilton, 2008), but data of these events is scarce and the effects of storms on dunes near tidal inlets is only investigated for a limited number of places. Also information of the effect of waves and tides on geological timescales is not fully known, so only the effect of hydrodynamic forcing on a timescale from years to decades is taken into account in this research. The introduction given in this chapter is not exhaustive and a more elaborate overview of processes in and around tidal inlet systems is given by De Swart & Zimmerman (2009).

1.2. Research gap and objective

It is hypothesized that tidal inlets have an influence on nearby dune systems, for example because some parts of the tidal inlet may be sheltered from wave attack or because there is more or less sediment input into the beach-dune system. The tidal inlet system and its relation to the adjacent beach-dune system is complex and needs further investigation to test this hypothesis.

A first step in assessing what the influence of a tidal inlet is on the adjacent dune system is to assess the relation between inlet behaviour and dune development. It is possible that the important processes can be identified using this information. The objective of this research is thus to describe the relation between the behaviour of tidal inlet systems and the development of adjacent dune systems. This will aid in the development of a conceptual model that can describe and predict dune development near tidal inlets. This model can be used as a first step in designing Building with Nature solutions in tidal inlet systems.

1.3. Study area

This research aims at getting a global overview of the relations between the tidal inlet system and adjacent dune systems. This can only be done if inlets from all over the world are used. Due to limitations in time and budget it is not feasible to assess all existing inlets, therefore five areas are selected which are divided in a total of eight sub-areas (see Appendix A):

- Europe: Atlantic coast, Wadden coast
- Contiguous United States: Atlantic coast, Pacific coast, Gulf coast
- Brazil
- Africa: Atlantic Coast
- Australia

Inlets from these areas are assessed in this research. South East Asia is not taken into account, because not much coastal dunes can be found there (Hesp, 2008). The areas mentioned above are selected because they have a different hydrodynamic forcing and climate. The northern Atlantic and Pacific coast experience swell, while this is much less the case at the Gulf coast and Wadden coast (Gulev, Grigorieva, & Sterl, 2006). The tidal range varies from micro-tidal along the Gulf coast to macro-tidal along parts of the Brazilian coast (Davidson-Arnott, 2009).

North-western Europe and large parts of the US east and west coast experience a maritime climate, while the Brazilian coast, excluding the southern part of the country, and the northern Australian coast has a tropical climate. In the southern part of Brazil and on the southern coast of Australia a maritime climate is present. Large parts of the west coast of Australia experience a hot desert climate (Peel, Finlayson, & McMahon, 2007).

1.4. Research questions

Multiple research questions are formulated to meet the objective mentioned in the previous paragraph:

1.4.1. Main Question

What is the influence of the hydrodynamic forcing and migratory behaviour of tidal inlets on dune systems near tidal inlets?

1.4.2. Subquestions

1. Where in the study area do tidal inlets occur that have a dune system on one or both sides of the inlet channel?
2. What are the characteristics of the selected tidal inlets and their adjacent dune systems?
3. What relations can be found between the parameters that describe inlet behaviour and the parameters that describe the dune systems?

1.4.3. Approach

The subquestions are answered with different methods. An elaborate overview is given in chapter 2, but here a quick overview is given. Subquestion 1 is answered with the help of visual assessment of satellite imagery. Inlets are selected based on a number of criteria. Subquestion 2 is answered using data found in literature or open-source databases. The found data is summarized in maps. The last subquestion is answered using categorical regression analysis.

1.5. Thesis outline

This thesis can be divided in two main parts. The first part is the selection and characterization of tidal inlets based on selected variables. The second part is the analysis of the found data. The methodology of this research is discussed in chapter 2. In chapter 3 the selection of the tidal inlets and the characterization is discussed. In chapter 4 the statistical analysis is presented. The results from this analysis are explained and discussed in chapter 5. After this the limitations of this research and some general remarks are made in chapter 6. Finally, in chapter 7 the conclusions and some suggestions for future research are presented.

2. Methodology

This chapter describes the methods that are used to get to the results as presented in the following chapters.

2.1. Selection of tidal inlets

The tidal inlets that will be researched are selected within the search area defined in paragraph 1.3. Inlets without dunes and inlets that are fixed on both sides by jetties and/or seawalls are not selected. From the inlets with dunes, a minimum of forty inlets is selected. To ensure spatial spreading of the inlets, a minimum of three inlets is selected per sub-area. The selection within a sub-area is governed by the differences in tidal range, wave climate and climate along the coast within the sub-area. The variation in the hydrodynamic forcing and climate is used as a proxy to get the biggest spread in characteristics in the final data inventory. The total number of forty inlets is used to get enough observations to get reliable result from the categorical regression analysis (2.3.2).

The selection procedure described here will lead to a list of inlets that are further characterized in the third part of the research. The number of selected inlets will be compared to an approximation of the total number of inlets that were assessed. The reason for not selecting inlets will be given too. The remark ‘structures in the inlet’ means that the inlet was fixed by jetties and/or seawalls or there was urban development up to the shoreline on both sides of the inlet. The remark ‘no dunes present’ means that no dunes could be seen on (aerial) photographs. The remark ‘no information about inlet’ means that no information about the inlet could be found on the internet, which was only the case with some inlets in Africa.

2.2. Characterize inlets and dune systems

To characterize tidal inlet systems and their adjacent dune systems it is necessary to have certain variables that can theoretically be determined for all systems. The choice of those variables is discussed in the first part. The methods used to get the data is discussed in the second part.

2.2.1. Choosing variables

To assess the dependencies of dune development on the behaviour of a tidal inlet, it is important to characterize the dune system. The development of a dune system is reliant on a number of processes (Figure 2) that relate to the hydrodynamics of the ocean or sea, the climate and the geology and geomorphology as described by Reed, Davidson-Arnott, & Perillo, (2009). This framework is used to choose variables for this research.

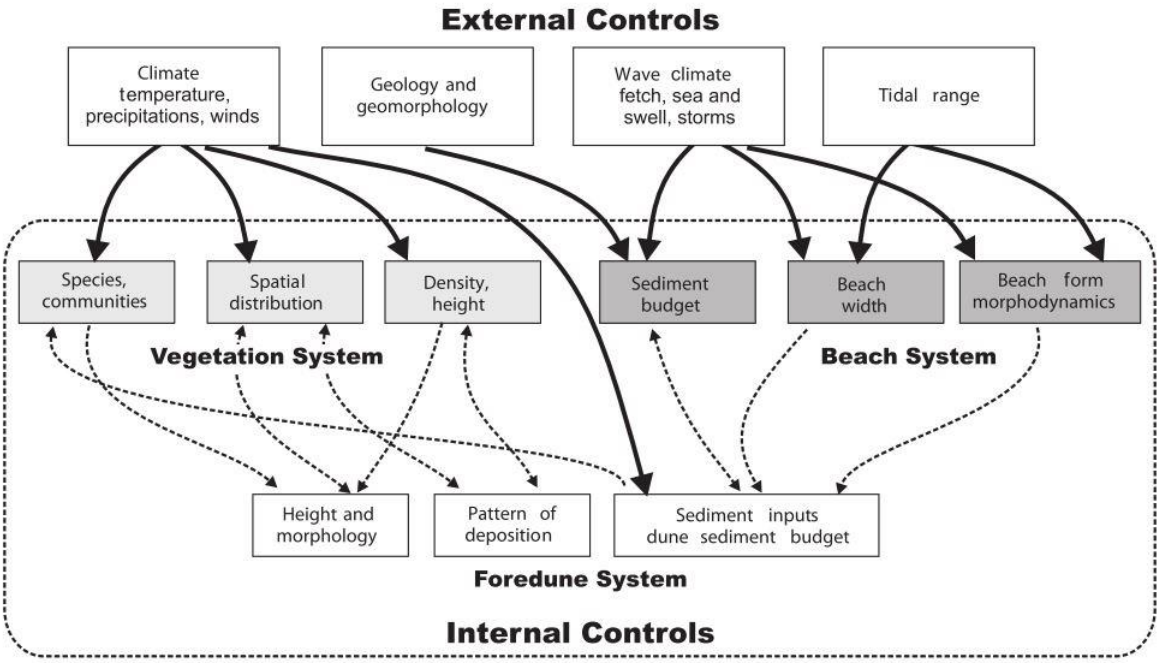

Figure 2: Framework that shows the controls on dune development (Reed et al., 2009)

To develop dunes, it is necessary to have sediment supply from the beach to the backshore. In general it can be said that coastal dunes develop where there is enough available sediment, a sufficient fetch to transport the sediment and vegetation to capture the sediment (Houser & Ellis, 2013). The availability of sediment and the fetch are directly related with the beach width (Bauer & Davidson-Arnott, 2003). The width of beaches along tidal inlets is not well-defined and it has approximately the same range as beaches along open coasts, so this is not of interest when assessing the effect of tidal inlets on dune development. The wind characteristics can be of interest, because the coast along a tidal inlet is not straight. The wind thus has a varying effect along the shore, so mean annual wind speed and most occurring wind direction are also taken into account. The wind direction is determined with respect to shore-normal to account for the different effect of wind from the same direction on a differently orientated inlet system.

A measure for the sediment supply from the beach to the dune systems and the vegetation characteristics is the dune height. The dune height can be limited, because developing dune ridges can be disconnected from their sediment supply by a new ridge (van Heteren, Oost, van der Spek, & Elias, 2006). The old ridge then becomes vegetated and stabilized (Reed et al., 2009). The maximum dune height is chosen as a proxy for the mean dune height in the dune system, because the mean dune height cannot easily be obtained. It is not well-defined which local maxima in a dune system can be regarded as the top of a dune. Values for the maximum dune height are also readily available in literature for some inlets (e.g. Sawakuchi et al., 2008). Furthermore, for every dune system is assessed if the dune system is fully or partly stabilized.

Individual dunes and dune systems can be classified in a number of ways (Doody, 2005; Hesp, 2012a), but it is difficult to assess individual dunes based on limited data and experience. It is easier to assess the dune system as a whole. The main variable is the overall development of the dune system. There will be looked if the dune system is expanding, retreating or on a fixed position. The value ‘none’ means that there is no dune system present at one side of the inlet. A variable that is also used in the classification of individual dunes is the vegetation type and cover. It is not feasible to assess the vegetation type for every dune system in this research, but it is possible to assess the vegetation cover based on aerial photographs. The type and amount of vegetation is partly dependent on the local climate (Hesp, 2012a). Therefore, the Köppen-Geiger climate class is assessed for every dune system (Peel et al., 2007).

The sediment supply towards the beach that is needed to have enough supply towards the backshore is controlled by marine processes in the tidal inlet system. The size of an inlet and its morphology is controlled by hydrodynamic forcing in the form of waves and tides (FitzGerald, 1996). This forcing can be characterized using the mean significant wave height and the mean tidal range. Using this two values it can be determined if the inlet is wave-dominated, tide-dominated or mixed-energy using a graph proposed by Davis & Hayes (1984).

Migration of an inlet channel controls erosion and/or accretion of the headlands. This has influence on the sediment supply towards the dunes. The migration direction and rate is dependent on the governing direction of incoming waves and the local geology. If the waves mostly come in from one direction and the bed is erodible, the inlet will migrate in downdrift direction (Wang & Beck, 2012). It can be that a spit is formed. This spit can be breached and then a new inlet channel is opened. If the bed is erodible, but the waves come in from different directions, it can be that the inlet displays an erratic migration behaviour. If the headlands cannot be eroded, because there are fixed by hard constructions or bedrock, the inlet will be on a fixed position (van Heteren et al., 2006). The wave direction will be determined with respect to shore-normal to account for the effect that come from the same direction towards differently orientated inlet systems.

Sediment transport inside the inlet channel is mainly done by tidal currents. The flood current deposits the sediment at the landward side of the inlet in a flood delta, while the ebb current deposits sediment on the seaward side in an ebb-tidal delta (Fiechter, Steffen, Mooers, & Haus, 2006). Not all the sediment is trapped in the ebb-tidal delta or the flood delta. Part of the sediment bypasses the inlet and is transported towards the downdrift headland. The two deltas act as sediment traps (de Swart & Zimmerman, 2009), but the ebb tidal delta also releases sediment in the form of shoals that migrate towards the coast (Ridderinkhof, de Swart, van der Vegt, & Hoekstra, 2016). Flood deltas do not release sediment in the form of shoals. This is due to the limited wave impact at the landward side of the inlet (Dyer & Huntley, 1999). The shoals originating from the ebb-tidal delta merge with the coast and form a large sediment input (van Heteren et al., 2006). The morphology of an ebb-tidal delta and the morphodynamics of shoals are influenced by the number of tidal channels in the inlet. The number of channels possibly has an influence on the migration velocity and attachment frequency of shoals (Ridderinkhof et al., 2016). The effect of shoal attachments on dune development is not yet known, but it could be that the number of inlet channels has indirect influence on the dunes. Therefore, the number of inlet channels is assessed for every inlet.

The variables as mentioned in Table 1 are used to characterize tidal inlet systems and their adjacent dune systems. The methods that are used to determine the values of those variables are given in the next chapter. Relationships between these variables are hypothesized in chapter 4.1.

Table 1: variables that characterize tidal inlet and coastal dune systems

Tidal inlet system	Coastal dune system
Mean tidal range $[m]$	Development $[none/fixed/expanding/retreating]$
Mean significant wave height $[m]$	Active part [fully active/partly active]
Dominant forcing $[wave, tide, mixed]$	Maximum dune height $[m]$
Mean wave direction $[°shore\ normal]$	Vegetation cover $[x/8]$
Migration style $[one\ direction, multiple\ directions, fixed]$	Wind speed $[m/s]$
Migration rate $[m/year]$	Wind direction $[°shore\ normal]$
Number of channels	Climate $[Köppen - Geiger\ climate\ class]$

2.2.2. Getting values for the selected variable

The inlet systems that were selected in the first part of the research will be characterized based on the selected variables (Table 1). The needed data will be gathered from open sources. If there is already a case study done on the inlet of interest, the data and/or results from that study will be used. If this is not the case, the data is gathered according to the method described below (see also: Table 2).

Table 2: method per variable

Variable	Method
Mean tidal range	Buoy data / Location data / XTide
Mean significant wave height	Buoy data / WaveWatch III
Dominant forcing	Graph as proposed by Davis & Hayes (1984)
Mean wave direction	Buoy data
Migration style	Visual assessment of satellite imagery
Migration rate	Measure displacement of channel centre line using satellite imagery
Number of channels	Visual assessment of satellite imagery
Dune development	Comparing polygons drawn over satellite imagery
Maximum dune height	Visual assessment of Digital Elevation Maps (DEM)
Vegetation cover	Visual assessment of satellite imagery in combination with appendix B
Wind speed	Weather station data / Windfinder
Wind direction	Weather station data / Windfinder
Climate	Climate map as proposed by Peel et al. (2007)

For some locations only the neap and spring tidal ranges are known. The mean tidal range can be determined by calculating the arithmetic mean of the two values, because the factor between the spring tidal range and the mean tidal range is the same as the factor between the neap tidal range and the mean tidal range (Baker, 1991). The tides can be approximated using models that predict the astronomical tide using tidal components, such as XTide (Pentcheff, 2010). Wave data can be found using data from the various wave buoys. In the Netherlands those buoys are maintained and operated by Rijkswaterstaat (RWS), In the United States this is done by the National Data Buoy Center (NDBC). In the German part of the North Sea a large measuring platform called FINO1 is operated by the Federal Ministry of Economic Affairs and Energy (BMWi) and a project Organisation (PTJ). If there is no local wave data available, the wave climate can be approximated using WaveWatch III, a global ocean wave model. The graph shown in Figure 3 is used to assess whether an inlet is wave-dominated, tide-dominated or mixed-energy.

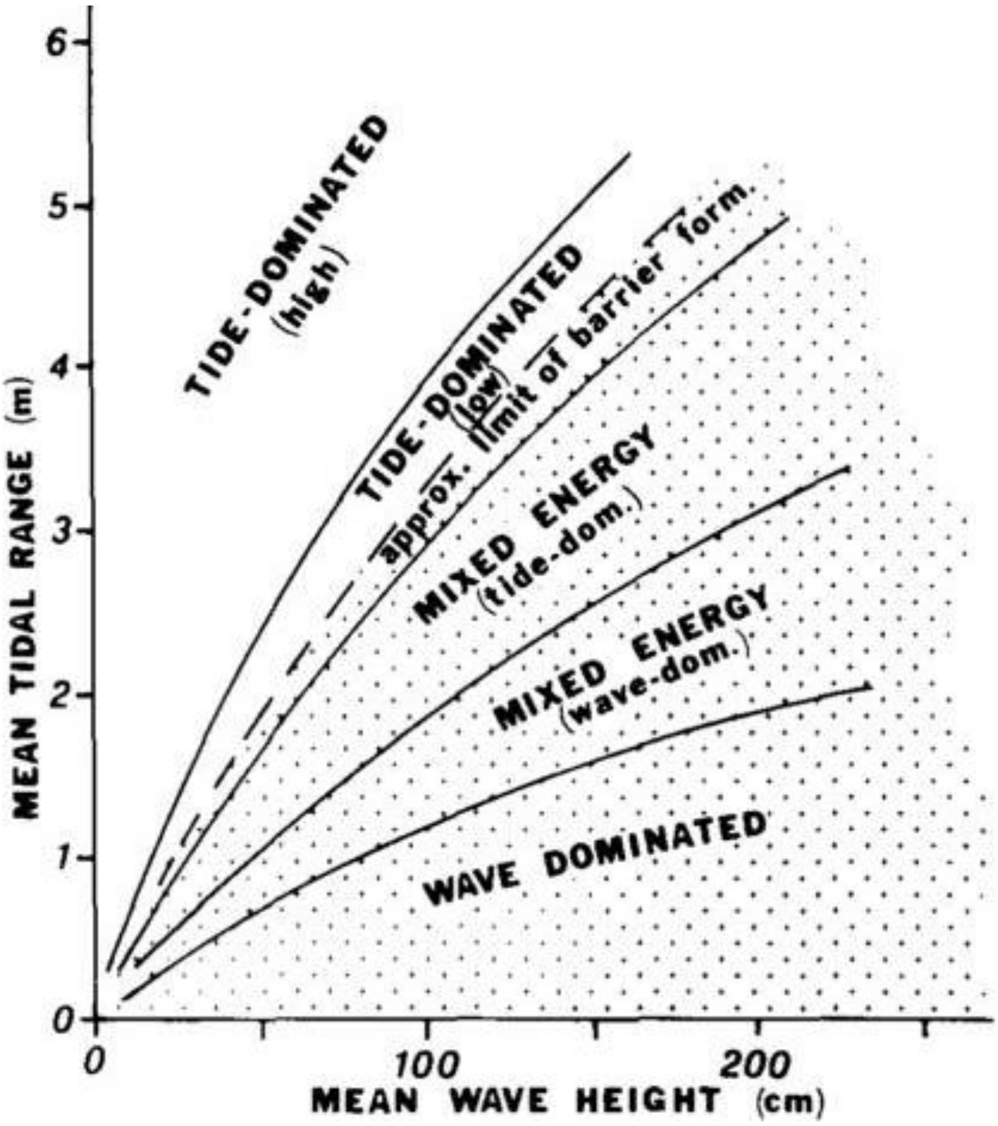

Figure 3: classification of coasts and tidal inlets as proposed by Davis & Hayes (1984)

Migration of the inlet, number of channels, dune development and vegetation cover are assessed using satellite imagery and aerial photographs that are available in for example Google Earth®. The migration style of the inlet is determined using visual assessment of time series of satellite imagery. The migration rate of the inlet is determined by determining the displacement of the centre line of the inlet over a known number of years. If the inlet is moving back-and-forth, the migration rate is determined using the maximum displacement of the inlet and the number of years it needed to reach this displacement. Dividing the displacement by the number of years yields a migration rate in m/year. Inlets with a migration rate of less than 1 m/year are considered stable due to the inaccuracy of the estimation method. The number of channels can be seen in most aerial photographs, because of the colour differences in the water. For some locations, the image quality is to low or water turbidity is too high to recognize channels. The dune development is assessed by looking at the movement of the seaward boundary of the dune system during. If there are dunes on both sides of the inlet, the dune development and the vegetation cover is determined for both sides separately. Which side is updrift and which side is downdrift is determined using the migration of the inlet or the wave direction on the fixed inlets. The updrift side is called UD and the downdrift side is called DD. If the dunes are present on a sand spit, they are characterized as being updrift (UD). The vegetation cover is only determined for the dunes closest to the inlet, because most dune systems become more vegetated when going inland. The vegetation cover is described using octas (eights), so 0/8 means that there is no vegetation and 8/8 means that the dune system is fully vegetated. This method is more commonly used to assess cloud cover (Met Office, 2015). Reference images for this rating can be found in appendix B.

The maximum height of dunes in a dune system is determined as the crest elevation from Digital Elevation Maps (DEMs) which are assessed using a Geographic Information System. DEMs for the Netherlands are available as part of the AHN (Algemeen Hoogtebestand Nederland). A global DEM mosaic is available through the National Center for Environmental Information (NCEI). The global DEM mosaic is built from various DEMs with different resolutions. If the individual dune ridges or the inlet itself are not recognizable on the DEM, the resolution is to coarse to determine the maximum dune height. The vertical accuracy of the DEMs differs between 5 centimetre and 1 meter.

The mean wind speed and most occurring wind direction are determined using data from local weather stations. This data is for example available for the Netherlands through the Royal Netherlands Meteorological Institute (KNMI). The Brazilian National Meteorological Institute (INMET) has wind data for some inlets on the Brazilian coast. When the data is not easily accessible via national weather institutions, Windfinder will be used to get the values for wind speed and wind direction. Windfinder is a global weather service that is aimed at wind related activities, such as surfing and sailing. Statistics at their sites are calculated based on measurements at weather stations that are done during daytime (Windfinder, 2017). If there is no data from Windfinder available, the wind data from WaveWatch III is used. WaveWatch III stores the data as a u-component and a v-component. The wind speed and direction are calculated as follows:

$$Wind\ speed = \sqrt{U_{wind}^2 + V_{wind}^2} \tag{1}$$

$$Wind\ direction = 270 - \text{atan}^2\left(\frac{V_{wind}}{U_{wind}}\right) \tag{2}$$

The wind direction and wave direction are converted from degrees from North to degrees from shore normal. Shore normal is determined as the direction of the centreline of the inlet pointing seaward.

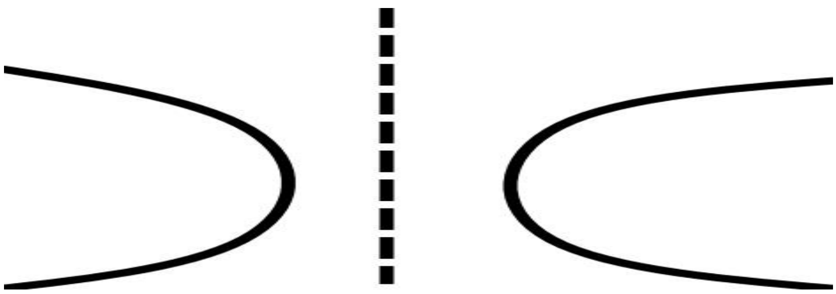

Figure 4: definition of shore normal (dotted line) in tidal inlets.

When all the classification is done, there is a big table that summarizes it all. The table will be organized with on every row an inlet and on every column a variable.

2.3. Find and explain dependencies

In the previous part of the research a data inventory was built. This inventory is further analysed using an algorithm for categorical regression called CATREG. The first step is to bin all numeric data into categories, so that all variables become categorical. This is necessary for the use of CATREG, because it only supports categorical data. In the second part of this paragraph more information about CATREG is given.

2.3.1. Categorize data

The data inventory built up in the previous part of the research consists of both numeric and categorical data. For statistical analysis, it is preferred to have the same data type throughout the whole data set. Therefore, the numeric data is binned into categories. The categorical data will be further analysed. The number of channels can be easily categorized in single channel or multiple channels. For the other numeric data a different approach is used.

The tidal range is categorized using the classification of tidal ranges proposed by Davies (1964). This means that the tidal ranges will be categorized in three categories, namely micro-tidal, meso-tidal and macro-tidal. Davies (1964) did the classification based on the spring tidal range, but in this research the mean tidal range will be used. Values of a mean tidal range below 2 m are considered micro-tidal. Values between 2 and 4 m are considered meso-tidal and tidal ranges of more than 4 m are macro-tidal.

The mean significant wave height is binned using the Beaufort Scale (Table 3). The wave heights given in the last column of the table refer to well-developed wind waves of the open sea. The categories are collapsed to get a total of three categories. The first category includes Beaufort Scale 0, 1, 2, 3 and 4 and consists of waves with a mean significant wave height of less than 1.5 m. The second category is 5 on the Beaufort Scale and consists of waves with a mean significant wave height between 1.5 m and 2.5 m. Waves higher than 2.5 m are placed in the last category.

Table 3: Beaufort Scale (modified from Met Office (2016))

<table>
<tr><th>Beaufort wind scale</th><th>Limits of wind speed [m/s]</th><th>Wind speed categories</th><th>Probable wave height [m]</th><th>Mean significant wave height categories</th></tr>
<tr><td>0</td><td><1</td><td rowspan="4">Calm</td><td>0</td><td rowspan="5">Low</td></tr>
<tr><td>1</td><td>1-2</td><td>0.1</td></tr>
<tr><td>2</td><td>2-3</td><td>0.2</td></tr>
<tr><td>3</td><td>4-5</td><td>0.6</td></tr>
<tr><td>4</td><td>6-8</td><td>Moderate</td><td>1.0</td></tr>
<tr><td>5</td><td>9-11</td><td rowspan="8">Heavy</td><td>2.0</td><td>Moderate</td></tr>
<tr><td>6</td><td>11-14</td><td>3.0</td><td rowspan="7">High</td></tr>
<tr><td>7</td><td>14-17</td><td>4.0</td></tr>
<tr><td>8</td><td>17-21</td><td>5.5</td></tr>
<tr><td>9</td><td>21-24</td><td>7.0</td></tr>
<tr><td>10</td><td>25-28</td><td>9.0</td></tr>
<tr><td>11</td><td>29-32</td><td>11.5</td></tr>
<tr><td>12</td><td>>33</td><td>>14</td></tr>
</table>

The wind speed is also categorized using the Beaufort Scale (Table 3). The Beaufort Scale is collapsed to get three wind speed categories. The categories 0, 1, 2 and 3 of the Beaufort Scale are collapsed to form the first category of wind speed with wind speed of less than 5 m/s. Category 4 of the Beaufort Scale forms the middle category with wind speeds of 5-8 m/s. The rest is placed in the last category with wind speeds above 8 m/s.

The wave and wind direction are categorized in respectively two and four categories. The wave directions can vary from 0° to 90°. A value of 0° means that the waves come in perpendicular to the coast, while a value of 90° means that the waves travel along the coast. The wave direction is categorized in two bins with the central bin edge at 45°. The wind direction can vary from 0° to 180°, where 0° means that the wind comes from the sea and 180° means that the wind comes from the land. The wind direction is binned in four categories, namely 0° - 45°, 45° - 90°, 90° - 135° and 135° - 180°.

The dune height is categorized in three categories. There is no existing classification scheme for dune heights, so the bin edges are chosen somewhat arbitrarily. The first category consists of dunes with a maximum height of less than 7 m. The second category has a maximum dune height of 7 – 25 m. The last category has a maximum dune height of more than 25 m.

The migration rate is categorized in three categories. To make it possible to correctly bin the numeric data, a range of values must be determined. Therefore, the migration rates from 0 – 5 m/year are put into the first category. The edge between the second and third category is less straight forward and must be chosen arbitrarily. A value of 20 m/year is chosen as the border between the second and third category. The second category has thus migration rates of 5 – 20 m/year, while the third category has values of more than 20 m/year.

The climate is already categorical data, but it has more than five categories. Therefore, the climate categories are collapsed based on the main climate groups. This will lead to a maximum of five categories (A, B, C, D and E).

2.3.2. Statistical analysis

Statistical analysis techniques are used to determine what relations exist between the behaviour of a tidal inlet system and the adjacent dune systems. The behaviour of a tidal inlet system is characterized by a number of variables which are used as predictor variables (first column in Table 4). The behaviour of the dune system is described by a number of variables which are used as response variables (second column in Table 4). The vegetation cover of the both dune system is used both as an predictor and as a response variable. First hypotheses about possible relations are formulated. After that the hypothesized relations are modelled and tested using a categorical regression algorithm (CATREG) which is developed by Van der Kooij (2007). The objective of this test is to determine which categorical predictor variables have a significant influence on the categorical response variables.

Table 4: response and predictor variables and their scaling

Predictor variable (scaling)	Response variable (all ordinal)
Mean significant wave height (ordinal)	Development of the updrift dune system
Mean wave direction (nominal)	Development of the downdrift dune system
Tidal range (ordinal)	Active part of the updrift dune system
Dominant hydrodynamic forcing (nominal)	Active part of the downdrift dune system
Migration style of the inlet (nominal)	Maximum dune height
Migration rate of the inlet (ordinal/nominal)	
Number of inlet channels (ordinal)	
Mean wind speed (ordinal)	
Mean wind direction (nominal)	
Climate (nominal)	
Vegetation cover of the updrift dune system	
Vegetation cover of the downdrift dune system	

CATREG scales categorical data by assigning numeric values to the different categories of the categorical data. This way an optimal linear regression equation for the scaled variables can be made. The standard approach used for linear and categorical regression is expanded to simultaneously include nominal, ordinal and numeric data. The CATREG objective is to find the set of scaled variables and regression coefficients, such that the objective function (3) is minimalized under a normalization restriction (4) and a restriction that centres the scaling of the response variable (5). This procedure is done separately for every response variable.

$$\sigma(y_r;\beta;y_j) = \left(G_r y_r - \sum_{j\in J_p}(\beta_j G_j y_j)\right)' W \left(G_r y_r - \sum_{j\in J_p}(\beta_j G_j y_j)\right) \quad (3)$$

$$y_r' D_r y_r = 0 \quad (4)$$

$$u' W G_r y_r = 0 \quad (5)$$

$$R^2 = n^{-1/2}(G_r y_r)' W v (v' W v)^{-1/2} \quad (6)$$

n Number of analysis cases (objects)
w_i Weight of object ($w_i = 1$)
W Diagonal $n \times n$ matrix with w_i on the diagonal
p Number of predictor variables
J_p Index set of predictor variables $j \in J_p$
k_j Number of categories of variable j
G_j Indicator matrix for variable j of order $n \times k_j$

$$g_{(j)ir} = \begin{cases} 1 & \text{when the ith object is in the rth category of variable } j \\ 0 & \text{when the ith object is not in the rth category of variable } j \end{cases}$$

G_r Indicator matrix for the response variable
D_r Matrix containing the weighted univariate marginals ($D_r = G_r' W G_r$)
u n-vector of ones
β Regression coefficients for the predictor variables
y_r Scaled categories for the response variable
y_j Scaled categories for the predictor variable j
v Accumulated contributions of predictor variables: $\sum_{j\in J_p}(\beta_j G_j y_j)$

After the data is discretized, as described in 2.3.1, the right scaling procedure must be chosen. If the categories are ordered and equally spaced, the numeric scaling level can be used. If there is an order between the categories but no equal spacing, the ordinal scaling level can be used. This way the order of the categories is preserved in the scaled variable. If the order of the categories is not of interest, the nominal scaling level can be used. If this scaling level is used, only the grouping into the categories is preserved. The scaling that is used is given in Table 4. For the migration rate the scaling is separately determined for every response variable by looking for the best fitting model.

After the data is scaled, there is assessed whether multicollinearity exists in the regression after the variables are scaled. Multicollinearity is the amount of linear correlation between variables. Low values of the correlations between the original and transformed variables indicate that there is no multicollinearity between variables. If there is moderate to strong multicollinearity between two variables (correlation > 0.5), one of those variables can be omitted from the analysis with only a minimal impact on the predictive behaviour of the model.

After there is made sure that there is no multicollinearity within the model, the output is further examined. For every predictor variable a F-test (J. C. Davis, 2002) is done to assess whether omission of the variable would significantly worsen the predictive capability of the model. If there are multiple predictors with statistically insignificant coefficients, they must be omitted one at a time before rerunning the model. This iterative process is repeated until there is a regression model where all predictors are significant for the predictive behaviour of the model. The amount of variability that can be explained by the regression model is R^2 (6). The (cumulative) change of this value is presented to show the effect of omitting predictor variables. Besides the regression coefficients it is important to look at the Importance and the Tolerance of the predictors. The Importance is calculated as Pratt's measure of relative importance, which is the product of the regression coefficient and the zero-order correlation divided by the squared multiple regression coefficient, R^2, to yield a total of 1 (Pratt, 1987). Large individual importances relative to the other importances correspond to predictors that are crucial to the regression. The Tolerance quantifies how much the independent variables are linearly related to another. It is the proportion of a variable's variance not accounted for by other independent variables. A value near 1 indicates that the variable cannot be predicted very well from the other predictors. A low value of the Tolerance means that the predictor contributes little information to the model. The value of the Tolerance is presented for the predictor variables before and after the scaling procedure has taken place.

Predictor variables are omitted and the algorithm is rerun until all variables have a significance value less than 0.1. The value of 0.1 is chosen instead of the more common 0.05, because the number of observations is limited and there is a lot of variability in the data. In the end, the goal of the statistical analysis is to have a regression model for each response variable where all remaining predictors are significant for the predictive capabilities of the model. The values of the Tolerance must be as high as possible with a minimum value of 0.5 to make sure that there is not much collinearity between the predictors. The value of R^2 does not matter because the main aim of the model is to describe the relationship between the predictors and the response variable (Frost, 2014). The aim is not to predict the response variable. A low value of R^2 means that the error in a prediction based on the given regression model is big, but it does not negate a significant predictor or its coefficient.

The results are shown in tables that summarize the iterations that were done to achieve the final model (Table 5). The first column shows the predictors that were used to build the model. The columns labelled p give the significance levels of the test that is conducted to determine whether removal of that predictor significantly impacts the predictive capabilities of the model. The column β gives the regression coefficient for the predictors that are used in the final model. The columns *Importance* and *Tolerance* give the values for Pratt's Importance and the Tolerance for the predictors. Furthermore, the values for R^2 and the (cumulative) change of R^2 are given to show the effect that omitting a variable has on the model capabilities regarding the explanation of variability.

Table 5: example of table that shows CATREG output

Predictor	p	p	p	p	β	Importance	Tolerance	
							after	before
A	0,010	0,008	0,003	0,001	0,480	0,400	0,956	0,932
B	0,250	0,222	0,390					
C	0,400							
D	0,002	0,001	0,002	0,000	0,535	0,600	0,854	0,932
E	0,160	0,300						
R^2	**0,370**	**0,356**	**0,224**	**0,198**				
ΔR^2		**-0,014**	**-0,132**	**-0,026**				
$\sum\Delta R^2$		**-0,014**	**-0,146**	**-0,172**				

The example shown in Table 5 shows that the analysis is started with 5 predictor variables, namely A, B, C, D and E. After four iterations only A and D are found to be significant. The value for the Importance shows that D is a bit more important than A, but the difference is not that big. The tolerance shows that there is little multicollinearity between the two variables. The values of β need to be assessed in combination with the corresponding transformation plots. Figure 5 shows an example of a transformation plot. The categories 1, 2 and 3 of the original predictor variable are transformed to numeric values. The more positive or negative the value, the more effect that category has on the regression. A similar transformation plot can be made for the response variable. The sign and value of β in combination with the sign and value of the transformed predictor category yields the effect on the response variable.

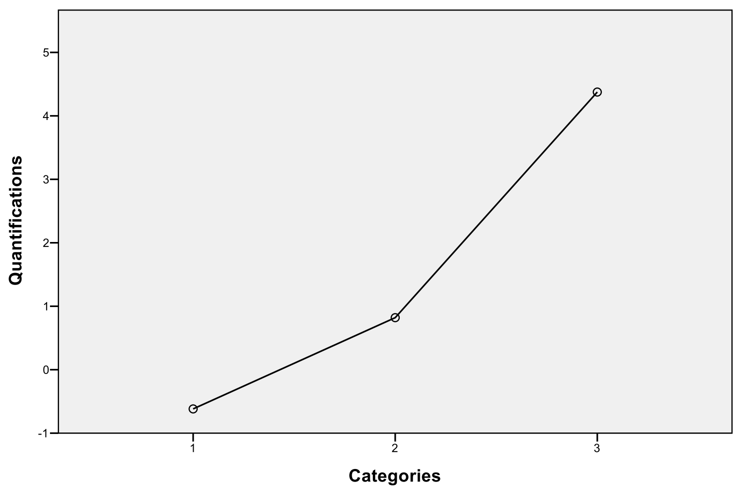

Figure 5: example of a transformation plot

3. Results: selection and characterization

There are many tidal inlets systems present in the study area as defined in paragraph 1.3. 106 inlets were assessed for their suitability for this research. 45 tidal inlet systems are selected for further research (Table 6). Especially along the east coast and Gulf coast of the contiguous United States a lot of inlets were fixed by inlet and/or the shoreline was heavily urbanized. This was also the case on the Atlantic coast of Europe. The west coast of the United States was mostly rocky, so not much dunes could be found there. Little information could be found about dunes and inlets on the African coast and in some cases it was unclear if the dunes were really coastal dunes or just desert dunes near the coast.

The global overview of the selected inlets is given in appendix C. The characterization per inlet is presented in appendix D. The complete dataset with all raw and categorical data is given in appendix E.

Table 6: number of selected inlets compared to the total number of assessed inlets

Area		**Assessed**	**Selected**	**Main exclusion criteria**
Europe	Wadden coast	12	10	No dunes, but seawalls
	Atlantic coast	14	5	No dunes present or structures in the inlet
United States	Atlantic coast	26	9	No dunes present or structures in the inlet
	Gulf coast	20	4	Structures in the inlet
	Pacific coast	5	3	No dunes, mainly rocky coast
Brazil		12	7	No dunes present
Australia		6	3	Structures in the inlet
Africa		17	3	No dunes present or no information about inlet
Total		**106**	**45**	

The categorized characteristics of all selected inlets are given in the maps in Figure 6 up to and including Figure 13. Multiple variables are shown per map. Symbol shapes and colours are used to differentiate between the categories. The vegetation cover is presented as a number that shows the amount of octas.

3.1. Europe

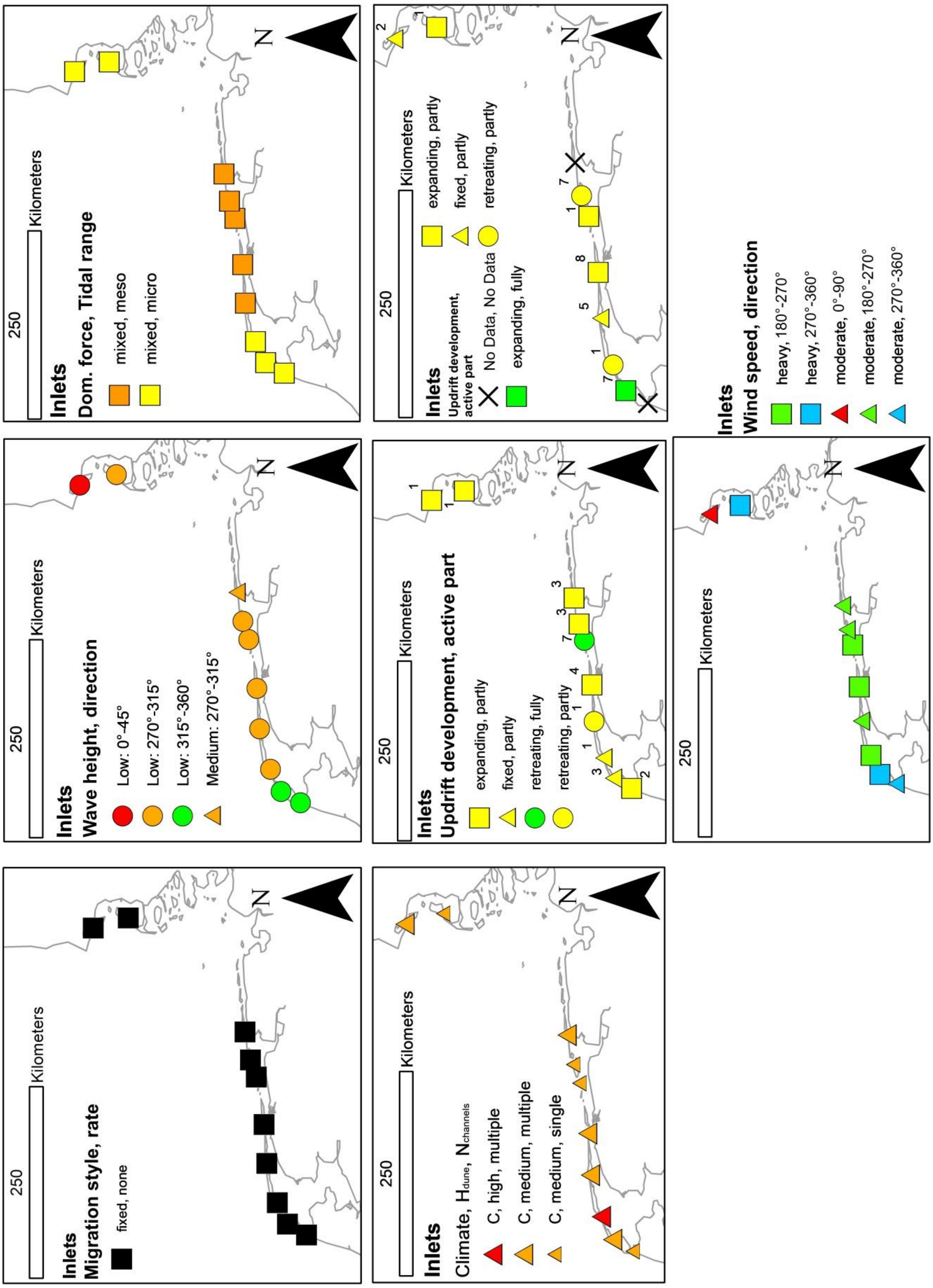

Figure 6: maps regarding the characterization of the Wadden Sea area

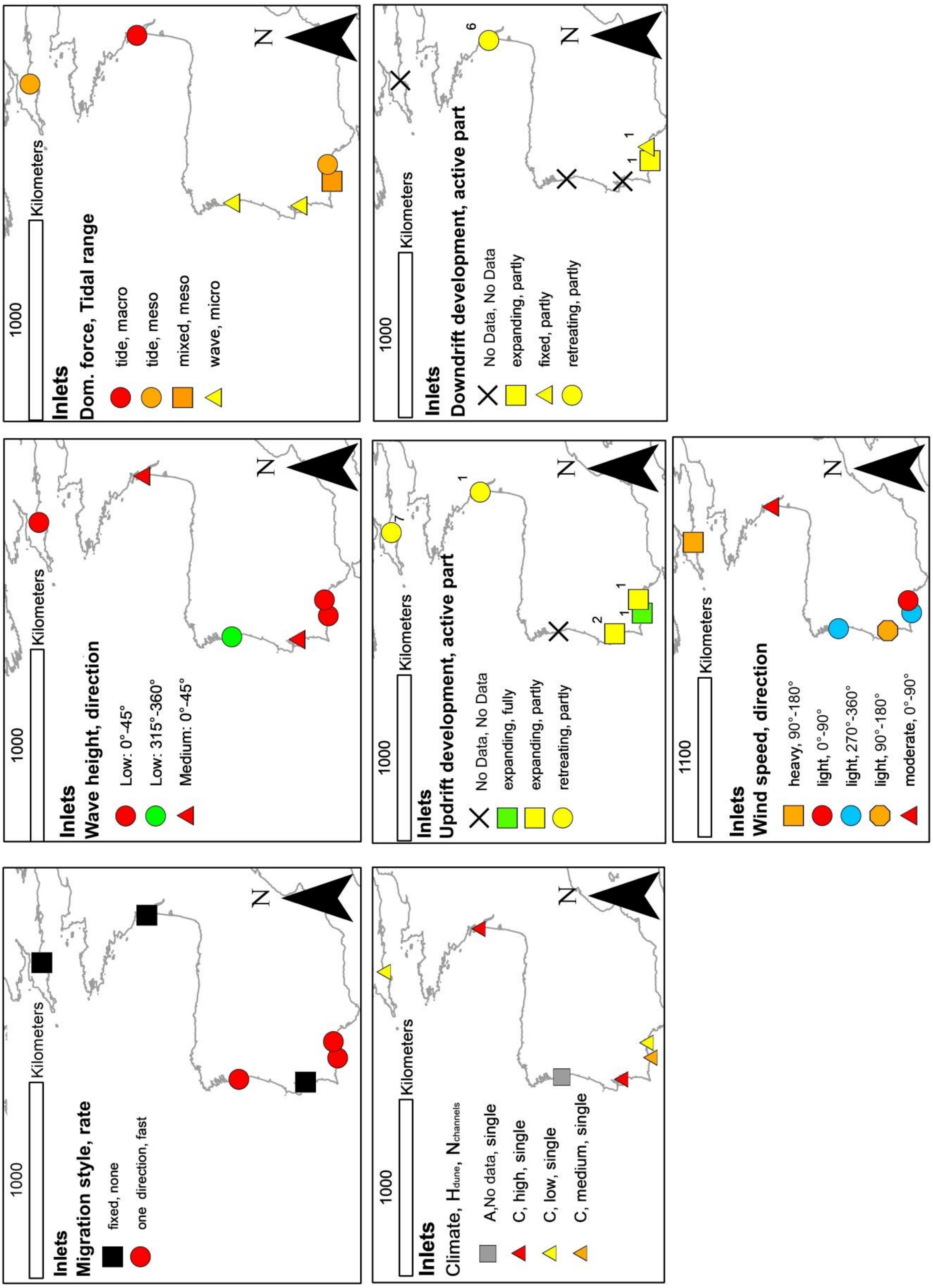

Figure 7: maps regarding the characterization of the European Atlantic coast

3.2. United States

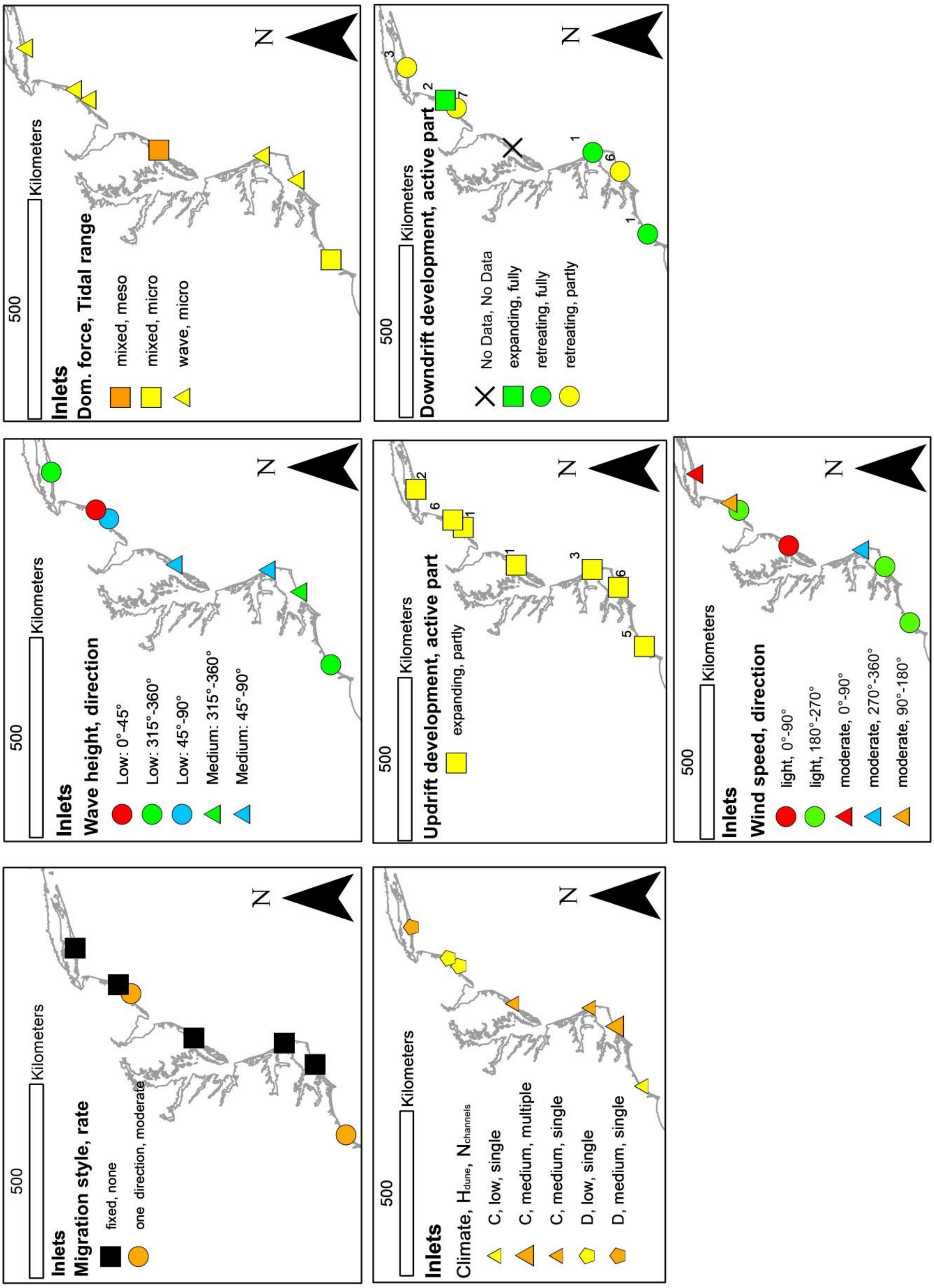

Figure 8: maps regarding the characterization of the northern part of the US east coast

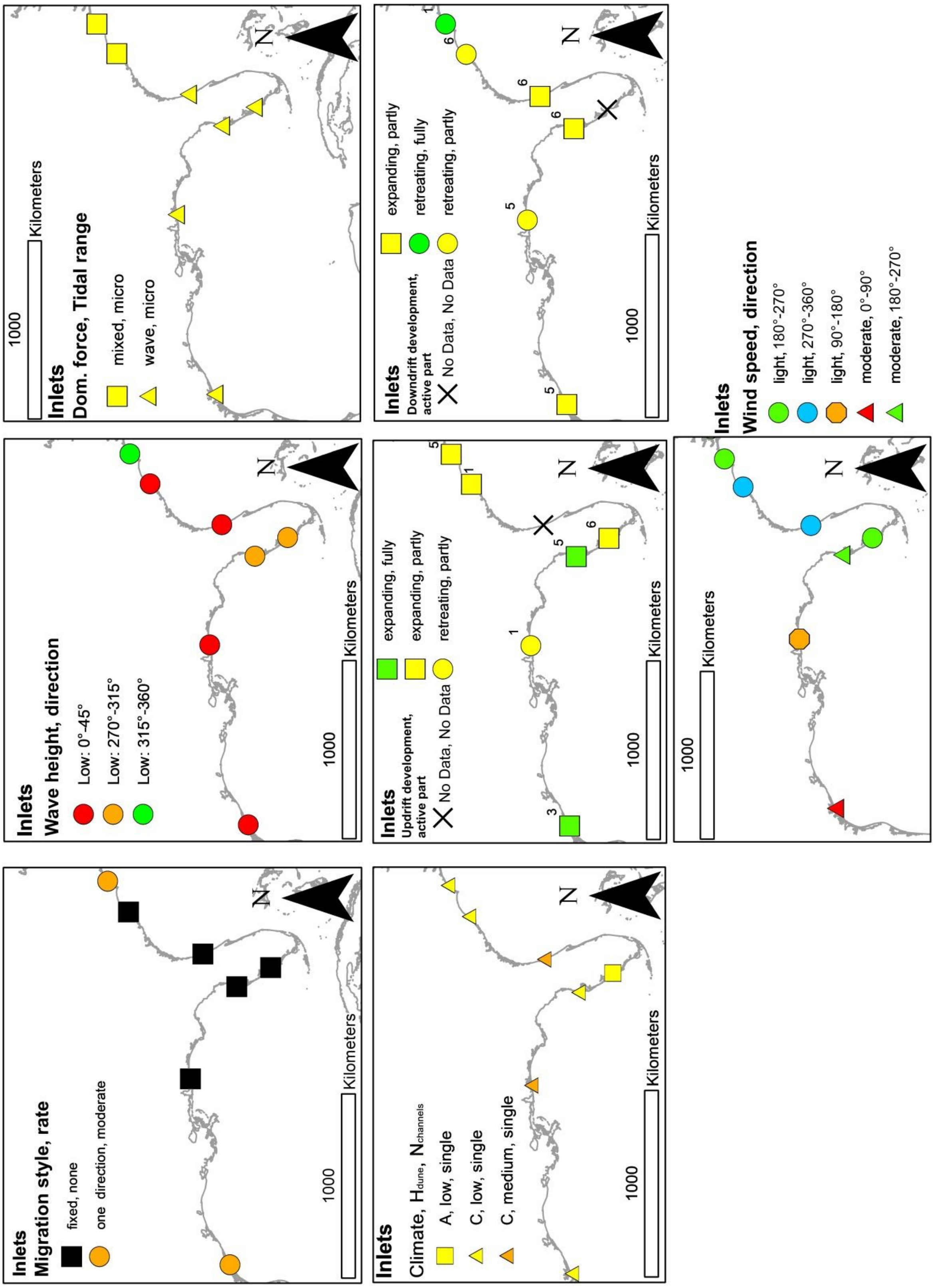

Figure 9: maps regarding the characterization of the Gulf coast and the southern part of the east coast

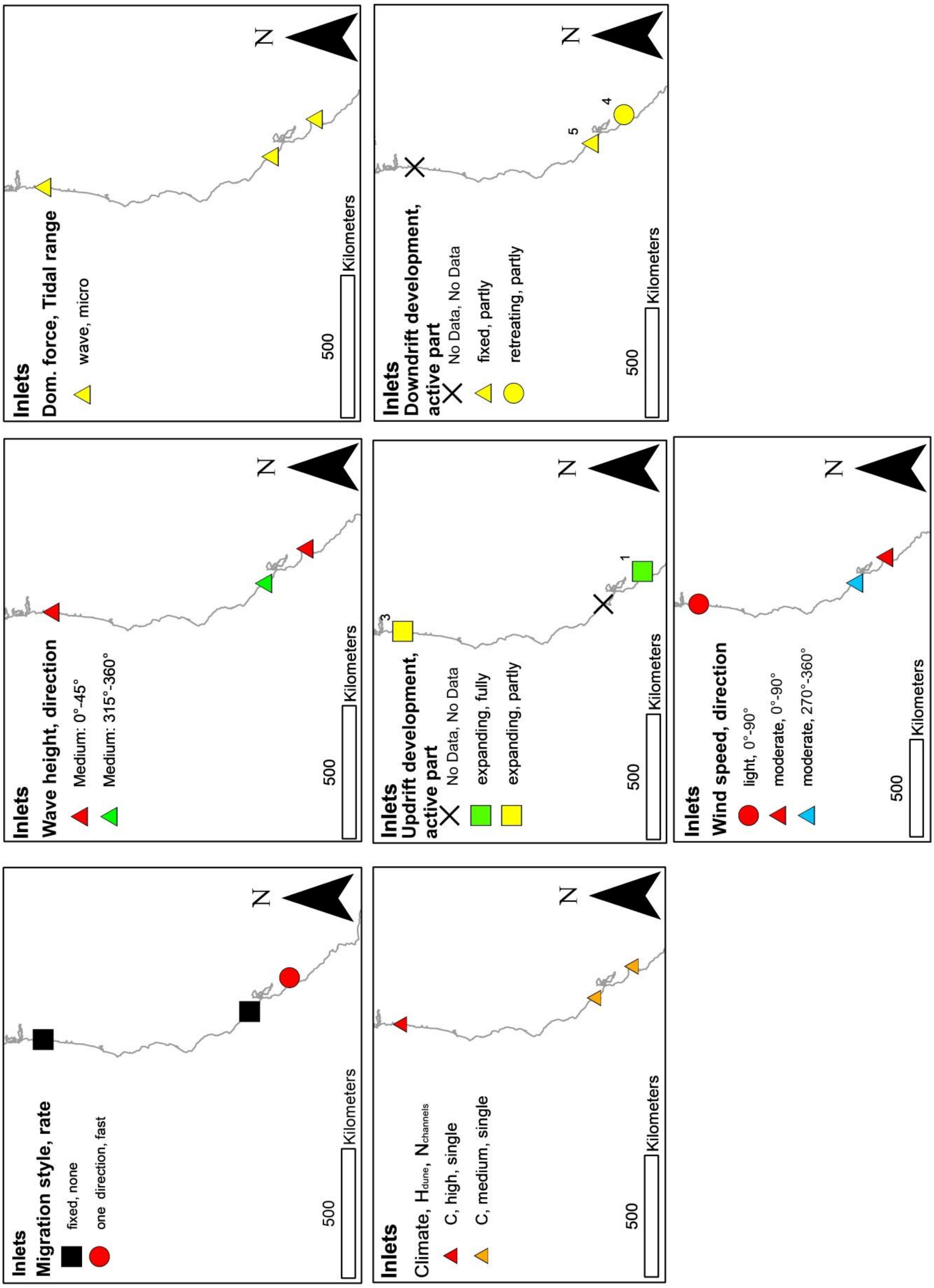

Figure 10: maps regarding the characterization of the US west coast

3.3. Brazil

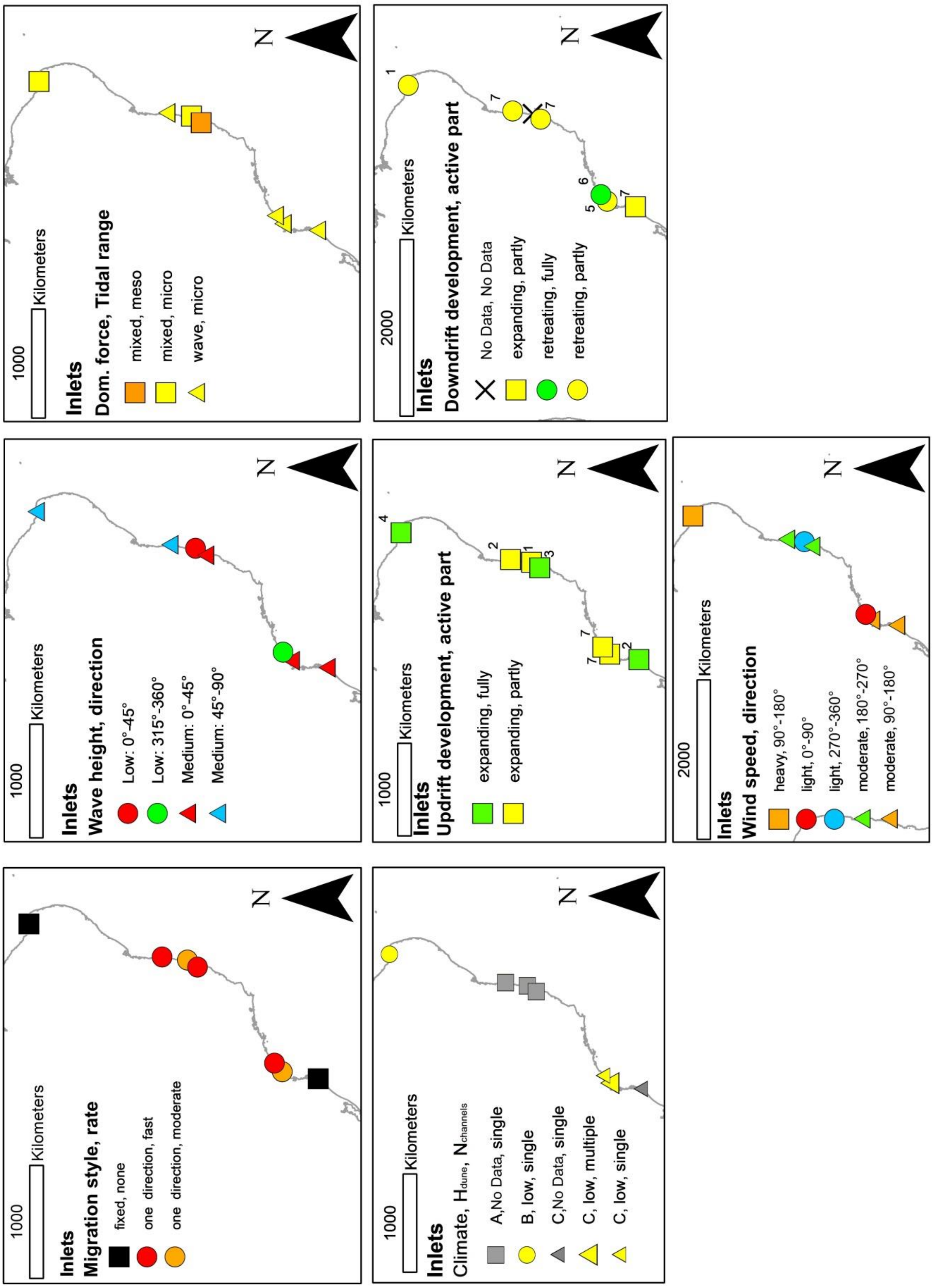

Figure 11: maps regarding the characterization of the Brazilian coast

3.4. Australia

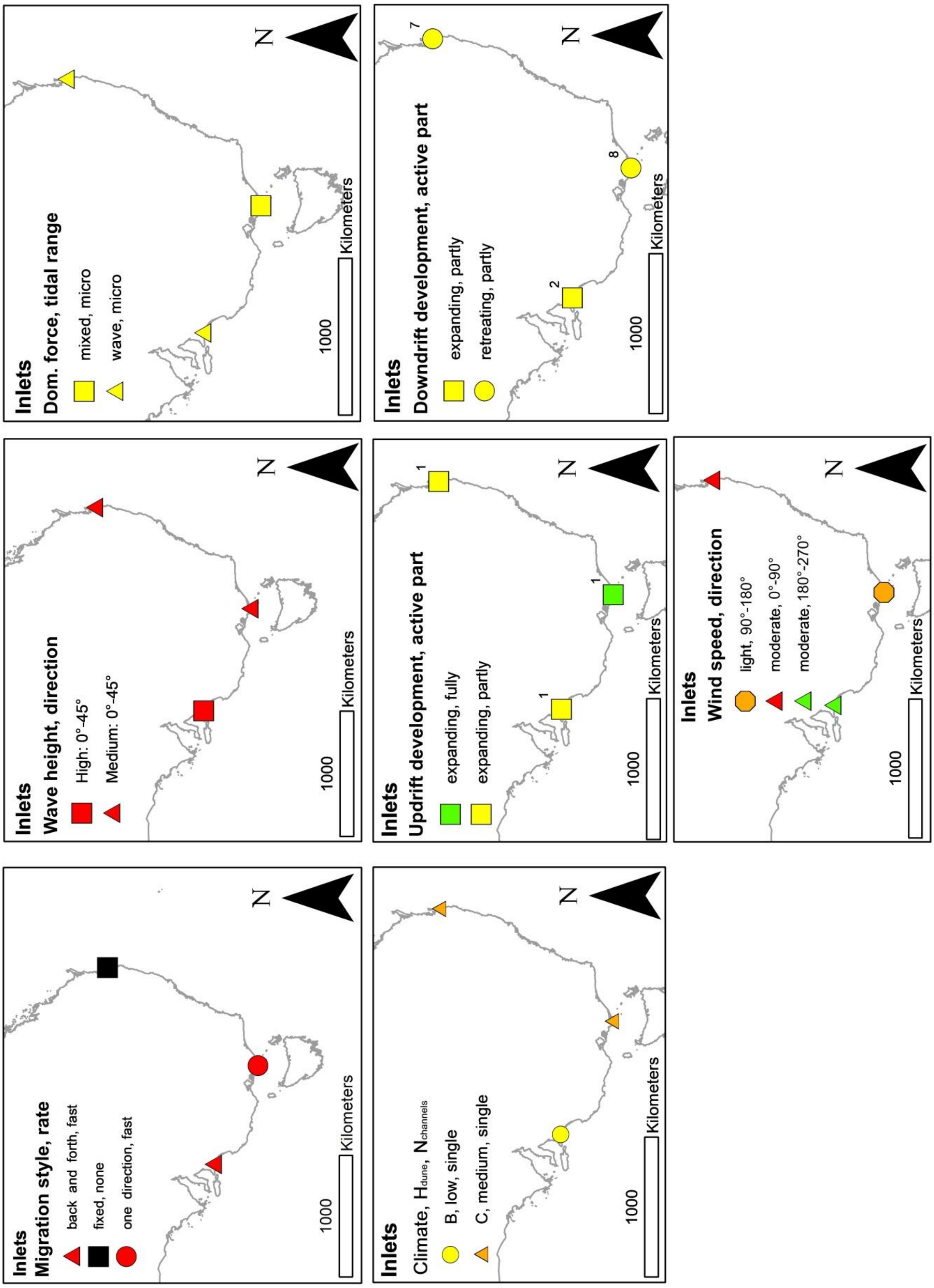

Figure 12: maps regarding the characterization of the Australian coast

3.5. Africa

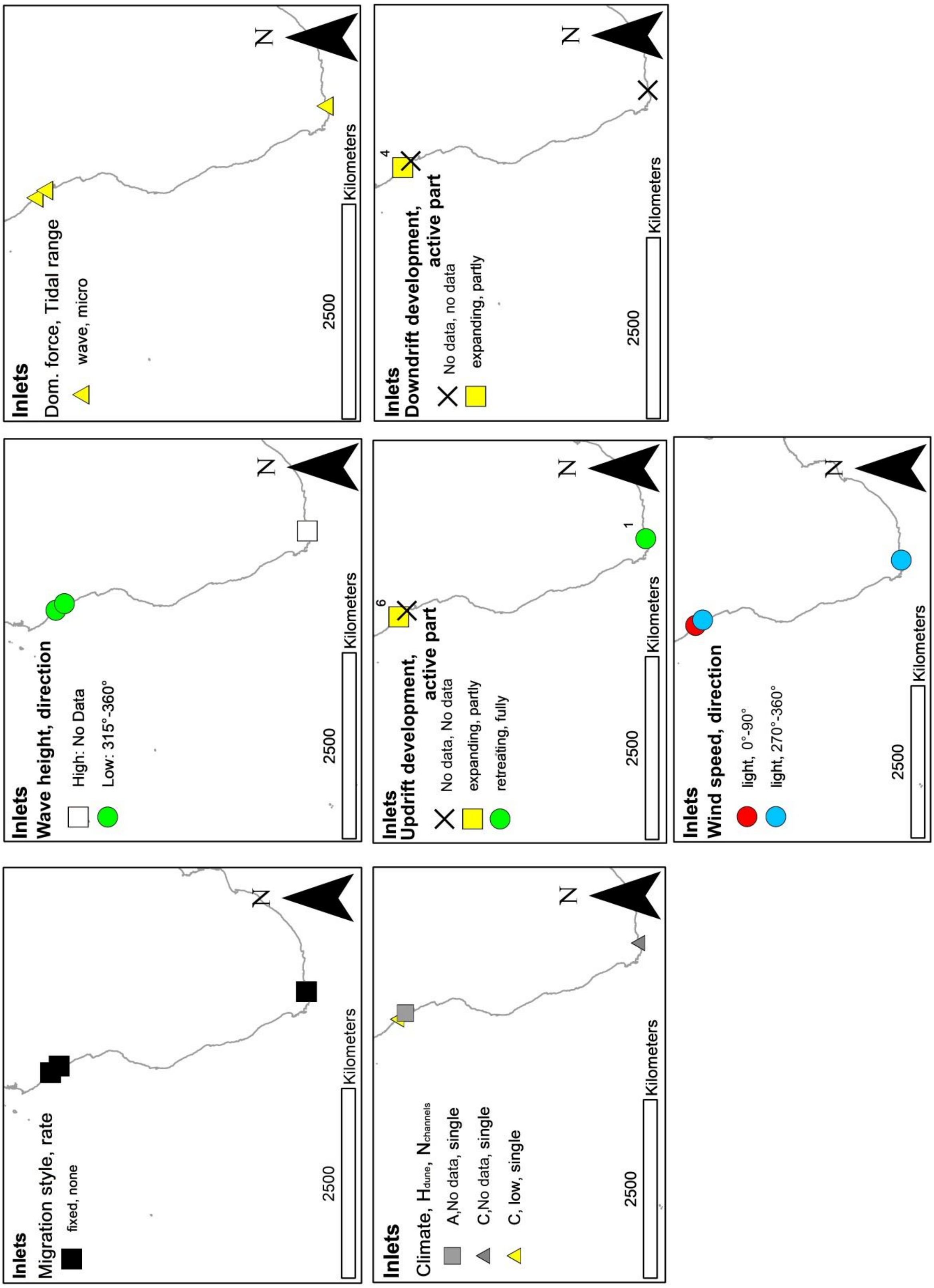

Figure 13: maps regarding the characterization of the African coast

4. Results: statistical analysis

The data from the different inlets is analysed to find relations between the behaviour of the tidal inlet system and the adjacent dune system(s). It is not feasible to assess all possible relations, so hypotheses are made. The hypothesized relations can be found in Table 7. The results of the statistical test on the hypotheses are shown in Table 15.

4.1. Hypotheses

The hypotheses that are presented in this chapter are based on literature. Table 7 gives an overview of the hypothesized relations.

Table 7: hypothesized relations between responses and predictors

Response	Hypothesized predictors
Development of the updrift dune system	Migration style of the inlet Dominant hydrodynamic forcing Mean significant wave height
Development of the downdrift dune system	Migration style of the inlet Dominant hydrodynamic forcing Mean significant wave height Mean wave direction
Extent of active part of updrift dune system	Climate Mean wind speed Mean wind direction Migration style of the inlet Mean significant wave height
Extent of active part of downdrift dune system	Climate Mean wind speed Mean wind direction Migration style of the inlet Mean significant wave height
Maximum dune height	Migration style of the inlet Climate Mean wind speed Mean wind direction Vegetation cover of the updrift dune system Vegetation cover of the downdrift dune system Mean significant wave height
Vegetation cover of updrift dune system	Migration style of the inlet Climate Mean wind speed Mean wind direction Dominant forcing
Vegetation cover of downdrift dune system	Migration style of the inlet Climate Mean wind speed Mean wind direction Dominant forcing

It is hypothesized that the development of the updrift dune system is mainly controlled by the migration style of the inlet, the dominant hydrodynamic forcing and the mean significant wave height. The mean wave direction is not taken into account as a predictor for the dune development of the updrift dune system, because it has an direct influence on the migration style of the inlet (FitzGerald, 1996). The development of the downdrift dune system is hypothesized to be dependent on the migration style of the inlet, the dominant hydrodynamic forcing, the mean significant wave height and the mean wave direction. The mean wave direction is taken into account here because it has an influence on the littoral drift.

The extent of the active part is hypothesized to be dependent on the vegetation cover and the maximum dune height. The maximum dune height is hypothesized to be dependent on the vegetation cover, the climate, the wind, the migration style of the inlet and the mean significant wave height. This means that the extent of the active part is also dependent on those variables. Therefore, it is hypothesized that the extent of the active part of the updrift (downdrift) dune system is dependent on the climate, the mean wind speed, the mean wind direction, the migration style of the inlet and the mean significant wave height. The vegetation cover is not included as an hypothesized predictor, because the vegetation cover is only determined for the active part of a dune system, so the method of determining the vegetation cover and the extent of the active part are largely correlated.

Development of dune system is mainly governed by sediment supply and transport (Houser & Ellis, 2013). The sediment supply is partly dependent on the beach width (Sherman & Bauer, 1993), which is determined by the hydrodynamic forcing and migration of the inlet. If an inlet migrates, it leaves a sand flat in updrift direction. This sand flat will most probably become dry, because significant parts of the sand flat are only submerged during extreme events (van Heteren et al., 2006). A wider dry beach means that there is more potential for aeolian sand transport (Bauer & Davidson-Arnott, 2003). More onshore directed aeolian transport leads to more dune growth (Houser & Ellis, 2013). There are dune systems present along all tidal inlets that were assessed, so it is assumed that the mean wind speed and mean wind direction are such that there is enough sediment transport towards the backshore for dunes to develop.

The downdrift beach is becoming smaller due to the migration (Hayes & FitzGerald, 2013). The dune system on the downdrift side of the barrier is thus exposed to erosional processes. Dune erosion mainly takes place as a result of wave action (Sherman & Bauer, 1993). Normally dunes mainly erode during storm surges (D'Alessandro & Tomasicchio, 2016), but if the beach is eroded away by an inlet channel, the dunes are continuously exposed to wave action. This will lead to a retreat of the dune system.

To develop dunes, it is imperative to have sufficient sediment supply towards the backshore. The first requirement is that there must be enough sediment on the beach (Hesp, 2002). The tides have an influence on the nearshore sediment budget, because they generate a net current which transports sediment alongshore (The Open University, 1999b). The nearshore sediment budget influences the sediment budget on the beach. This sediment is brought from the nearshore to the beach by waves (The Open University, 1999a). Tidal fluctuations of the water level lead to current through tidal inlets. These currents are capable of moving sediment through the inlet channel. Once the flow comes into the basin or the open ocean/sea, the flow slows down and the sediment deposits. This leads to the formation of flood deltas and ebb-tidal deltas (de Swart & Zimmerman, 2009). The morphology of these deltas is dependent on the dominant hydrodynamic forcing (FitzGerald, 1996). The absolute value of the tidal range is not important (R. A. Davis & Hayes, 1984). Wave action can also lead to the formation of shoals on ebb-tidal deltas. These shoals migrate towards the downdrift coast, where they can form a large input of sediment to the beach (Ridderinkhof et al., 2016). This may lead to expansion of the downdrift dune system. Waves that come in obliquely to the coast lead to a current parallel to the shore, the so-called littoral drift (Davidson-Arnott, 2009). This leads to an asymmetrical ebb-tidal delta and to sand bypassing (de Swart & Zimmerman, 2009; Sha, 1989). The sediment that bypasses the inlet channel can be beneficial for the development of downdrift dune systems, because the sediment is transported towards the downdrift shore. Migration of tidal inlets is associated with obliquely incoming waves too (FitzGerald, 1996).

The part of the dune system where deposition or erosion of sediment takes place is called the active part of a dune system. The extent of the active part of the dune system is controlled by the vegetation cover of the dunes and the sediment transport (Houser & Ellis, 2013). If the vegetation is dense, the sediment will be deposited in a small strip along the backshore, while less dense vegetation allows the sediment to be transported further into the dune system (Arens, Baas, Van Boxel, & Kalkman, 2001). Overwash events also lead to the transport of sediment further into the dune system. Overwash occurs when storm waves overtop low dunes or when a dune ridge is breached (Davidson-Arnott, 2009). This means that the dune height has an influence on the frequency of occurrence of overwash. Dune systems with little vegetation and low dunes are thus probably completely active, while dune systems that have established dunes and more vegetation are only active at the most seaward dune ridge. Considering all this it is hypothesized that whether the dune system is completely or only partly active is dependent on the vegetation cover and the maximum dune height.

A dune can grow as long as it receives enough sediment and if there is vegetation to capture the sediment (Houser & Ellis, 2013). The supply of sediment is dependent on the wind speed, the wind direction and the width of the dry beach (Bauer & Davidson-Arnott, 2003). The width of dry beach is controlled by the migration style of the inlet (Hayes & FitzGerald, 2013) and the hydrodynamic forcing (The Open University, 1999a). Furthermore, rainfall and dampness of the air can hinder sediment transport (Hesp, 2012a). The largest dunes will occur at the backshore of dissipative beaches, while the smallest dunes occur at the backshore of reflective beaches. Whether a beach is dissipative, reflective or intermediate is controlled by the mean significant wave height (Short & Hesp, 1982). The occurrence of vegetation that is capable of trapping sediment is controlled by the climate and whether the vegetation can thrive with burial. If the first dune ridge is already largely vegetated, sediment will not be transported further into the dune system (Houser & Ellis, 2013). This will lead to stabilization of the older dune ridges (van Heteren et al., 2006). It is hypothesized that the maximum dune height in a dune system is controlled by the wind speed, wind direction, migration style of the inlet, the climate, the vegetation cover of the updrift and downdrift dune system and the mean significant wave height.

The vegetation cover is not only a predictor for the behaviour of a dune system, but it is also part of the response of a dune system. The vegetation cover is largely dependent on the type of vegetation and the rate of burial. The rate of burial is hooked on the sediment supply towards the dunes, which is mainly controlled by the wind speed and wind direction. The type of vegetation is dependent on the climate and the rate of burial (Houser & Ellis, 2013). The vegetation cover of the most seaward dune ridge is also directly connected with the overall development of the dune system. An expanding dune system has incipient dunes as the most seaward dunes. These dunes are only vegetated with pioneer vegetation (Hesp, 2012a). A retreating or stable dune system has older dunes at its seaward boundary. Older dunes are often more vegetated (Houser & Ellis, 2013). It is thus hypothesized that the vegetation cover on both the updrift and downdrift dune system can be predicted using the climate, the mean wind speed, the mean wind direction and the migration style of the inlet and the dominant forcing. The effect of the predictors on the response is probably different for updrift and downdrift system.

4.2. Categorical regression

The hypotheses formulated in the previous paragraph are tested whether they can be confirmed using statistical testing of the data collection (see paragraph 2.3.2). In this paragraph the main characteristics of the results are given. In appendix F the transformation plots are presented that show the original variables plotted against the transformed variables. The values of β are related to the transformed variables so they have to be examined together with the transformation plots.

4.2.1. Results per response variable

The migration style of the inlet and the dominant hydrodynamic forcing are found to be significant for the development of the updrift dune system (Table 8). The dominant hydrodynamic forcing is the most important of the two variables. The values of β in combination with the transformation plots (Figure 66, Figure 67 and Figure 68) tells us that an wave-dominated, migrating inlet has an expanding dune system. If an inlet is mixed-energy or tide-dominated, the probability of having an expanding dune system decreases. The same is true when an inlet is fixed or migrating back-and-forth.

Table 8: development of the updrift dune system

Predictor	p	p	β	Importance	Tolerance	
					after	before
Migration style of the inlet	0,004	0,000	0,318	0,381	1,000	0,999
Dominant hydrodynamic forcing	0,015	0,026	-0,405	0,619	1,000	0,999
Mean significant wave height	0,354					
R^2	**0,345**	**0,263**				
ΔR^2		**-0,082**				

The development of the downdrift dune system was hypothesized to be dependent on four predictors, but only the mean wave direction proved to be significant (Table 9).

Table 9: development of the downdrift dune system

Predictor	p	p	p	p	β
Migration style of the inlet	0,340	0,276	0,341		
Mean significant wave height	0,202	0,282			
Mean wave direction	0,017	0,020	0,001	0,000	0,398
Dominant hydrodynamic forcing	0,593				
R^2	**0,291**	**0,271**	**0,193**	**0,158**	
ΔR^2		**-0,02**	**-0,078**	**-0,035**	
$\sum\Delta R^2$		**-0,02**	**-0,098**	**-0,133**	

The extent of the active part of the updrift dune system was hypothesized to be dependent on five predictors, but only the climate and the migration style of the inlet were found to be significant (Table 10). The two significant predictors are of almost equal importance for the extent of the active part of the updrift dune system. When an inlet is migrating in one direction, it is more likely that the updrift dune system will be fully active (Figure 71).

Table 10: extent of the active part of the updrift dune system

Predictor	p	p	p	p	β	Importance	Tolerance	
							after	before
Climate	0,008	0,002	0,001	0,001	0,471	0,415	0,654	0,932
Mean wind speed	0,220	0,111	0,361					
Mean wind direction	0,365							
Migration style of the inlet	0,001	0,000	0,002	0,005	0,505	0,584	0,654	0,932
Mean significant wave height	0,156	0,119						
R^2	**0,366**	**0,352**	**0,224**	**0,198**				
ΔR^2		**-0,014**	**-0,128**	**-0,026**				
$\sum\Delta R^2$		**-0,014**	**-0,142**	**-0,168**				

The extent of the active part of the downdrift dune system was also hypothesized to be dependent on five predictors, but only the mean wind direction proved to be significant (Table 11).

Table 11: extent of the active part of the downdrift dune system

Predictor	p	p	p	p	p	β
Climate	0,528	0,483	0,281	0,255		
Mean wind speed	0,921					
Mean wind direction	0,204	0,113	0,083	0,074	0,076	0,215
Migration style of the inlet	0,453	0,557	0,577			
Mean significant wave height	0,738	0,731				
R^2	**0,121**	**0,115**	**0,109**	**0,090**	**0,046**	
ΔR^2		**-0,006**	**-0,006**	**-0,019**	**-0,044**	
$\sum\Delta R^2$		**-0,006**	**-0,012**	**-0,031**	**-0,075**	

The maximum dune height was hypothesized to be dependent on seven predictors and only four were significant (Table 12). The mean significant wave height is found to be of lesser importance than the other three significant predictors, which are all of almost equal importance. Migrating inlets lead to lower dunes. The same is true when there is an arid climate, lower wave heights and lower vegetation cover.

Table 12: maximum dune height

Predictor	p	p	p	p	β	Importance	Tolerance	
							after	before
Migration style of the inlet	0,062	0,006	0,000	0,000	0,468	0,290	0,822	0,986
Climate	0,156	0,012	0,001	0,002	0,514	0,282	0,688	0,887
Mean significant wave height	0,257	0,012	0,019	0,007	0,455	0,054	0,609	0,881
Mean wind speed	0,257	0,335						
Mean wind direction	0,419	0,267	0,154					
Vegetation cover of the updrift dune system	0,031	0,000	0,000	0,000	-0,486	0,374	0,954	0,938
Vegetation cover of the downdrift dune system	0,928							
R^2	**0,756**	**0,740**	**0,706**	**0,681**				
ΔR^2		**-0,016**	**-0,034**	**-0,025**				
$\sum\Delta R^2$		**-0,016**	**-0,05**	**-0,075**				

The vegetation cover of the updrift dune system was hypothesized to be dependent on five predictor variables, but at the end only the migration style of the inlet and the mean wind direction proved to be significant (Table 13). The mean wind direction is the most important one. Wind that are blowing seaward are leading to more vegetation cover.

Table 13: vegetation cover of the updrift dune system

Predictor	p	p	p	p	β	Importance	Tolerance	
							after	before
Migration style of the inlet	0,065	0,035	0,040	0,067	0,244	0,201	0,985	0,996
Climate	0,304	0,082	0,152					
Mean wind speed	0,347							
Mean wind direction	0,008	0,003	0,001	0,000	0,445	0,799	0,985	0,996
Dominant hydrodynamic forcing	0,233	0,392						
R^2	**0,367**	**0,318**	**0,255**	**0,231**				
ΔR^2		**-0,049**	**-0,063**	**-0,024**				
$\sum\Delta R^2$		**-0,049**	**-0,112**	**-0,136**				

The vegetation cover of the downdrift dune system was hypothesized to be dependent on five variables. Finally, two variables were found to be significant (Table 14): the climate and the mean wind direction. The climate is more important than the mean wind direction. Especially an arid climate leads to lower vegetation cover. Offshore winds lead to higher vegetation cover.

Table 14: vegetation cover of the downdrift dune system

Predictor	p	p	p	p	β	Importance	Tolerance	
							after	before
Migration style of the inlet	0,022	0,612						
Climate	0,093	0,121	0,012	0,002	0,449	0,705	0,996	0,976
Mean wind speed	0,363	0,508	0,506					
Mean wind direction	0,072	0,288	0,253	0,044	0,299	0,295	0,996	0,976
Dominant hydrodynamic forcing	0,419							
R^2	**0,468**	**0,299**	**0,285**	**0,274**				
ΔR^2		**-0,169**	**-0,014**	**-0,011**				
$\sum\Delta R^2$		**-0,169**	**-0,183**	**-0,194**				

4.2.2. Summary

The relations that are given in the tables above are summarized in Table 15. The reason why 'migration style of the inlet' is in italic is given in chapter 5.

Table 15: overview of found relations between the response and predictor variables

Response variable	**Predictor variable**
Development of the updrift dune system	*Migration style of the inlet* Dominant hydrodynamic forcing
Development of the downdrift dune system	Mean wave direction
Extent of the active part of the updrift dune system	Climate *Migration style of the inlet*
Extent of the active part of the downdrift dune system	Mean wind direction
Maximum dune height	*Migration style of the inlet* Climate Vegetation cover of the updrift dune system Mean significant wave height
Vegetation cover of the updrift dune system	*Migration style of the inlet* Mean wind direction
Vegetation cover of the downdrift dune system	Climate Mean wind direction

5. Discussion: results of the statistical test

In the previous chapter a series of relations between the inlet behaviour and the dune behaviour were presented. Those relations are supported by the statistics and in this chapter the physical explanation is given based on published literature and the maps given in chapter 3. Overall, it can be said that the migration style of the inlet was the only variable that was directly connected to tidal inlet systems. The other significant variables are also present on straight coasts, but they may be influenced by the tidal inlet system (de Swart & Zimmerman, 2009; FitzGerald, 1996).

5.1. Development of the updrift dune system

In Figure 14 the expansion of the downdrift dune system at Brigantine Inlet is shown. Brigantine Inlet is a wave-dominated, migrating inlet. The same behaviour can be seen at for example Pelican Inlet on the wave-dominated Gulf coast. From Figure 12 can be seen that the inlets in Australia do have different migratory behaviour, but all inlets are mixed-energy or wave-dominated and all updrift dune systems are expanding. Also all selected tidal inlets along the Brazilian coast (Figure 11) have an expanding updrift dune system, while there are no tide-dominated inlets. Two out of three tidal inlet systems along the US west coast (Figure 10), which are all wave-dominated, have expanding updrift dune systems too. The third tidal inlet does not have an updrift dune system. The two inlets along the European Atlantic coast with a retreating updrift dune system, namely Maumusson Inlet and Exmouth Inlet, are both tide dominated.

Figure 14: Brigantine Inlet, a wave dominated and migrating inlet, in 2016. The black line shows the border of the updrift dune system in 1984.

The behaviour as stated in the previous paragraph is supported by the outcome of the statistical analysis. The statistical test namely showed that the development of the updrift dune system is significantly controlled by the migration style of the inlet and the dominant hydrodynamic forcing.

The mean significant wave height is possible not significant because its effect is also partly present in the dominant hydrodynamic forcing. The dominant hydrodynamic forcing is namely determined by the ratio between the mean significant wave height and the mean tidal range (R. A. Davis & Hayes, 1984). The mean significant wave height can have an influence on the beach geometry too (Short & Hesp, 1982), but this effect is most probably subordinate to the effects of the migration style and the dominant hydrodynamic forcing. This can explain why the mean significant wave height is not a significant predictor variable.

5.2. Development of the downdrift dune system

In Figure 15 the expansion of the updrift dune system at Hurricane Pass is illustrated. The waves come in obliquely from the west. Little Egg Inlet on the US east coast is an example of a fixed inlet where the waves come in very oblique to the coast. This inlet has an expanding downdrift dune system. This is in contrast with the downdrift dune systems at Jumpinpin Inlet and Murray Mouth which both have retreating downdrift dune system, while the waves are also coming in oblique to the coast. The same is true for Maumusson Inlet at the European Atlantic coast.

Figure 15: the updrift coast of Hurricane Pass, A mixed energy inlet with waves coming from 270°-315° with respect to shore normal, in 2017. The black line shows the border of the dune system in 1984.

The development of the downdrift dune system influenced by the mean wave direction according to the results of the statistical test. The migration style of the inlet, the dominant hydrodynamic forcing and the mean significant wave height are not significant variables according to the statistical test. The reason can be the variability in the data, because no clear examples can be found that support an significant influence of these variables.

5.3. Extent of the active part of the updrift dune system

The extent of the active part of the updrift dune system is dependent on the climate and the migration style of the inlet. On the west coast of the United States it can for example be seen that there is one inlet with a fully active updrift dune system and one inlet with a partly active updrift dune system. The inlet with the fully active dune system is migrating, while the other one is on a fixed position. A dune system can also be stabilized as a result of dune growth due to a migrating inlet. This happened on Moreton Island near Jumpinpin Inlet, where a transgressive dune field was stabilized due to the development of foredunes (Levin, Jablon, Phinn, & Collins, 2017). The effect of the climate can be seen clearest when looking at the updrift dune systems near inlet in tropical regions (Climate type A). All but one of these inlets is partly active.

The mean wind speed, mean wind direction and the mean significant wave height are not significant according to the statistical test. The variability regarding the mean wind direction is too big to visually see a relation with the extent of the active part of the updrift dune system. For example, all updrift dune systems on the East coast of the United States are partly active, but all categories of the mean wind direction are present there. Comparable observations can be made for the relation between the mean wind speed and the extent of the active part of the updrift dune system. Regarding the mean significant wave height it can also be seen that it seemingly does not matter whether the waves are high, medium or low.

5.4. Extent of the active part of the downdrift dune system

The extent of the active part of the downdrift dune system is dependent on the mean wind direction according to the statistical test. On the US east coast can clearly be seen that the inlet with wind from land are fully active, while the inlets with wind from the sea are only partly active. This is also true for two out of three inlets with a downdrift dune system along the European Atlantic coast.

The climate, the mean wind speed, the migration style and the mean significant wave height are not significant according to the statistical test. This is supported by the maps, because no clear examples that point towards a possible relations could be found regarding the four insignificant predictor variables.

The vegetation cover of a dune has a clear relation with the extent of the active part of the dune. When a dune is fully vegetated, deposition of sediment will only take place in the first row of vegetation, while sedimentation takes place over a broader area when the dune is less vegetated (Arens et al., 2001). This means that the dune system is only partly active when the level of vegetation cover is high. The vegetation cover as used in this research is determined as the cover of the active part of the dune system. Using the vegetation cover as a predictor for the extent of the active part would thus lead to biased results. This is why the vegetation cover is not used as a predictor for the extent of the active part.

5.5. Maximum dune height

The results from the statistical test show that the maximum dune height is significantly influenced by the migration style of the inlet, the climate, the vegetation cover of the updrift dune system and the mean significant wave height.

The two inlets with the highest dunes on the European Atlantic coast, namely Maumusson Inlet and Sado River Inlet, are both on a fixed position and have the largest mean significant wave height in that area.

The effect of the climate on the maximum dune height can be seen in the results from the characterization. There are only dunes in the highest category on locations with a temperate climate (C). In the arid (B) and tropical (A) climates only dunes from the lowest category were found.

The maximum dune height is shown to be dependent on the vegetation cover of the updrift dune system, while the vegetation cover of the downdrift system does not have a significant effect. This can be due to the low number of observations on the vegetation cover of the updrift and downdrift dune systems. Vegetation extracts momentum from the air and causes sediment to settle (Houser & Ellis, 2013). This process is the same on the updrift and the downdrift side of the inlet channel. The amount of aeolian transport towards the dunes can differ significantly between the updrift and the downdrift side of the inlet due to the difference in sediment budget and fetch length (Bauer & Davidson-Arnott, 2003), so the exact impact of the vegetation is different between the updrift and downdrift. Because the process does not differ between the updrift and the downdrift side, it is assumed that the maximum dune height is dependent on the local vegetation cover. No distinction is being made between updrift and downdrift dune systems.

The mean wind speed and the mean wind direction were not significant predictors for the maximum dune height. This can be due to the relatively high number of hypothesized predictors compared to the number of observations. The mean wind speed and mean wind direction were hypothesized, because they have an effect on the amount of aeolian transport into the dune system (Bauer & Davidson-Arnott, 2003). Aeolian transport mostly takes place in turbulent flow, so when the velocity field is fluctuating (Durán, Claudin, & Andreotti, 2011). This fluctuation is not taken into account when using the mean wind speed and mean wind direction. This can only be done using on site measurements.

5.6. Vegetation cover of the updrift dune system

The vegetation cover of the updrift dune system is significantly influenced by the mean wind direction and the migration style of the inlet. On the US east coast it is observed that the highest vegetation covers are present near fixed tidal inlet system with the wind coming from land. The highest vegetation cover at the European Atlantic coast is observed at Exmouth Inlet, which is an fixed tidal inlet system with a mean wind direction from the land too.

Texel Inlet is a prime example of an inlet where migration led to more vegetation of the updrift dune system. The southward migration of the inlet led to the development of new dune rows, which cut off the sediment supply towards the older dunes. The older dunes then became more vegetated and stabilized (van Heteren et al., 2006).

The effect of the wind direction and the migration style on the vegetation cover is mainly due to aeolian sediment transport and sedimentation rates on the dunes. It is clear that the sedimentation rate has an influence on the vegetation cover, but no clear quantitative relationship could be established (Keijsers et al., 2015).

5.7. Vegetation cover of the downdrift dune system

The vegetation cover of the downdrift dune system is influenced by the climate and the mean wind direction. Some observations about this can be made from the maps shown in chapter 3. The highest vegetation cover on downdrift dune systems at the Brazilian coast is found at locations with wind blowing from land. This is also the case at the US east coast.

Regarding the effect of the climate, especially the difference between the vegetation cover in a tropical and an arid climate are notable. This can be due to the difference in precipitation and temperature (Peel et al., 2007), which lead to different vegetation types (Houser & Ellis, 2013). The effect of the wind direction is analogous to the effect as described in the previous paragraph about the vegetation cover of the updrift dune system.

The results from the statistical analysis show that the vegetation cover of the downdrift system is dependent on both the climate and the mean wave direction, while the vegetation cover of the updrift system is dependent on the mean wave direction and the migration style of the inlet. No tidal inlet is so big that both sides of the inlet experience a different climate class according to the Köppen-Geiger climate scale (Peel et al., 2007). Therefore, it is assumed that the climate the same effect on the vegetation cover of both updrift and downdrift dune systems. The fact that the climate is not a significant predictor for the vegetation cover of the updrift dune system can be due to the limited number of observations (45) in combination with the hypothesized number of predictors (5).

6. Discussion: limitations and remarks

The methods used to get the result that are presented in the previous chapter need to be put in perspective to draw reasonable conclusions. This chapter thus gives an overview of the limitations and the remarks that can be made about the research.

The tidal inlet systems were selected from a limited geographic area. Asia and Antarctica were excluded because there are only limited amounts of dunes present there, let alone dunes along tidal inlets (Forbes & Hansom, 2011; Hesp, 2008). The climate in the study area is as widespread as possible excluding the polar climate, but not for every climate an equal number of inlets was selected. This means that not every type of climate is equally present in the data set. This could lead to biased results when doing the statistical analysis, but because every climate type is presents more than one time, the bias is assumed to be small.

Based on Reed et al. (2009), most of the aspects are represented, with the exception of geology and the long term geomorphology. This effect can for example be characterized using the grain diameter, because this is an important parameter in the formation of bedforms (Dyer & Huntley, 1999). This data is not widely available, so these variables were not used in the research. Variables such as ebb tidal delta volume and orientation can also be used to assess the geomorphology of tidal inlet system, but these type of variables are difficult to assess for a lot of systems within the available timespan using only open-source data.

The wind data used in this research mainly comes from Windfinder, an online weather service for surfers and sailors. The statistics on Windfinder are computed based on observations made during daytime hours (06:00-18:00) so the effects of day and night on the wind, such as sea breeze, are not taken into account. The sea breeze effect can have an influence on the mean wind speed and the mean wind direction, because the sea breeze leads to onshore winds during the afternoon in the hot summer months. The local topography has a large influence on the behaviour of the sea breeze (Arrillaga, Yagüe, Sastre, & Román-Cascón, 2016), so it is virtually impossible to correct all values of the mean wind speed and the mean wind direction for the sea breeze effect. Also the effect of gusts and other fluctuations of the wind speed and wind direction were not taken into account. These factors can influence the amount of aeolian transport, but they are very difficult to characterize (Durán et al., 2011). The values for the mean wind speed and mean wind direction that were not taken from Windfinder are comparable to the values in Windfinder (2017), so there is no noticeable bias regarding the wind data from different sources.

A total number of 45 inlets was selected and characterized. For 2 inlets (Conkouati, Lagoa Massabi Inlet) no data could be found about the dune system, so these cases were excluded from the statistical analysis. Furthermore not every inlet has dune systems on both, which lead to more excluded observations in some analyses. The data from WaveWatch III (2017) shows that the waves at the model node closest to the Breede River Mouth are directed offshore, so this value was omitted from the analysis. Finally a minimum number of 34 observations ($N = 34$) was used to do the statistical analysis. Using a low number of observations does lead to higher standard errors for the coefficients, so it is less likely that coefficients are significant (Van der Kooij, 2007).

The discretization of the raw numeric data of the mean significant wave height, the mean wind speed, the mean wave direction, the mean wind direction and the maximum dune height was done using bin edges that were chosen a bit arbitrarily. The outcome of CATREG seemed to be relatively insensitive to the choice of the number of bins and the bin edges. There were no other significant variables when the number of bins was changed ±1 or when the bin edges where shifted up to 25%.

At first the final goal of this research was to get a conceptual model that linked the hydrodynamics and behaviour of a tidal inlet to the development of adjacent dune systems. The data does not fully support a complete conceptual model, but it identifies the important processes that influence dunes along tidal inlets so a start can be made with a model comparable to what Reed et al. (2009) present (Figure 2). It is not possible to quantify any relations, because the uncertainty of the data and the statistical test is too big. Qualitative relations can be made, but should be treated with caution.

7. Conclusions and recommendations

Inlets from Europe, the United States, Brazil, Africa and Australia are assessed to find the influence of the hydrodynamic forcing in tidal inlets on the dune systems near those inlets. Variables regarding the hydrodynamics and the migratory behaviour of tidal inlets and the overall development and characteristics of dune system are used to characterize every inlet. The overall data set gives us insight in the relations between the inlet processes and the development and characteristics of the adjacent dune system, but the relations must be reviewed critically and may not be the truth in all situations. This chapter gives the answers to the research questions and some recommendations for future research.

7.1. Answers to the research questions

Subquestion 1: Where in the selected geographical areas do tidal inlets occur that have a dune system on one or both sides of the inlet channel?

For every selected geographical area (see appendix A for an overview) a minimum of three tidal inlets was found that had dune systems on one or both sides of the inlet. At the end 45 inlets where selected from the 106 inlets that were assessed. In Europe those inlets can mainly be found along the coast of northwest Europe where there is a line of barrier island between the North Sea and the Wadden Sea. Tidal inlets with adjacent dune systems can be found along the European Atlantic coast too. Furthermore, there are many tidal inlets along the east coast and Gulf coast of the contiguous United States, but many of them are heavily urbanized. The west coast of the contiguous United States is mostly rocky, so tidal inlets with adjacent dune systems are rare in this area. The Brazilian coast and the west coast of Africa both have numerous tidal inlets, and many of them also have a dune system on one or both sides of the inlet. On the African coast it is not always clear if the dunes are really coastal dunes or just desert dunes that are located close to the ocean. On the Australian coast are numerous tidal inlets too, especially along the east coast. Many inlets are heavily urbanized, but some inlets with adjacent dune systems can be found.

Subquestion 2: What are the characteristics of the selected tidal inlets and their adjacent dune systems?

There are tidal inlets and dune systems in various shapes and sizes. The hydrodynamic forcing varies from high waves with very little tidal ranges to low waves with high tidal ranges. Moreover, the climate and wind regime varies per location.

Tidal inlets can be in the form of small channels that are not permanently open or big multichannel systems. The inlets show a varying migratory behaviour considering the timescale involved. 31 inlets are on a fixed position and 13 are migrating in one direction. Only one inlet showed migration in various directions. The rate at which the inlets migrate differs from a meter per year to almost 80 meters per year.

The dune systems display diverse behaviour. The systems can be expanding, stable or retreating. Also the amount of vegetation and the extent of the active part differs between the various systems. The maximum observed dune height differs from a few meters to circa 30 meters.

Subquestion 3: What relations can be found between the parameters that describe inlet behaviour and the parameters that describe the dune systems?

The table below shows the variables that have an effect on the various aspects of a dune system. Quantitative relations could not be established and the qualitative relations should be handled with care and assessed per situation.

Table 16: relations between the parameters that describe inlet behaviour and the parameters that describe the dune system

Response variable	Predictor variable
Development of the updrift dune system	*Migration style of the inlet*
	Dominant hydrodynamic forcing
Development of the downdrift dune system	Mean wave direction
Extent of the active part of the updrift dune system	Climate
	Migration style of the inlet
Extent of the active part of the downdrift dune system	Mean wind direction
Maximum dune height	*Migration style of the inlet*
	Climate
	Vegetation cover of the updrift dune system
	Mean significant wave height
Vegetation cover of the updrift dune system	*Migration style of the inlet*
	Mean wind direction
Vegetation cover of the downdrift dune system	Climate
	Mean wind direction

Main question: What is the influence of the hydrodynamic forcing and migratory behaviour of tidal inlets on dune systems near tidal inlets?

The overall development of a dune system near a tidal inlet seems to be controlled by the migration of the inlet and the hydrodynamic forcing. Furthermore, the dune height appears to be controlled by the climate and the vegetation cover, which in turn looks like to be influenced by the wind direction and the climate.

The migration of a tidal inlet is the only process that only takes place in tidal inlet systems that significantly influences the nearby dune systems. The other significant processes, such as the hydrodynamics and wind, are also present near straight coasts. The morphology and topography in and near tidal inlet has an influence on the local hydrodynamics and wind conditions, so the exact influence of those processes on nearby dune systems may be different than on straight coasts.

As a conclusion it can be said that the migration of inlets is the most direct factor leading to dune systems behaving differently near tidal inlet than on straight coasts. Other processes, for example hydrodynamics, are also present near straight coasts, but they may be influenced by the morphology of the tidal inlet. The processes and relations as we know for straight coast remain applicable to dune systems near tidal inlets.

7.2. Recommendations

The research presented in this thesis can be continued and expanded in several ways. One of the options is to use a similar methodology, but time series are used instead of using a single value for the different variables. This will lead to more data being used when determining the relations, which can improve our confidence in the results. The main drawback of this method is the limited availability of validated time series. A second option for further research is to use idealized models to investigate the effect of the various relations. Quantitative relations can be obtained this way. This option is more suitable for specific situations and locations.

References

AHN. (2017). AHN Viewer. Amersfoort: Algemeen Hoogtebestand Nederland. Retrieved from https://ahn.arcgisonline.nl/ahnviewer/

Arens, S. M., Baas, A. C. W., Van Boxel, J. H., & Kalkman, C. (2001). Influence of reed stem density on foredune development. *Earth Surface Processes and Landforms*, *26*(11), 1161–1176. https://doi.org/10.1002/esp.257

Arrillaga, J. A., Yagüe, C., Sastre, M., & Román-Cascón, C. (2016). A characterisation of sea-breeze events in the eastern Cantabrian coast (Spain) from observational data and WRF simulations. *Atmospheric Research*, *181*, 265–280. https://doi.org/10.1016/j.atmosres.2016.06.021

Baker, A. C. (1991). *Tidal Power*. Stevenage: Peter Peregrinus Ltd.

Bauer, B. O., & Davidson-Arnott, R. G. D. (2003). A general framework for modeling sediment supply to coastal dunes including wind angle, beach geometry, and fetch effects. *Geomorphology*, *49*(1), 89–108. https://doi.org/10.1016/S0169-555X(02)00165-4

Bertin, X., Chaumillon, E., Weber, N., & Tesson, M. (2004). Morphological evolution and time-varying bedrock control of main channel at a mixed energy tidal inlet: Maumusson Inlet, France. *Marine Geology*, *204*(1–2), 187–202. https://doi.org/10.1016/S0025-3227(03)00353-0

Bird, E. C. F. (2010). West Africa. In *Encyclopedia of the World's Coastal Landforms* (1st ed., pp. 915–974). Springer. https://doi.org/10.1007/978-1-4020-8640-3

Ceia, F. R., Patrício, J., Marques, J. C., & Dias, J. A. (2010). Coastal vulnerability in barrier islands: The high risk areas of the Ria Formosa (Portugal) system. *Ocean and Coastal Management*, *53*(8), 478–486. https://doi.org/10.1016/j.ocecoaman.2010.06.004

Channel Coastal Observatory. (2016). Dawlish Statistics. Retrieved March 6, 2017, from http://www.channelcoast.org/data_management/real_time_data/charts/?chart=103&tab=stats&disp_option=&data_type=table&year=All years

Charles, E., Idier, D., Thiébot, J., Cozannet, G. Le, Pedreros, R., Ardhuin, F., & Planton, S. (2012). Present wave climate in the Bay of Biscay: Spatiotemporal variability and trends from 1958 to 2001. *Journal of Climate*, *25*(6), 2020–2039. https://doi.org/10.1175/JCLI-D-11-00086.1

Cleveringa, J., Israël, C. G., & Dunsbergen, D. W. (2005). *De westkust van Ameland; Resultaten van 10 jaar morfologisch onderzoek in het kader van de Rijkswaterstaat programma's KUST2000 en KUST2005.* https://doi.org/Rapport RIKZ/2005.029

Costa, M., Silva, R., & Vitorino, J. (2001). Contribuição Para O Estudo Do Clima De Agitação Marítima Na Costa Portuguesa. *2as Jornadas Portuguesas de Engenharia Costeira E Portuária - Associação Internacional de Navegação*, (October 2001), 20.

D'Alessandro, F., & Tomasicchio, G. R. (2016). Wave-dune interaction and beach resilience in large-scale physical model tests. *Coastal Engineering*, *116*, 15–25. https://doi.org/10.1016/j.coastaleng.2016.06.002

Davidson-Arnott, R. G. D. (2009). *Introduction to Coastal Processes & Geomorphology*. *Journal of Coastal Research* (1st ed., Vol. 226). Cambridge: Cambridge University Press. https://doi.org/10.2112/1551-5036(2006)22[1589:BR]2.0.CO;2

Davies, J. L. (1964). A Morphogenec Approach to World Shorelines. *Zeitschrift Für Geomorphologie*, *8*, 127–142.

Davis, J. C. (2002). *Statistics and Data Analysis in Geology* (3rd ed.). Wiley.

Davis, R. A., & Hayes, M. O. (1984). What is a Wave-Dominated Coast? *Marine Geology*, *60*(C), 313–329. https://doi.org/10.1016/S0070-4571(08)70152-3

de Ferranti, J. (2017). Elevation Data. Retrieved March 9, 2017, from http://viewfinderpanoramas.org/Coverage map viewfinderpanoramas_org3.htm

de Swart, H. E., & Zimmerman, J. T. F. (2009). Morphodynamics of Tidal Inlet Systems. *Annual Review of Fluid Mechanics*, *41*, 203–229. https://doi.org/10.1146/annurev.fluid.010908.165159

Doody, J. P. (2005). Sand dune inventory of Europe. *Proceedings Dunes and Estuaries International Conference on Nature Restoration Practices in European Coastal Habitats*, (OCTOBER 2005), 45–54.

Dronkers, J. (2016). *Dynamics of coastal systems* (2nd ed.). World Scientific.

Durán, O., Claudin, P., & Andreotti, B. (2011). On aeolian transport: Grain-scale interactions, dynamical mechanisms and scaling laws. *Aeolian Research*, *3*(3), 243–270. https://doi.org/10.1016/j.aeolia.2011.07.006

Dyer, K. R., & Huntley, D. A. (1999). The origin, classification and modelling of sand banks and ridges. *Continental Shelf Research*, *19*(10), 1285–1330. https://doi.org/10.1016/S0278-4343(99)00028-X

Elias, E. P. L. (2006). *Morphodynamics of Texel Inlet*. IOS Press. Retrieved from https://books.google.nl/books?id=bN-fpZrBgtAC&pg=PA54&lpg=PA54&dq=mean+wave+height+Texel&source=bl&ots=xWpp9yynij&sig=xIyJs8IGV5BwYyfufhKFtqSxRF0&hl=nl&sa=X&ved=0ahUKEwjp4ZrJo_HRAhUEaxQKHWbLD_oQ6AEIHzAA#v=onepage&q=mean wave height Texel&f=false

Fiechter, J., Steffen, K. L., Mooers, C. N. K., & Haus, B. K. (2006). Hydrodynamics and sediment transport in a southeast Florida tidal inlet. *Estuarine, Coastal and Shelf Science*, *70*(1–2), 297–306. https://doi.org/10.1016/j.ecss.2006.06.021

FINO1. (2017). Significant wave height and wave direction 2014-2016. Federal Ministry for Economic Affairs and Energy (BMWi), Project Executing Organisation (PTJ).

FitzGerald, D. M. (1996). Geomorphic Variability and Morphologic and Sedimentologic Controls on Tidal Inlets. *Journal of Coastal Research*, (23), 47–71. https://doi.org/10.2307/25736068

Fitzgerald, D. M., Penland, S., & Nummedal, D. (1984). Control of barrier island shape by inlet sediment bypassing: East Frisian Islands, West Germany. *Marine Geology*, *60*(1–4), 355–376. https://doi.org/10.1016/0025-3227(84)90157-9

Forbes, D. L., & Hansom, J. D. (2011). Polar Coasts. In *Treatise on Estuarine and Coastal Science* (pp. 245–283). https://doi.org/10.1016/B978-0-12-374711-2.00312-0

Frost, J. (2014). How High Should R-squared Be in Regression Analysis? Retrieved May 2, 2017, from http://blog.minitab.com/blog/adventures-in-statistics-2/how-high-should-r-squared-be-in-regression-analysis

Gonçalves, C., Brogueira, M. J., & Nogueira, M. (2015). Tidal and spatial variability of nitrous oxide in Sado estuary (Portugal). *Estuarine, Coastal and Shelf Science*, *167*(2), 466–474. https://doi.org/10.1016/j.ecss.2015.10.028

Grasmeijer, B., & Pasmans, I. (2013). *Hydromorfologie Eems-Dollard estuarium; Achtergrondstudie t.b.v. OTB MER vaarweg Eemshaven*. Emmeloord. Retrieved from http://www.platformparticipatie.nl/Images/12. Bijlage J hydromorfologisch onderzoek_tcm318-354310.pdf

Gulev, S. K., Grigorieva, V., & Sterl, A. (2006). *Global Atlas of Ocean Waves*. Moscow. Retrieved from http://www.sail.msk.ru/atlas/

Hayes, M. O., & FitzGerald, D. M. (2013). Origin, Evolution and Classification of Tidal Inlets. *Journal of Coastal Research*, (69), 14–33. https://doi.org/10.2112/SI

Hesp, P. A. (2002). Foredunes and blowouts: initiation, geomorphology and dynamics. *Geomorphology*, *48*(1–3), 245–268. https://doi.org/10.1016/S0169-555X(02)00184-8

Hesp, P. A. (2008). Coastal Dunes in the Tropics and Temperate regions: Location, Formation, Morphology and Vegetation Processes. In *Coastal Dunes* (pp. 29–49). https://doi.org/10.1016/B978-0-12-374739-6.00310-9

Hesp, P. A. (2012a). *Dune Coasts*. *Treatise on Estuarine and Coastal Science* (Vol. 3). Elsevier Inc. https://doi.org/10.1016/B978-0-12-374711-2.00310-7

Hesp, P. A. (2012b). Surfzone-beach-dune interactions. *NCK-Days 2012 : Crossing Borders in Coastal Research : Jubilee Conference Proceedings*, 35–40. https://doi.org/10.3990/2.168

Houser, C., & Ellis, J. (2013). Beach and Dune Interaction. *Treatise on Geomorphology*, *10*, 267–288.

Houser, C., Hapke, C., & Hamilton, S. (2008). Controls on coastal dune morphology, shoreline erosion and barrier island response to extreme storms. *Geomorphology*, *100*(3), 223–240. https://doi.org/10.1016/j.geomorph.2007.12.007

INMET. (2017). Estações Convencionais. Retrieved April 10, 2017, from http://www.inmet.gov.br/portal/index.php?r=estacoes/estacoesConvencionais

ISO. (2011). *ISO 3166-1*. Geneva, Switzerland.

Keijsers, J. G. S., De Groot, A. V., & Riksen, M. J. P. M. (2015). Vegetation and sedimentation on coastal foredunes. *Geomorphology*, *228*, 723–734. https://doi.org/10.1016/j.geomorph.2014.10.027

Kidson, C. (1964). Dawlish Warren, Devon: Late stages in sand spit evolution. *Proceedings of the Geologists' Association*, *75*(2), 167–184. https://doi.org/10.1016/S0016-7878(64)80003-1

KNMI. (2011). *Klimaattabel De Kooy*. *Klimaatatlas*. De Bilt. Retrieved from http://www.klimaatatlas.nl/tabel/stationsdata/klimtab_8110_210.pdf

Lawson, J. (1709). *A New Voyage to Carolina; Containing the Exact Description and Natural History of That Country: Together with the Present State Thereof. And A Journal of a Thousand Miles, Travel'd Thro' Several Nations of Indians. Giving a Particular Account of Their Cus*. London.

Leatherman, S. P. (1985). Geomorphic and stratigraphic analysis of Fire Island, New York. *Marine Geology*, *63*, 173–195.

Lessa, G. C., Angulo, R. J., Giannini, P. C., & Araújo, A. D. (2000). Stratigraphy and Holocene evolution of a regressive barrier in south Brazil. *Marine Geology*, *165*(1–4), 87–108. https://doi.org/10.1016/S0025-3227(99)00130-9

Levin, N., Jablon, P.-E., Phinn, S., & Collins, K. (2017). Coastal dune activity and foredune formation on Moreton Island, Australia, 1944–2015. *Aeolian Research*, *25*, 107–121. https://doi.org/10.1016/j.aeolia.2017.03.005

Loureiro, E., Granja, H., & Pinho, J. L. S. (2005). Morphodynamics of the Cávado Estuary Inlet (NW Portugal). In *International Coastal Symposium*. Braga.

Matias, A., Ferreira, Ó., Vila-Concejo, A., Garcia, T., & Dias, J. A. (2008). Classification of washover dynamics in barrier islands. *Geomorphology*, *97*(3–4), 655–674. https://doi.org/10.1016/j.geomorph.2007.09.010

Maun, M. A. (2004). Burial of Plants as a Selective Force in Sand Dunes. In M. L. Martínez & N. P. Psuty (Eds.), *Coastal Dunes: Ecology and Conservation* (pp. 119–135). Berlin, Heidelberg: Springer Berlin Heidelberg. https://doi.org/10.1007/978-3-540-74002-5_8

Maun, M. A., & Lapierre, J. (1984). The Effects of Burial by Sand on Ammophila Breviligulata. *Journal of Ecology*, *72*(3), 827–839. Retrieved from http://www.jstor.org/stable/2259534

Mccauley, E., & Tomlinson, R. (2006). *The evolution of Jumpinpin Inlet*. Indooroopilly Qld. Retrieved from http://www.ozcoasts.gov.au/pdf/CRC/62-jumpinpin.pdf

Met Office. (2015). How we measure cloud amount. Retrieved June 21, 2017, from http://www.metoffice.gov.uk/guide/weather/observations-guide/how-we-measure-cloud

Met Office. (2016). Beaufort Scale. Retrieved April 4, 2017, from http://www.metoffice.gov.uk/guide/weather/marine/beaufort-scale#

Morales, J. A., Borrego, J., Jiménez, I., Monterde, J., & Gil, N. (2001). Morphostratigraphy of an ebb-tidal delta system associated with a large spit in the Piedras Estuary mouth (Huelva Coast, Southwestern Spain). *Marine Geology*, *172*(3–4), 225–241. https://doi.org/10.1016/S0025-3227(00)00135-3

Morales, J. A., Delgado, I., & Gutiérrez-Mas, J. M. (2015). Bedform variability and flow regime in a barrier-inlet system. *Geologica Acta*, *13*(2), 137–153. https://doi.org/10.1344/GeologicaActa2015.13.2.5

NCEI. (2016). Global DEM Mosaic. Retrieved March 15, 2017, from http://noaa.maps.arcgis.com/home/item.html?id=c876e3c96a8642ab8557646a3b4fa0ff

NDBC. (2013). Bouy Data Summaries. National Oceanic and Amospheric Administration.

NOAA. (2013). Tidal Datums. *Tides and Currents*. National Oceanic and Amospheric Administration. Retrieved from https://tidesandcurrents.noaa.gov/stations.html?type=Datums

Peel, M. C., Finlayson, B. L., & McMahon, T. A. (2007). Updated world map of the Köppen-Geiger climate classification. *Hydrology and Earth System Sciences*, *4*, 439–473. https://doi.org/10.1127/0941-2948/2006/0130

Pentcheff, D. (2010). WWW Tide/Current Predictor. Retrieved from http://tbone.biol.sc.edu/tide/

Pianca, C., Mazzini, P. L. F., & Siegle, E. (2010). Brazilian offshore wave climate based on

NWW3 reanalysis. *Brazilian Journal of Oceanography*, *58*(1), 53–70. https://doi.org/10.1590/S1679-87592010000100006

Pilkey Jr., O. H., Neal, W. J., Monteiro, J. H., & Dias, J. A. (1989). Algarve Barrier Islands : A Noncoastal-Plain System in Portugal. *Journal of Coastal Research*, *5*(2), 239–261.

Pratt, J. W. (1987). Dividing the indivisible: using simple symmetry to partition variance explained. In T. Pukkila & S. Puntanen (Eds.), *Proceedings of the Second International Conference in Statistics* (pp. 245–260). Tampere, Finland: University of Tampere.

Rebelo, L. P., Ferraz, M., & Brito, P. O. (2009). Troia Peninsula Evolution: The Dune Morphology Record. *Journal of Coastal Research*, *2009*(56), 352–355. https://doi.org/10.2307/25737596

Reed, D. J., Davidson-Arnott, R. G. D., & Perillo, G. M. E. (2009). Estuaries, coastal marshes, tidal flats and coastal dunes. *Geomorphology and Global Environmental Change*, *30*(3), 130–157. https://doi.org/10.1017/CBO9780511627057.006

Ridderinkhof, W., de Swart, H. E., van der Vegt, M., & Hoekstra, P. (2016). Cyclic behavior of sandy shoals on the ebb-tidal deltas of the Wadden Sea. *Continental Shelf Research*, *115*, 14–26. https://doi.org/10.1002/2016JF003823

Riggs, S. R., & Ames, D. V. (2009). *Impact of the Oregon Inlet Terminal Groin on Downstream Beaches of Pea Island, NC Outer Banks*.

RWS. (2017). Watergegevens. Retrieved March 8, 2017, from www.watergegevens.rws.nl

Sawakuchi, A. O., Kalchgruber, R., Giannini, P. C. F., Nascimento, D. R., Guedes, C. C. F., & Umisedo, N. K. (2008). The development of blowouts and foredunes in the Ilha Comprida barrier (Southeastern Brazil): the influence of Late Holocene climate changes on coastal sedimentation. *Quaternary Science Reviews*, *27*(21–22), 2076–2090. https://doi.org/10.1016/j.quascirev.2008.08.020

SCOPAC. (2003). *Holcombe to Straight Point (including Exe estuary)*. *Sediment Transport Study*.

Sedigh, M., Tomlinson, R., Cartwright, N., & Etemad-Shahidi, A. (2016). Numerical modelling of the Gold Coast Seaway area hydrodynamics and littoral drift. *Ocean Engineering*, *121*, 47–61. https://doi.org/10.1016/j.oceaneng.2016.05.002

Sha, L. P. (1989). Variation in ebb-delta morphologies along the West and East Frisian Islands, The Netherlands and Germany. *Marine Geology*, *89*(1–2), 11–28. https://doi.org/10.1016/0025-3227(89)90025-X

Shand, T., & Carley, J. (2011). Long-term trends in NSW coastal wave climate and derivation of extreme design storms. *NSW Coastal …*, *2*(Figure 1), 1–12. Retrieved from http://www.coastalconference.com/2011/papers2011/Tom Shand Full Paper.pdf

Sherman, D. J., & Bauer, B. O. (1993). Dynamics of beach-dune systems. *Progress in Physical Geography*, *17*(4). https://doi.org/10.1177/030913339301700402

Short, A. D., & Hesp, P. A. (1982). Wave, beach and dune interations in Southeastern Australia. *Marine Geology*, *48*(1982), 259–284.

Shuttleworth, B., Woidt, A., Paparella, T., Herbig, S., & Walker, D. (2005). The dynamic behaviour of a river-dominated tidal inlet, River Murray, Australia. *Estuarine, Coastal and Shelf Science*, *64*(4), 645–657. https://doi.org/10.1016/j.ecss.2005.04.007

The Open University. (1999a). Beaches. In *Waves, Tides and Shallow Water Processes* (2nd ed., pp. 125–148). Oxford: Butterworth-Heinemann.

The Open University. (1999b). Tides. In *Waves, Tides and Shallow Water Processes* (2nd ed., pp. 50–86). Oxford: Butterworth-Heinemann.

The Open University. (1999c). Waves. In *Waves, Tides and Shallow Water Processes* (2nd ed., pp. 11–49). Oxford: Butterworth-Heinemann.

USACE. (2014). Chincoteague Inlet Federal Navigation Project. Retrieved March 23, 2017, from http://www.nao.usace.army.mil/About/Projects/ChincoteagueNav.aspx

Vallés, S. M., Gallego Fernández, J. B., & Dellafiore, C. M. (2011). Dune Vulnerability in Relation to Tourism Pressure in Central Gulf of Cádiz (SW Spain), a Case study. *Journal of Coastal Research*, *272*(2), 243–251. https://doi.org/10.2112/JCOASTRES-D-09-00125.1

Van der Kooij, A. J. (2007). *Appendices A_B_C_References*. *Predition Accuracy and Stability of Regression with Optimal Scaling Transformations*. Leiden University, Leiden. Retrieved from https://openaccess.leidenuniv.nl/handle/1887/12096

van Heteren, S., Oost, A. P., van der Spek, A. J. F., & Elias, E. P. L. (2006). Island-terminus evolution related to changing ebb-tidal-delta configuration: Texel, The Netherlands. *Marine Geology*, *235*(1–4), 19–33. https://doi.org/10.1016/j.margeo.2006.10.002

Wang, P., & Beck, T. M. (2012). Morphodynamics of an anthropogenically altered dual-inlet system: John's Pass and Blind Pass, west-central Florida, USA. *Marine Geology*, *291–294*, 162–175. https://doi.org/10.1016/j.margeo.2011.06.001

WaveWatch III. (2017). WaveWatch III hindcast 2014-2016. National Oceanic and Amospheric Administration. Retrieved from ftp://polar.ncep.noaa.gov/pub/history/waves/multi_1/

Windfinder. (2017). Statistieken. Retrieved March 6, 2017, from https://www.windfinder.com/

Xu, Z., Mason, J. A., & Lu, H. (2015). Vegetated dune morphodynamics during recent stabilization of the Mu Us dune field, north-central China. *Geomorphology*, *228*, 486–503. https://doi.org/10.1016/j.geomorph.2014.10.001

Appendices

A. Study area

RUSSIA
MONGOLIA
CHINA
KAZAKHSTAN
INDIA
IRAN
IRAQ
SAUDI ARABIA
TURKEY
UKRAINE
POLAND
ITALY
EGYPT
LIBYA
SUDAN
CHAD
ALGERIA
NIGER
MALI
ZAMBIA
NAMIBIA
INDONESIA
AUSTRALIA
GREENLAND (DENMARK)
CANADA
UNITED STATES OF AMERICA
MEXICO
ALASKA (USA)
BRAZIL
BOLIVIA
PERU
COLOMBIA
ARGENTINA

B. Reference images vegetation cover

0/8

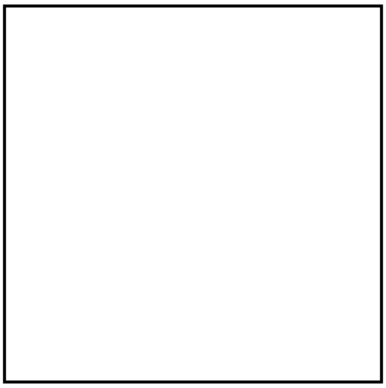

1/8

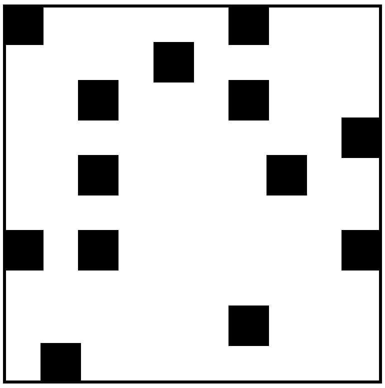

2/8

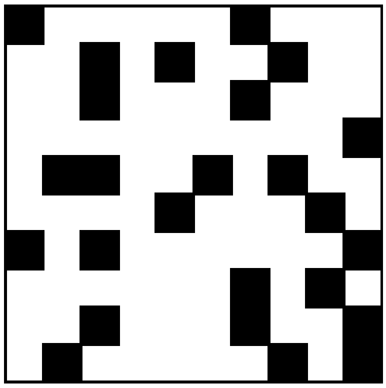

3/8

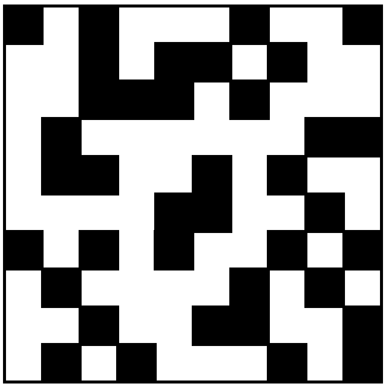

4/8

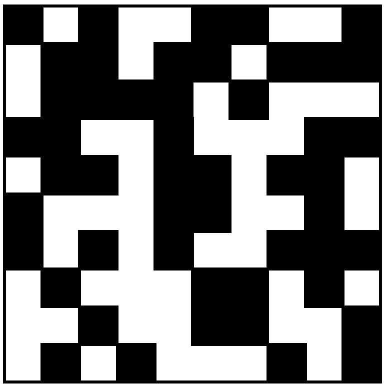

5/8

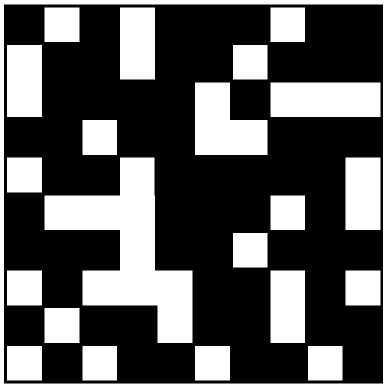

6/8

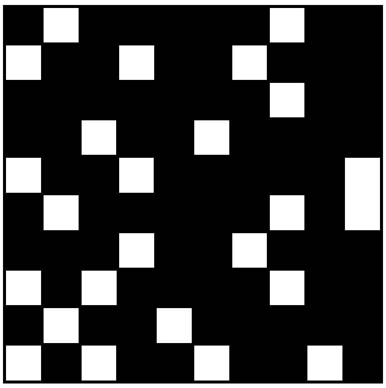

7/8

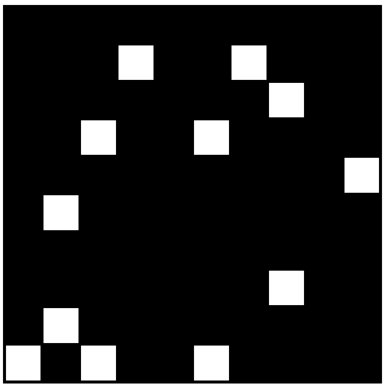

8/8

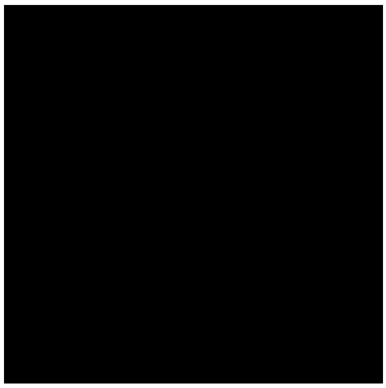

C. Global overview of selected inlets

ID	Country[1]	Inlet Name	ID	Country[1]	Inlet Name
1	NL	Texel Inlet	17	US	Fire Island Inlet
2		Eierlandse Gat	18		Little Egg Inlet
3		Vlie Inlet	19		Brigantine Inlet
4		Ameland Inlet	20		Chincoteague Inlet
5		Frisian Inlet	21		Oregon Inlet
6		Eems-Dollard Inlet	22		Ocracoke Inlet
7	DE	Osterems	23		New Topsail Inlet
8		Norderneyer Seegat	24		North Inlet
9	DK	Listerdyb	25		Matanzas Inlet
10		Graadyb	26		Big Carlos Pass
11	GB	Exmouth Inlet	27		Hurricane Pass
12	FR	Maumusson Inlet	28		Pensacola Pass
13	PT	Cávado Estuary Inlet	29		Pelican Inlet
14		Sado River Inlet	30		Netarts Bay Inlet
15		Armona Inlet	31		Tomales Bay Inlet
16	ES	Piedras River Mouth	32		Pajaro River Mouth
33	BR	Galinhos Inlet			
34		Barra das Canavieiras			
35		Barra das Barra Velha			
36		Itaúnas River Mouth			
37		Icapara Inlet			
38		Ararapira Channel			
39		Ibiraquera Channel			
40	AU	Shallow Inlet			
41		Murray Mouth			
42		Jumpinpin Channel			
43	CG	Conkouati			
44	AO	Lagoa Massabi Inlet			
45	SA	Breede River Mouth			

[1] Country codes are the Alpha-2 codes according to ISO3166-1 (ISO, 2011)

D. Characterization

All selected inlets were characterized based on a few selected variables. For all inlets the most recent aerial photograph is given. Almost all of them have a few black lines and outlined polygons in them to indicate the development of the dune system. Some of them also have an outlined polygon to show the sector where the vegetation cover is determined. The legend for those figures is given in Table 17. The caption below the figures gives the location and the years for which the seaward boundary of the dune system is presented.

Table 17: legend for the figures shown at the characterization of the inlets

8pt black line		Seaward boundary of dune system
Outlined polygon with 5pt black line		Sector where the vegetation cover is determined

Europe

On the European coast a total of 26 inlets was assessed. Some inlets were on a rocky coast or in heavily urbanized areas, so sixteen inlets are selected for further research. From the sixteen selected inlet systems in Europe, ten are inlets connecting the Wadden Sea to the North Sea. These inlets are situated in The Netherlands, Germany and Denmark (Table 18). Also inlets from England, France, Portugal and Spain were selected (Figure 16). The Wadden Sea region experiences a temperate climate without a dry season and a mild summer, thus it is class Cfb according to the Köppen-Geiger climate scale. The climate along the Atlantic coast varies from a temperate climate without a dry season (Cfb) on the British Isles and in France to a temperate climate with a dry season and a hot summer (Csa) in the southern part of Spain and Portugal.

Table 18: Inlets in Europe

Country	Inlet name	Country	Inlet name
The Netherlands	Texel Inlet	Denmark	Listerdyb
	Eierlandse Gat		Graadyb
	Vlie Inlet	England	Exmouth Inlet
	Amelander Inlet	France	Maumusson Inlet
	Frisian Inlet	Portugal	Cávado Estuary Inlet
	Eems-Dollard Inlet		Sado River Inlet
Germany	Osterems		Armona Inlet
	Norderneyer Seegat	Spain	Piedras River Mouth

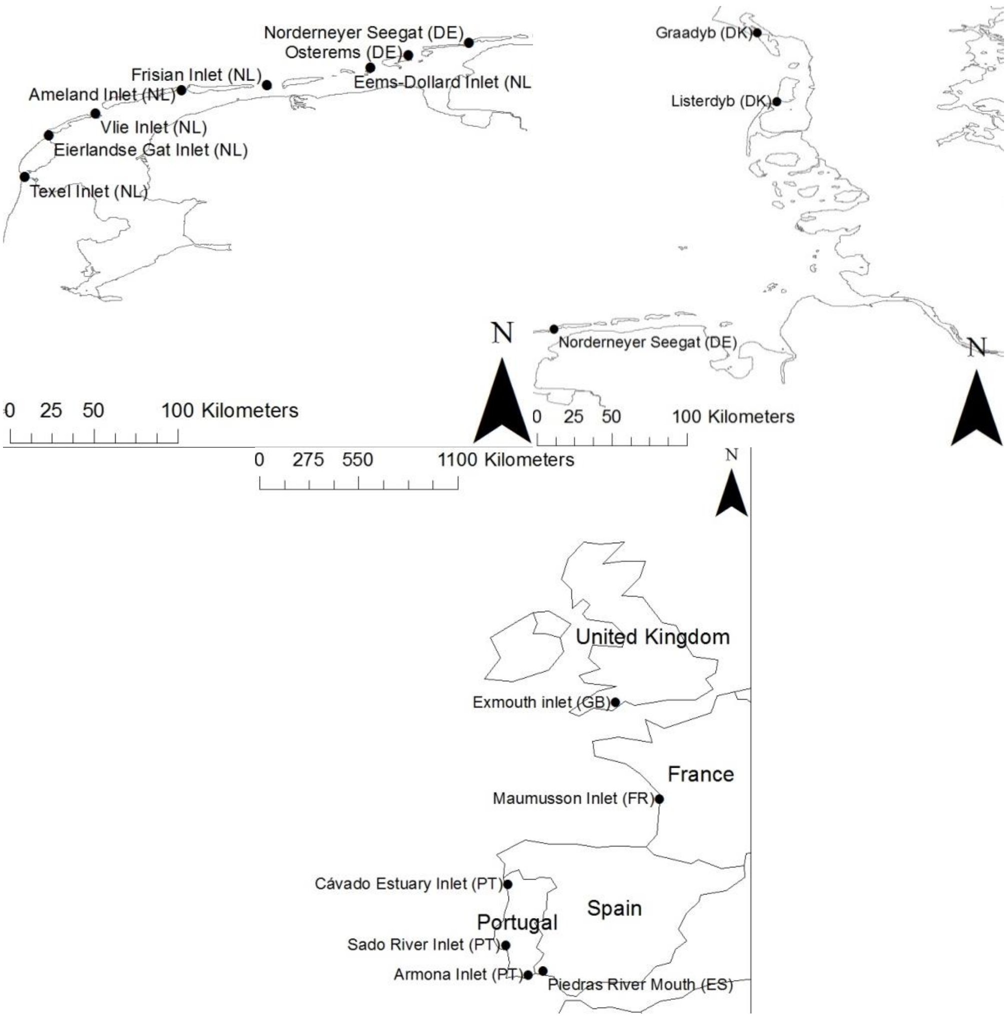

Figure 16: selected tidal inlet systems in the Wadden Sea region (upper) and on the Atlantic coast (lower)

Wadden coast

The Wadden area extents from Den Helder in the northwest of the Netherlands to Esbjerg in Denmark. The area consists of a row of barrier islands which shield the Wadden Sea from the North Sea. Sha (1989) states that the wave climate along the Frisian Islands is more or less constant, but this assumption is not used in this research. This is done because there is better data available from multiple measuring buoys and platforms in the North Sea (e.g. FINO 1). All inlets are assumed to be on a fixed position, because Fitzgerald, Penland, & Nummedal (1984) state that the movement of barrier islands in the Wadden Sea is done by inlet narrowing rather than inlet allocation. The net current along the Wadden islands is from the southwest to the east (Sha, 1989).

Texel Inlet

Texel Inlet is the most western and biggest inlet that connects the Dutch Wadden Sea with the North Sea. It is located between the city of Den Helder and the biggest Dutch Wadden Island, Texel. Between the island and the mainland there is one channel, namely the Marsdiep. The channel bifurcates on both ends into multiple smaller channels that continuously change configuration (van Heteren et al., 2006). The inlet has a tidal range of 1.4 meter, which in combination with a mean significant wave height of 1.3 m means that the inlet qualifies as mixed energy. The mean wave direction is 245°N (Elias, 2006). Under natural circumstances the inlet wants to migrate to the south, but the southern coastline is fixed by a seawall, so the inlet stays on a fixed position (van Heteren et al., 2006).

Coastal dunes with heights up to 15 meters are present on the southern part of Texel. The dune system is expanding as a result of shoal mergers, mainly the Hors, that led to a large sand flat at the southern tip of the island. The sand is blown towards the backshore and captured by pioneer vegetation (van Heteren et al., 2006). The vegetation cover is estimated as 2/8. If the dune is stabilized and cut off from the sediment supply by a new dune ridge, the dunes become fully vegetated (van Heteren et al., 2006). The prevailing wind direction and wind speed at Texel Inlet is assumed the same as on De Kooy Naval Air Station (NAS) in Den Helder, because the NAS is located only 6 kilometres from Texel Inlet. According to KNMI (2011) the prevailing wind direction at this location is 240°N with a mean wind speed of 5.8 m/s.

Figure 17: South shore of Texel on the downdrift side of Texel Inlet (1984-2016)

Eierlandse Gat

Eierlandse Gat is an inlet between the islands Texel and Vlieland connecting the Wadden Sea to the North Sea. The inlet has two channels, namely Robbengat en Engelsmansgat. The inlet has a tidal range of 1.7 meters (Dronkers, 2016). The waves in the inlet have a mean significant height of 1.3 m and a mean direction of 245°N (Elias, 2006). This means that the inlet is mixed energy according to Davis & Hayes (1984).

Coastal dunes are present on both sides of the inlet. The dunes on the northern part of Texel are called the Eierland Dunes and they can reach heights up to 20 meters. The dunes on Vlieland are not that high with maximum heights up to 17 meters (AHN, 2017). The vegetation cover on the first dune ridge on Texel is estimated to be 3/8. The dunes on the Vliehors have a vegetation cover of 7/8. The dunes on Texel show almost no expansion, but the dunes on Vlieland do expand in southwest direction. Especially some patches on the Vliehors showed growth in the period from 1984 until 2016. Wind characteristics are assumed to be equal to the wind characteristics at the Vliehors weather station at Vlieland, which shows a prevailing wind direction of 225°N and a mean wind speed of 8 m/s (Windfinder, 2017).

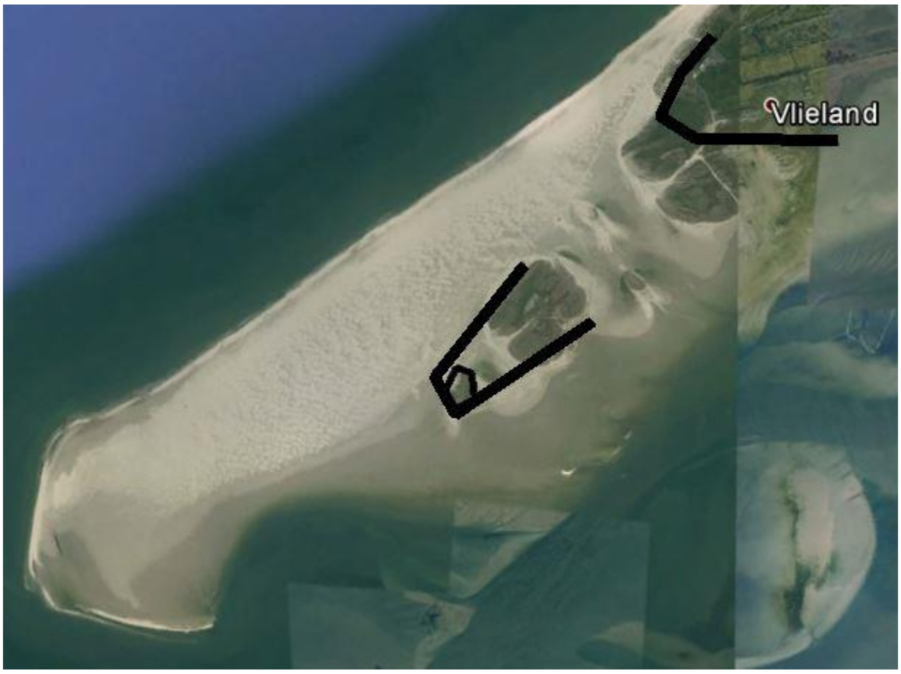

Figure 18: Southwest side of Vlieland at the downdrift side of the Eierlandse Gat Inlet (1984-2016)

Vlie Inlet

Vlie Inlet is the inlet between Vlieland and Terschelling connecting the Wadden Sea to the North Sea. The inlet has two channels, Vliestroom and Schuitengat, with the first being the main channel. The inlet experiences a tidal range of 1.9 meters (Dronkers, 2016). Measurement data from buoy Stortemelk Oost in the Vlie Inlet shows a mean significant wave height of 0.7 m and a mean wave direction of 270°N (RWS, 2017). This which means that the inlet is mixed energy according to Davis & Hayes (1984).

Coastal dunes are present on Vlieland and Terschelling. The dunes at the northern tip of Vlieland reach a maximum height of 23 meters, while some dunes at the southwest tip of Terschelling reach a height of 30 meters (AHN, 2017). The dune system at the eastside of Vlieland remains on a fixed position, while the dune system on the western side of Terschelling shows some retreat. There is pioneer vegetation visible on the first dune ridge on both islands, so the vegetation cover is 1/8. The largest dunes are fully vegetated. Wind characteristics are assumed to be equal to the wind characteristics at the Vliehors weather station at Vlieland, which shows a prevailing wind direction of 225°N and a mean wind speed of 8 m/s (Windfinder, 2017).

Figure 19: The southwest coast of Terschelling at the downdrift side of Vlie (1984-2016)

Ameland Inlet

Ameland Inlet is the inlet between Terschelling and Ameland connecting the Wadden Sea to the North Sea. At this moment the inlet has two channels, but Cleveringa, Israël, & Dunsbergen (2005) state that the inlet changes from one channel to two channels and back within a period of 50-60 years. The inlet has a tidal range of 2.1 m (Dronkers, 2016). Data from buoy 12 in the Ameland Inlet shows a mean significant wave height of 1.2 m (RWS, 2017). The inlet is thus mixed energy according to the graph proposed by Davis & Hayes (1984). The wave direction at the Vlie Inlet and the Eems-Dollard Inlet are both 270°N, thus this direction is also assumed for Ameland Inlet.

There are dunes on both sides of the Ameland Inlet. On Terschelling it is a dunefield that covers almost the whole eastern side of the island. This dune system is cut through by a series of creeks that flow out into the Wadden Sea. The maximum dune height in this system is 9 meter (AHN, 2017). The dune system is retreating as a result of coastline retreat. The most seaward dunes have a vegetation cover of 1/8, because there is only some pioneer vegetation available. The dunes on Ameland have a width of approximately a kilometre on the seaward side of the inlet which decreases to around 150 m at the landward side of the inlet. The dunes in this system are higher than the dunes at the other side of the inlet, they have a maximum height of 20 m. The dune system is more or less stable and the first dune rows are vegetated with a cover of 5/8. The wind characteristics at the Ameland Inlet are retrieved using the data from the weather station at Hoorn, Terschelling. This station shows a prevailing wind direction of 225°N with a mean wind speed of 7 m/s (Windfinder, 2017).

Figure 20: The northeast coast of Terschelling at the updrift side of Ameland Inlet (1984-2016)

Frisian Inlet

Frisian Inlet is the Inlet between Ameland and Schiermonnikoog and it connects the Wadden Sea with the North Sea. The inlet is a dual-inlet system with a shoal, The Engelsmanplaat, in the middle. The inlet has a tidal range of 2.3 m (Dronkers, 2016) and wave data from the Amelander Westgat Platform shows a mean significant wave height of 0.8 m and a mean wave direction of 270°N (RWS, 2017), which means that the inlet is mixed energy (R. A. Davis & Hayes, 1984).

Coastal dunes are present on both Ameland and Schiermonnikoog. Satellite imagery shows expansion of the dune systems on both islands. The vegetation cover on Ameland is 4/8, while the dunes at Schiermonnikoog are fully vegetated (8/8). There is even vegetation on the beach in front of the dune system. The dunes at the western side of Ameland reach heights up to 8 m, while there are dunes at the eastern part of Schiermonnikoog have heights up to 20 m (AHN, 2017). Data from Ameland Platform/Wierumergronden gives a prevailing wind direction of 202°N and a mean wind speed of 8 m/s (Windfinder, 2017).

Figure 21: Updrift (upper) and downdrift (lower) side of Frisian Inlet (1984-2016)

Eems-Dollard Inlet

The Eems-Dollard Inlet is part of the estuary of the Eems. The inlet is located between the German island Borkum and the Dutch island Rottumeroog. According to Grasmeijer & Pasmans (2013) the inlet experiences an tidal range of 2.15 m with an mean significant wave height of 1.1 m coming from the west (270°N). This means that the inlet is mixed energy (R. A. Davis & Hayes, 1984). The inlet consist of one channel (Westereems). The channels within the inlet and the estuary do migrate, but this has no influence on the location of the system as a whole (Grasmeijer & Pasmans, 2013).

Small dunes can be found in the retreating dune system on Rottumeroog, but they only reach a height of about 4 m. The dunes are largely vegetated (7/8). The dunes on Borkum can reach a height of 13 m (de Ferranti, 2017). Most dune development is on the seaward side of the island and aerial photographs show expansion of the dune system towards the north. The first dune ridge sparsely vegetated (1/8), which can indicate active dune development. According to Windfinder (2017) the mean wind speed at Huibertgat, just seaward of the inlet, is 8 m/s and the prevailing wind direction is 202°N.

Figure 22: Eems-Dollard Inlet (1984-2016)

Osterems

The Osterems is the northeast part of the Eems estuary. The inlet divides the German Wadden islands Borkum and Memmert. The inlet has one channel which is also called the Osterems. The inlet experiences a tidal range of 2.15 m and waves with a mean significant height of 1.1 m come in from a direction of 270°N (Grasmeijer & Pasmans, 2013). This means that the inlet is mixed energy (R. A. Davis & Hayes, 1984).

There are dunes present on Memmert and Borkum. The dunes at Memmert only reach a height of 4 m, while the dunes at the western part of Borkum are up to 11 m high. The dune system on Borkum is expanding. The dune system on Memmert is retreating as a result of movement of the whole island. Pioneer vegetation is present on the beach and the first dune ridge at Borkum, thus the vegetation cover is 1/8. The dunes at Memmert are almost fully vegetated (7/8). Data from the airport at Borkum shows a prevailing wind direction of 202°N with a mean wind speed of 6 m/s (Windfinder, 2017).

Figure 23: Osterems (1984-2016).

Norderneyer Seegat

The Norderneyer Seegat connects the Wadden Sea and the North Sea between the German Wadden Islands Juist and Norderney. The inlet has two channels, a tidal range of 2.4 m and an annual mean significant wave height of 1.6 m (Fitzgerald et al., 1984). Data from the FINO1 (2017) shows a mean wave direction of 245°N. The Norderneyer Seegat is mixed energy according to the graph presented by Davis & Hayes (1984).

Dunes are not present on the western part of Norderney. This part of the island is urbanized and the shoreline is fixed and protected by hard structures. The dune system on the western part of Juist shows expansion. Dunes in this dune system have a maximum height of 19 m. The foredunes are almost half vegetated (3/8). The prevailing wind direction is 225°N with a mean wind speed of 7 m/s according to the measuring station at Juist airport (Windfinder, 2017).

Figure 24: the northeastern shore of Juist at the downdrift side of the Norderneyer Seegat (1984-2016)

Listerdyb

Listerdyb is the tidal inlet that divides the German island Sylt and the Danish island Rømø. The inlet has a tidal range of 1.8 m (Dronkers, 2016). Hindcast data from WaveWatch III (2017) shows a mean significant wave height of 1.3 m and a mean wave direction of 238°N. The inlet is thus mixed energy (R. A. Davis & Hayes, 1984). The inlet has one tidal channel and it stays on a fixed position.

There are coastal dune systems present on both sides of the inlet. Both systems are expanding and the maximum observed dune height is 21 m (NCEI, 2016). The first dune ridge on both islands is vegetated by pioneer vegetation with a cover of 1/8. Data from the weather station at List/Ellenbogen shows a mean wind speed of 9 m/s with a mean wind direction of 225°N (Windfinder, 2017).

Figure 25: Listerdyb (1984-2016)

Graadyb

Graadyb is the tidal inlet that divides the Danish island Fanø and the Danish mainland. The inlet has a tidal range of 1.7 m (Dronkers, 2016). Hindcast data from WaveWatch III (2017) shows a mean significant wave height of 1.3 m and a mean wave direction of 238°N. The inlet is thus mixed energy (Davis & Hayes, 1984). The inlet has one tidal channel and it stays on a fixed position.

There are coastal dune systems present on both sides of the inlet. The downdrift system is expanding and the updrift system stays on a fixed position. The maximum observed dune height is 21 m (NCEI, 2016). The first dune ridge on Fanø is vegetated by pioneer vegetation with a cover of 1/8. The vegetation on the mainland has a cover of 2/8. Data from the weather station at Esbjerg Airport shows a mean wind speed of 7 m/s with a mean wind direction of 270°N (Windfinder, 2017).

Figure 26: northwestern shore of Fanø (1984-2016)

Atlantic Coast
The European Atlantic coast stretches from Gibraltar in the South to Norway in the north. For this research the area between Gibraltar and the United Kingdom was assessed.

Exmouth Inlet
Exmouth Inlet is situated between the towns Exmouth and Dawlish Warren in East Devon, England. The inlet forms the mouth of the river Exe and has a single channel. The inlet has a mean tidal range of 2.6 m (SCOPAC, 2003). Mean significant wave height as measured at Dawlish is 0.6 m with a mean direction of 163°N (Channel Coastal Observatory, 2016). Combining the tidal range and the mean significant wave height yields that the inlet is tide-dominated according to the classification of Davis & Hayes (1984). Assessment of aerial photographs from 1945 and 2016 shows no displacement of the inlet, which is logical because the inlet is fixed in his current position by bedrock outcrops (SCOPAC, 2003).

Coastal dunes are present on Dawlish Warren Spit. These dunes are under constant threat of wave attack and much of the historical dune field already disappeared (Kidson, 1964). The dunes that are still present are almost fully vegetated (7/8) as an attempt to stabilize the dunes and to prevent erosion (Kidson, 1964). The maximum dune height is 6 m. The wind climate at Exmouth Inlet can be approximated by the wind climate at the English Lightship in the English Channel. This buoy shows an average wind speed of 8 m/s with a mean direction of 225°N (Windfinder, 2017).

Figure 27: Dawlish Warren Spit (1945-2016)

Maumusson Inlet
Maumusson Inlet is located on the west coast of France and it connects the Atlantic Ocean with the Marennes-Oléron Bay via a single channel. The inlet separates Oléron Island to the north and Arvert Peninsula to the south. The yearly average significant wave height is 1.5 m with the majority of the waves coming from the west and northwest (Bertin, Chaumillon, Weber, & Tesson, 2004). The mean wave direction is approximated by getting the mean wave direction of a wave measuring buoy in the Bay of Biscay. This shows a mean wave direction of 288°N (Charles et al., 2012). The tidal range varies from 2 m to 6 m. The mean tidal range is thus approximated as 4 m. The inlet is tide-dominated according to Davis & Hayes (1984). The adjacent shorelines show some erosion and accretion as stated by Bertin et al. (2004), but overall the inlet remains stable.

Dunes are present on both sides of Maumusson Inlet. The dunes at Oléron Island experience retreat as a result of coastal erosion (Bertin et al., 2004). From aerial photographs it can be seen that the dune system at Avert Peninsula also experiences retreat over the last 32 years, but not as much as on Oléron Island. The maximum height of the dunes at Oléron Island is circa 24 m, while the dunes at the Arvert Peninsula reach up to 55 m in height. The dunes at Oléron Island are largely vegetated, but there are overwash features present. The first dune ridge is only sparsely vegetated (1/8). The first dune row at the Arvert Peninsula is more vegetated (6/8) and does not show overwash features. The prevailing wind direction is 292°N with a speed of 5 m/s according to statistics from the weather station Chassiron/Oléron at the northern tip of Oléron Island (Windfinder, 2017).

Figure 28: Maumusson Inlet (1984-2016)

Cávado Estuary Inlet
Cávado Estuary Inlet is located on the west coast of Portugal near the city Esposende. The inlet connect the Cávado Estuary with the Atlantic ocean. The tidal range is 3.7 m and the mean significant wave height is 2.1 m, which makes the inlet mixed energy (Loureiro, Granja, & Pinho, 2005). The waves are mainly coming in from the east (270°N). Satellite imagery from the years 1984-2016 shows no displacement of the inlet, but the end of the spit is breached during some years. The inlet then temporary has two channels with the southern channel merging with the northern (main) channel after a few years. Therefore, it is assumed that the inlet has a fixed position and one channel.

Coastal dunes can be found on the spit that divides the Cávado Estuary and the ocean. This spit is part of the Northern Littoral Nature Reserve. The dune field shows some expansion in northern direction. The highest dunes can be found on the south end of the sand spit with a maximum height of 21 m (de Ferranti, 2017). The vegetation cover of the northern part of the dune field is circa 1/8. According to Windfinder (2017) the mean annual wind speed is 3 m/s with a prevailing wind direction of 315°N (station Esponende/Rio Cávado).

Figure 29: Cávado Estuary Inlet (1984-2013)

Sado River Mouth

The Sado River Mouth is a tidal inlet that connects the Sado River with the Atlantic Ocean. The inlet experiences a tidal range of 1.1 m (Gonçalves, Brogueira, & Nogueira, 2015). The mean wave height is 2.4 m coming from a mean direction of 225°N (WaveWatch III, 2017). The inlet is thus wave-dominated (R. A. Davis & Hayes, 1984). Satellite images from 1984-2016 show that the inlet stays on a fixed position and has a single channel.

The Sado River and the Atlantic Ocean are partly divided by a sand spit called the Troia Peninsula. An expanding dune system is present on this sand spit (Rebelo, Ferraz, & Brito, 2009). The maximum dune height is 27 m according to Rebelo et al. (2009) and the dunes closest to the inlet have a vegetation cover of 2/8. The mean wind speed is 3 m/s coming from 315°N (Windfinder, 2017).

Figure 30: Sado River Inlet (1984-2016)

Armona Inlet

Armona Inlet is the second largest inlet that connects the Ria Formosa in southern Portugal with the Atlantic Ocean. The inlet is situated between Culatra Island in the south and Armona Island in the north. The mean tidal range is circa 2 m (Matias, Ferreira, Vila-Concejo, Garcia, & Dias, 2008) and the waves are mainly coming from the west-southwest (245°N) with a mean significant wave height of 1.0 m (Costa, Silva, & Vitorino, 2001). According to the graph proposed by Davis & Hayes (1984) this inlet is mixed energy. According to Ceia, Patrício, Marques, & Dias, (2010) the inlet migrates with 20 m/year. The inlet also became narrower during the last decades, but it is believed that it will stay open (Matias et al., 2008).

Both Culatra Island and Armona Island have dunes on them. Overwash is a very important process on those islands. The dunes can reach a maximum height of 9 m (Pilkey Jr., Neal, Monteiro, & Dias, 1989). The dune system on both sides of the inlet are expanding as a result of the narrowing inlet. The most seaward dunes on both sides of the inlet are sparsely vegetated (1/8). The prevailing wind direction is 90°N with a wind speed of 4 m/s as measured at weather station Ilha Deserta (Windfinder, 2017).

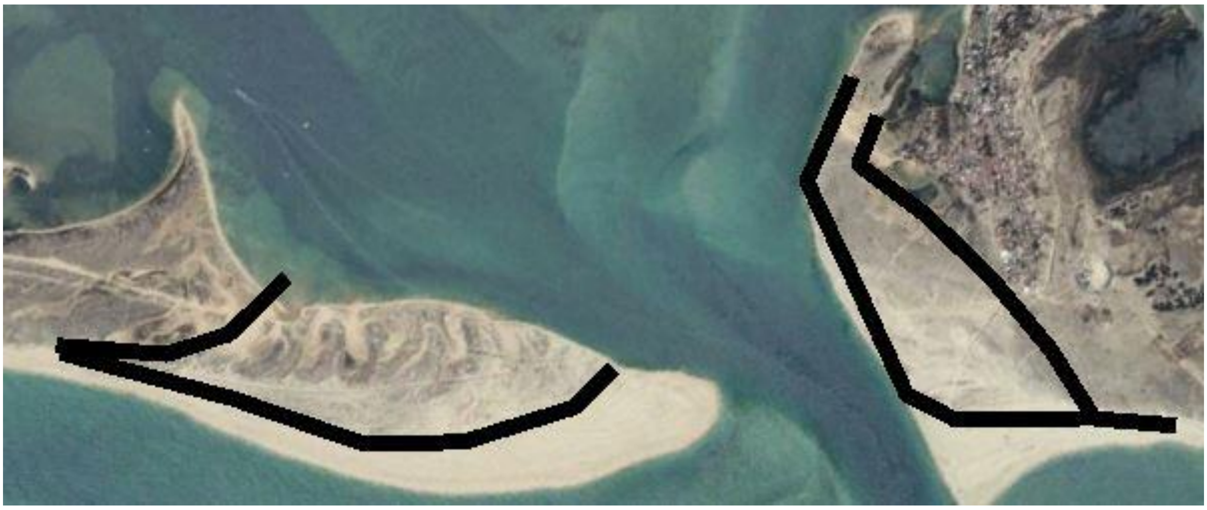

Figure 31: Armona Inlet (1984-2015)

Piedras River Mouth

Piedras River Mouth is an estuary on the Huelva coast in southeast Spain. The mean tidal range is 2.0 m and the prevailing waves have a mean significant wave height of 0.40 m coming from the southwest (235°N). These waves are associated with Atlantic swell (Morales, Borrego, Jiménez, Monterde, & Gil, 2001). Combining the tidal range and the wave height means that the inlet is tide-dominated. The sand spit which forms a barrier between the sea and the mainland grows eastward with 30 m/year (Morales, Delgado, & Gutiérrez-Mas, 2015).

Aeolian dunes are present on the sand spit. These dunes have heights ranging from 2 to 4 m high (Vallés, Gallego Fernández, & Dellafiore, 2011) and the dunes closest to the inlet are sparsely vegetated (1/8). The dune system is expanding as a result of the growth of the spit. The prevailing wind measured at Huelva is from 225°N with a speed of 3 m/s (Windfinder, 2017).

Figure 32: Piedras River Mouth (1984-2016)

United States

In total 51 inlets were examined along the coast of the United States. 37 (73%) of those inlets were fixed on both sides by jetties and/or seawalls or there was no recognizable dune system present. In the end 14 tidal inlet systems were selected. The selected inlet systems are mainly on the Atlantic and the Gulf coast in the east and the south (Figure 33). Three inlet on the west coast are also taken into account (Table 19: Oregon and California).

Table 19: Inlets in the United States

State	Inlet name
New York	Fire Island Inlet
New Jersey	Little Egg Inlet
	Brigantine Inlet
Virginia	Chincoteague Inlet
North Carolina	Oregon Inlet
	Ocracoke Inlet
	New Topsail Inlet
South Carolina	North Inlet
Florida (Atlantic coast)	Matanzas Inlet
Florida (Gulf coast)	Big Carlos Pass
	Hurricane Pass
	Pensacola Pass
Texas	Pelican Inlet
Oregon	Netarts Bay Inlet
California	Tomales Bay Inlet
	Pajaro River Mouth

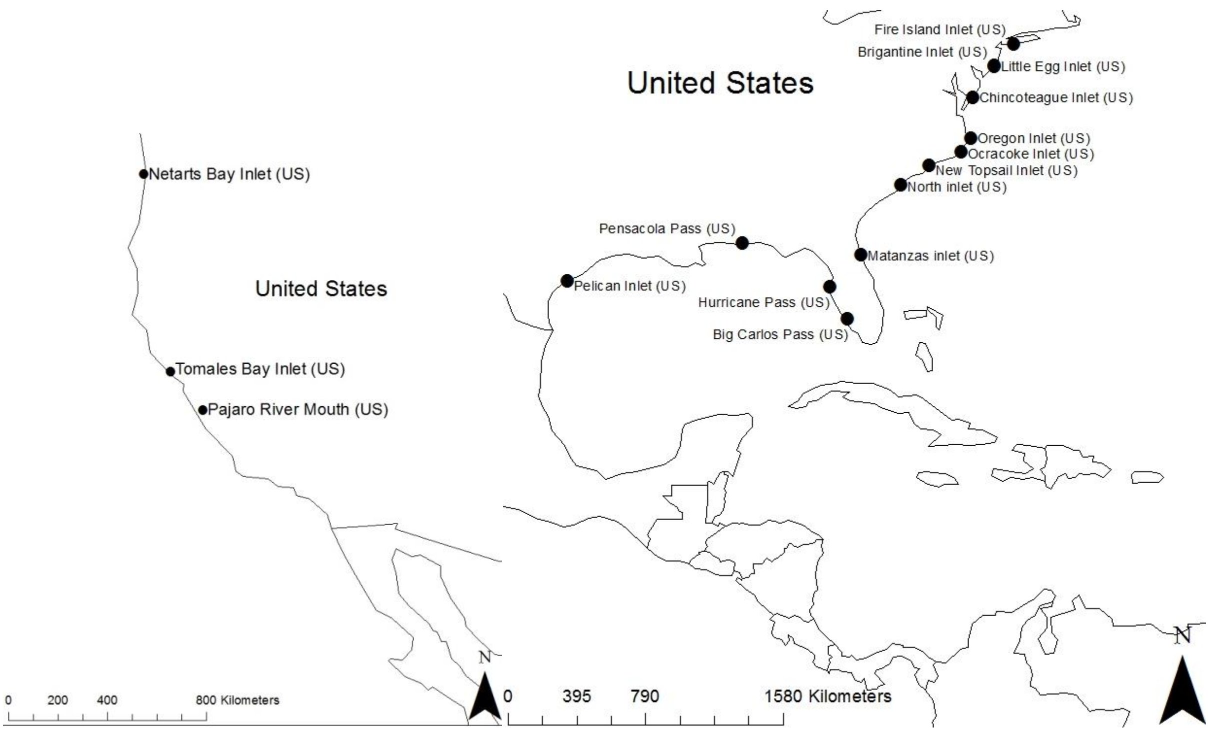

Figure 33: selected tidal inlet systems along coast of the United States

East Coast

The East Coast of the United States stretches from the Canadian border at circa 45°N to the southern tip of Florida at approximately 25°N. The climate along this coast varies from a continental climate without a dry season and a mild summer in the north (Dfa) to a tropical climate (A) in the southern tip of Florida. The largest part of the East Coast experiences a temperate climate without a dry season and with a hot summer (Cfa) according to Peel et al. (2007).

Fire Island Inlet

Fire Island Inlet is the inlet between Oak Island and Democrat Point on Fire Island in the state New York. The islands are part of a barrier system that runs parallel to the south shore of Long Island. The nearby tide monitoring station at Long Beach shows a mean tidal range of 1.4 m (NOAA, 2013). Data from buoy 44025 shows a mean significant wave height of 1.3 m with a mean wave direction of 160°N (NDBC, 2013). The inlet is wave-dominated according to the classification proposed by Davis & Hayes (1984). The inlet showed migratory behaviour in the past, but it is now on a fixed position. The single channel in the inlet is periodically dredged (Leatherman, 1985).

Dunes are present on both sides of the island. The dune system on Democrat Point is expanding, while the dune system on Oak Island is retreating. The first dune row at Democrat Point have a vegetation cover of 2/8. The most seaward dunes at Oak Island are slightly more vegetated with a cover of 3/8. The maximum observed dune height is 9 m (NCEI, 2016). Statistics from weather station Gilgo Beach shows a mean wind speed of 5 m/s with a mean direction of 202°N (Windfinder, 2017).

Figure 34: Fire Island Inlet (1984-2016)

Little Egg Inlet

Little Egg Inlet is one of the inlets connecting the Great Bay with the Atlantic Ocean at the coast of New Jersey. The inlet is situated north of Brigantine Inlet. The inlet experiences a mean tidal range of 1.1 m according to the tidal gauge at Brigantine Channel (NOAA, 2013).

Wave buoy 44009 shows a mean significant wave height of 1.2 m and a mean wave direction of 136° (NDBC, 2013), which means that the inlet is wave-dominated (R. A. Davis & Hayes, 1984). The inlet has a single channel that stays on a fixed position.

There are expanding dune systems present on both sides of Little Egg Inlet. The maximum dune height is circa 6 m (NCEI, 2016). The dune system at the north side of the inlet has a vegetation cover of 2/8, while the southern dune system has a cover of 5/8. The weather station at the Holgate Marina shows a mean wind speed of 5 m/s with a mean wind direction of 292°N.

Figure 35: Little Egg Inlet (1995-2016)

Brigantine Inlet

Brigantine is one of the inlets that connects the Great Bay in New Jersey with the Atlantic Ocean. The inlet is located south of Little Egg Inlet. The tidal gauge at Brigantine Channel shows that the inlet has a mean tidal range of 1.1 m (NOAA, 2013). Buoy 44009 shows that the inlet experiences waves with a mean significant height of 1.2 coming from 136° (NDBC, 2013), which means that the inlet is wave-dominated according to the classification of Davis & Hayes (1984). Satellite imagery from 1984 until 2016 shows that the inlet has one channel that migrates north with a rate of circa 12 m/year.

Dunes are present on both sides of Brigantine Inlet. The dunes at the updrift (south) side show expansion, while the dunes at the downdrift (north) side are retreating. The dunes are only a few metres high, with a maximum height of circa 5 m (NCEI, 2016). The seaward dunes at the south side of the inlet are sparsely vegetated with pioneer vegetation (1/8). The dunes at the north side are largely vegetated (7/8). The weather station at 8th Street in Brigantine shows a mean wind speed of 3 m/s with a mean direction of 292°N.

Figure 36: Brigantine Inlet (1995-2016)

Chincoteague Inlet

Chincoteague Inlet is located in the state of Virginia between Wallops Island and Fishing Point. It connects Chincoteague Bay with the Atlantic Ocean. The tidal gauge in the inlet shows a mean tidal range of 0.7 m (NOAA, 2013) and buoy 44009 shows a shows a mean significant wave height of 1.2 m with a mean direction of 136° (NDBC, 2013). The inlet is wave-dominated according to the classification of Davis & Hayes (1984). The inlet has one channel which is maintained by the United States Army Corps of Engineers (USACE, 2014). The inlet stays on a fixed position.

There are coastal dunes present on both sides of Chincoteague Inlet. Both dune systems are expanding. The dunes are up to a few metres high with a maximum height of circa 5 m (NCEI, 2016). The dunes at Fishing Point have a vegetation cover of 6/8, while the most seaward dunes at Wallops Island are 4/8 covered. A weather station at Chincoteague Island shows a mean wind speed of 4 m/s and a mean wind direction of 225°N (Windfinder, 2017).

Figure 37: Chincoteague Inlet (1994-2016)

Oregon Inlet

Oregon Inlet connects the Pamlico Sound with the Atlantic Ocean and is part of the North Carolina Outer Banks. The inlet separates Bodie Island to the north and Pea Island to the south. The tidal gauge at the Coast Guard Station shows that the inlet experiences a tidal range of 0.6m (NOAA, 2013). Wave measurements at buoy DSLN7 show that the mean wave height is 1.5 m (NDBC, 2013). The inlet is thus wave-dominated according to Davis &

Hayes (1984). The mean wave direction is estimated using WaveWatch III (2017) and this yielded a mean direction of 118°N. The inlet has a single channel which is periodically dredged by the USACE. Historically the inlet migrated south, but the south side of the inlet is fixed by a rock groin in 1991, so the inlet stays on a fixed position (Riggs & Ames, 2009).

There are coastal dunes present on both sides of Oregon inlet. The dunes at Bodie Island are expanding, while the dunes at Pea Island are retreating. The vegetation cover at Bodie Island is 3/8, while it is 1/8 at Pea Island. The maximum observed dune height near the inlet is 9 m (NCEI, 2016). The weather station at the Oregon Inlet Marina shows a mean wind speed of 5 m/s with a mean direction of 22°N (Windfinder, 2017).

Figure 38: Oregon Inlet (1993-2017)

Ocracoke Inlet

Ocracoke connects Pamlico Sound to the Atlantic Ocean and is part of the North Carolina Outer Banks. The inlet separates Ocracoke island to the west and Portsmouth Island to the east. The tidal gauge at Ocracoke Island shows that the inlet has a tidal range of 0.3 m (NOAA, 2013). The mean wave significant wave height is 1.5 m according to the measurements done at buoy 41025 (NDBC, 2013). The mean wave direction is estimated as 129°N (WaveWatch III, 2017). The inlet is wave-dominated according to Davis & Hayes (1984). The inlet has two channels which can be recognized from satellite imagery. This observation is supported by observations from Lawson (1709).

Coastal dunes can be found on both sides of Ocracoke Inlet. The dunes on Ocracoke Island are expanding and have a vegetation cover of 6/6. The dunes on Portsmouth Island are retreating and also have a vegetation cover of 6/6. The maximum observed dune height near the inlet is 7 m (NCEI, 2016). The weather station at Ocracoke Harbor shows a mean wind direction speed of 4 m/s with a mean direction of 45°N (Windfinder, 2017).

Figure 39: Ocracoke Inlet (1984-2017)

New Topsail Inlet
New Topsail Inlet is located south of Topsail Beach in the state North Carolina. It connects the marsh and several channels to the Atlantic Ocean. The inlet experiences a tidal range of 1.2 m according to the tidal gauge at Wrightville Beach (NOAA, 2013). The wave climate is characterized by waves with a mean significant height of 0.9 m and a mean wave direction of 147° as measured at buoy 14035 (NDBC, 2013), which means that the inlet is mixed-energy (R. A. Davis & Hayes, 1984). The inlet has one channel and the inlet migrates south with a rate of circa 10 m/year according to satellite imagery from the years 1984-2016.

Coastal dunes can be found on both sides of New Topsail Inlet. The dunes at the north side are expanding due to the migration of the inlet. The same migration also leads to the retreat of the dunes south of the inlet. The dunes are only up to 2 m high. The dunes at the north side are more than half vegetated (5/8), while the dunes closest to the inlet at the south side are sparsely vegetated (1/8). Statistics from the weather station at Topsail Beach/Boryk Canal show that the mean wind speed is 3 m/s with a mean direction of 0°N.

Figure 40: New Topsail Inlet (1993-2016)

North Inlet
North Inlet is located in the state South Carolina between Debidue Island in the north and North Island in the south. The inlet connects a salt marsh, several creeks and a number of bays to the Atlantic Ocean. The tidal gauge at Pawleys Island Pier shows that the inlet experiences a tidal range of 1.5 m (NOAA, 2013). The wave climate is measured at buoy 41004 and the mean significant wave height is 1.3 m with a mean wave direction of 131°N (NDBC, 2013). The inlet has a single channel and does not migrate.

There are dune systems on both sides of North Inlet, but the dunes are very small with observed heights up to 1 m (NCEI, 2016). The dune system at the south side shows expansion and the most seaward dunes are 1/8 vegetated. The dune system at the north side shows some retreat. The most seaward dunes are here 6/8 vegetated. The weather station North Inlet/Winyah Bay shows that the mean wind speed is 4 m/s with a mean direction of 67°N (Windfinder, 2017).

Figure 41: North Inlet (1994-2017)

Matanzas Inlet

Matanzas Inlet, Florida, connects the Matanzas River and Intracoastal Waterway with the Atlantic Ocean. The tidal gauge at Crescent Beach/Matanzas River shows that the inlet has a mean tidal range of 1.2 m (NOAA, 2013). The waves measured at buoy 41012 have a mean height of 1.2 m and a mean direction of 107°N (NDBC, 2013). The inlet is wave-dominated according to Davis & Hayes (1984). The inlet stays on a fixed location and has a single channel.

Dunes are only present on the north side of the inlet. This dune systems is expanding and has a maximum dune height of 7 m (NCEI, 2016). The dunes are largely vegetated (6/8). The weather station at Matanzas Inlet shows a mean wind speed of 3 m/s with a mean direction of 22°N (Windfinder, 2017).

Figure 42: North side of Matanzas Inlet (1995-2017)

Gulf Coast

The Gulf Coast is the southern coast of the United States stretching from the southern tip of Florida (81°W) to the Mexican border (97°W). The southern tip of Florida has a tropical climate (A), but the rest of the coast experiences a temperate climate without a dry season and with a hot summer (Cfa) (Peel et al., 2007).

Big Carlos Pass

Big Carlos Pass connects Estero Bay with the Gulf of Mexico and lays between Estero Island in the north and Black Island in the south. The gauge at Naples shows a mean tidal range of 0.6 m (NOAA, 2013). Waves are measured at buoy 42036 and statistics from this buoy show that the mean significant wave height is 0.9 m with a mean wave direction 168°N (NDBC, 2013). The inlet has one channel and stays on a fixed position.

Dunes are present on both sides of the inlet, but the dunes on Estero Island are heavily influenced and for some parts even removed. For this analysis only the dunes at Black Island are taken into account. The dunes at Black Island are part of Lovers Key State Park. The dunes are only up to 2 m high (NCEI, 2016) and the first dune ridge is only 2/8 vegetated. The weather station Sanibel Island shows a mean wind speed of 3 m/s and a mean wind direction of 67°N (Windfinder, 2017).

Figure 43: Big Carlos Pass (1995-2017)

Hurricane Pass

Hurricane Pass is the tidal inlet that connects St. Joseph Sound to the Gulf of Mexico. The inlet divides Honeymoon Island to the north and Caladesi Island to the south. The inlet experiences a tidal range of 0.6 m according to the gauge at Honeymoon Island South (NOAA, 2013). The wave climate is measured at buoy 42036. Statistics from this buoy gives a mean significant wave height of 0.9 m with a mean direction of 168°N (NDBC, 2013). The inlet is wave-dominated (R. A. Davis & Hayes, 1984) and stays on a fixed position. The inlet has a single channel.

There is a dune system on both sides of the inlet. Both systems expand and are more than half vegetated. The dunes at Caladesi Island are a little more vegetated (5/8) than the dunes at Honeymoon Island (4/8), but the difference is subtle. The maximum dune height in the area is circa 4 m (NCEI, 2016). A mean wind speed of 5 m/s with a mean direction of 122°N is measured at weather station Clearwater Beach (Windfinder, 2017).

Figure 44: Hurricane Pass (1995-2017)

Pensacola Pass

Pensacola Pass, Florida, connects the Pensacola Bay with the Gulf of Mexico. The tidal range at the Pensacola Naval Air Station (NAS) at the landward side of the inlet is 0.3 m (NOAA, 2013). The mean wave height is measured at buoy 42016 and is 0.5 m (NDBC, 2013). The mean wave direction is estimated at 168°N (WaveWatch III, 2017). The inlet is wave-dominated according to Davis & Hayes (1984). The inlet has a single channel and stays on a fixed location.

Retreating coastal dune systems are found on both sides of Pensacola Pass. The maximum observed dune height near the inlet is 7 m (NCEI, 2016). The vegetation cover is 1/8 at the west side and 5/8 at the east side of the inlet. The mean wind speed is 4 m/s with a mean direction of 337°N as measured at Pensacola NAS (Windfinder, 2017).

Figure 45: Pensacola Pass (1994-2017)

Pelican Inlet

Pelican Inlet, Texas, connects the Matagorda Bay with the Gulf of Mexico. The inlet is situated 6.5 km southwest of Matagorda Ship Channel Inlet. It is assumed that the tidal range in both inlets is the same. The tide gauge in the Matagorda Ship Channel Inlet shows that the mean tidal range 0.3 m is (NOAA, 2013). The wave climate is approximated using buoy 42035, which yields a mean significant wave height of 0.9 m and a mean wave direction of 150°N (NDBC, 2013). Pelican Inlet is wave-dominated according to the classification by Davis & Hayes (1984). Using imagery from the years 1990-2016 it could be determined that the inlet has a single channel and that it migrates to the north with a rate of circa 14 m/year.

Expanding dune systems are present on both sides of Pelican Inlet despite the migration of the inlet. The maximum observed dune height is circa 4 m (NCEI, 2016). The dunes at the southwest side of the inlet are 3/8 vegetated, while the dunes at the northeast side are 5/8 vegetated. The mean wind speed is 6 m/s and the mean wind direction is 157°N as measured at weather station Port O'Connor/Matagorda Bay (Windfinder, 2017).

Figure 46: Pelican Inlet (1984-2017)

West Coast

The West Coast stretches from the Canadian border (48°N) to the Mexican border (33°N) and faces the Pacific Ocean. The West Coast experiences a temperate climate with a dry and warm summer (Csb) (Peel et al., 2007).

Netarts Bay Inlet

Netarts Bay Inlet, Oregon, connects Netarts Bay to the Pacific Ocean. The bay and the ocean are divided by a sand spit called the Netarts Spit. The tidal range as measured at Netarts is 1.5 m (NOAA, 2013). The mean significant wave height is 2.3 m and the mean wave direction is 275°N as measured at buoy 46029 (NDBC, 2013) and the inlet is thus wave-dominated (R. A. Davis & Hayes, 1984). The inlet stays on a fixed position due to the bedrock at the northern side of the inlet. Most of the time there is a single channel, but on historic satellite imagery a small temporary channel can be seen in some periods.

The north side of Netarts Bay Inlet is a rocky coast, so no dunes are present here. There is an expanding dune system on the Netarts Spit with dune heights up to 26 m (NCEI, 2016). The most seaward dunes are 3/8 vegetated. Weather statistics from weather station Oceanside/OR show a mean wind speed of 2 m/s with a mean direction of 292°N (Windfinder, 2017).

Figure 47: Netarts Bay Inlet (1984-2017)

Tomales Bay Inlet

Tomales Bay Inlet, California, connect Tomales Bay with Bodega Bay, which borders the Pacific Ocean. The tidal range as measured at Sand Point/Tomales Bay is 1.1 m (NOAA, 2013) and the mean significant wave height as measured at buoy 46013 is 2.2 m. The mean wave direction at this buoy is 290°N (NDBC, 2013). Combination of tidal range and mean significant wave height yields that Tomales Bay Inlet is wave-dominated (R. A. Davis & Hayes, 1984). The inlet stays on a fixed location, because the south side is fixed by bedrock. From satellite imagery it could be derived that there is a single tidal channel.

Dunes are present at the north side of Tomales Bay Inlet. No expansion or retreat of this system could be seen in satellite imagery from 1993-2016. The most obvious change in the dune system is that the dunes became more vegetated. The most seaward dunes are now 5/8 vegetated. The maximum dune height as seen in DEMs is 17 m (NCEI, 2016). Weather station Bodega Bay shows a mean wind speed of 6 m/s with a mean direction of 315°N (Windfinder, 2017).

Figure 48: Tomales Bay Inlet

Pajaro River Mouth

The Pajaro River Mouth is the connection between the Pajaro River and Monterey Bay, which borders the Pacific Ocean. A tidal range of 1.1 m is measured at Moss Landing (NOAA, 2013). The wave climate is measured with buoy 46042, which yields a mean significant wave height of 2.2 m and a mean wave direction of 288°N (NDBC, 2013). The inlet is wave-dominated according to Davis & Hayes (1984). The inlet channel migrated towards the south and forming a sand spit in satellite images from the period 1993-2016 with a migration rate of circa 65 m/year.

The dune system at the north side of the inlet system shows expansion, while the dune system at the south retreats a result of the inlet migration. The youngest dunes in the northern system are vegetated by pioneer vegetation (1/8). The most seaward dunes in the southern system are 4/8 vegetated. The maximum observed dune height in the vicinity of the inlet is 14 m (NCEI, 2016). According to Windfinder (2017) a mean wind speed of 5 m/s and a mean wave direction of 292°N occurs at the Monterey Bay Buoy.

Figure 49: Pajaro River Mouth (1993-2017)

Brazil

In Brazil twelve inlets were assessed. Some of them had mangrove forests instead of coastal dunes, so finally a total of seven inlets was selected for this research (Table 20 and Figure 50). The Brazilian coast faces the Atlantic Ocean from 4°N to 34°S. The area north of 23°S has a tropical climate (A). The area south of 23°S has a temperate climate (C).

Table 20: Inlets in Brazil

State	Inlet name
Rio Grande do Norte	Galinhos Inlet
Bahia	Barra das Canavieiras
	Barra Velha
Espirito Santo	Itaúnas River Mouth
São Paulo	Icapara Inlet
Paraná	Ararapira Channel
Santa Catarina	Ibiraquera Channel

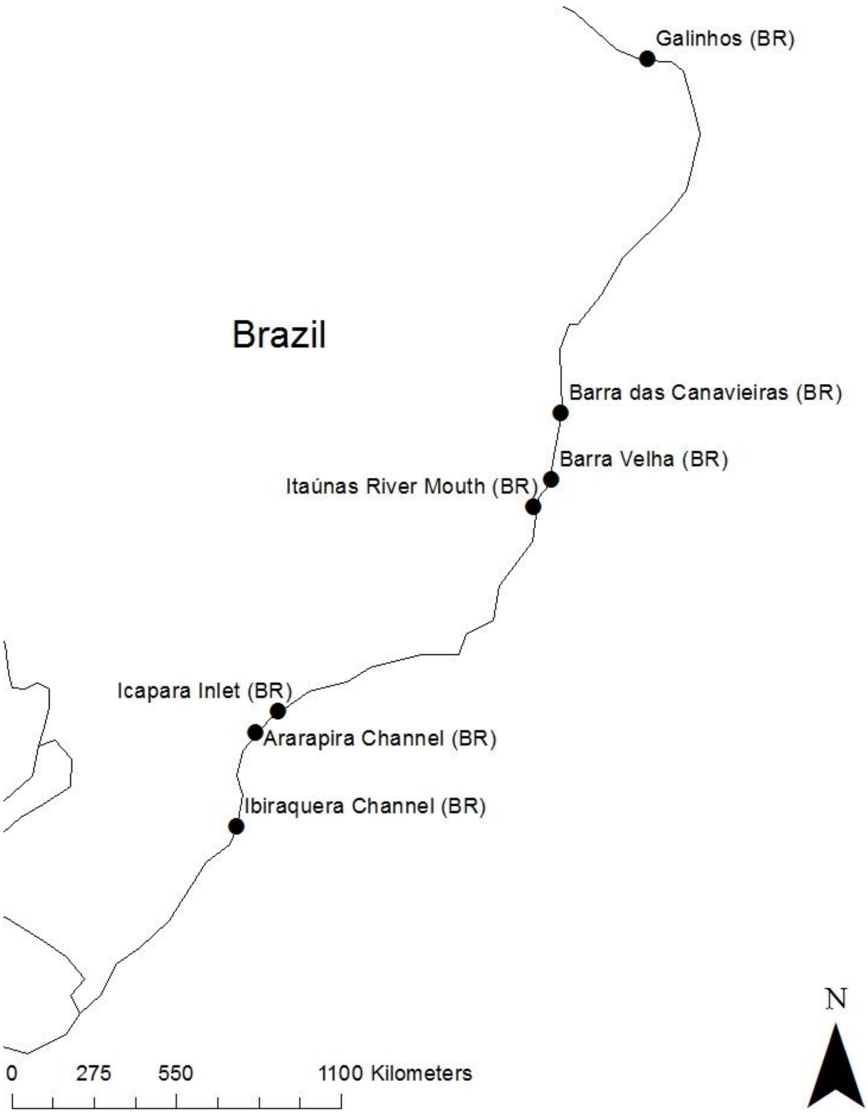

Figure 50: selected tidal inlet systems along the Brazilian coast

Galinhos Inlet

Galinhos Inlet is located on the north coast of Brazil and is connected with the Atlantic Ocean. The northeast shore of the inlet is a sand spit called Galinhos' Spit. The tidal range is 1.9 m (Pentcheff, 2010) and the offshore wave climate is characterized by a mean wave height of 1.7 m with a mean direction of 134° (WaveWatch III, 2017). This wave direction means that the waves go away from the inlet, so this value is not reliable. The values given by Pianca, Mazzini, & Siegle (2010) for the northernmost sector of Brazil are considered to be more representative, which leads to a mean wave direction of 82°. The inlet is mixed-energy according to Davis & Hayes (1984). The inlet has a single channel and satellite images from the period 1970-2016 shows no displacement of the inlet, so it is assumed that the inlet is on a fixed position.

Coastal dunes are present on both sides of Galinhos Inlet. The dunes on Galinhos' Spit are expanding and have a vegetation cover of 4/8. The dunes at the other side of the inlet are retreating and are barely vegetated (1/8). The maximum dune height is 6 m (NCEI, 2016). The mean wind speed offshore is 8.8 m/s with a mean direction of 138°N (WaveWatch III, 2017).

Figure 51: Galinhos Inlet (1970-2016)

Barra das Canavieiras

Barra das Canavieiras connects the delta of the Salsa River to the Atlantic Ocean. The tidal range is estimated to be 1.4 m (Pentcheff, 2010). The mean significant wave height is 1.8 m with a mean direction of 133°N (WaveWatch III, 2017), which means that the inlet is wave-dominated (R. A. Davis & Hayes, 1984). The inlet has one channel and migrates in southward direction with a rate of circa 20 m/year.

Coastal dunes can be found on both sides of Barra das Canavieiras. The dune system at the north side is expanding and has a vegetation cover of 2/8. The dune system at the south side is retreating and has a vegetation cover of 7/8. A maximum dune height could not be determined from the global DEM mosaic from the NCEI (2016). The mean offshore wind speed is 6.2 m/s with a mean direction of 289°N (WaveWatch III, 2017).

Figure 52: Barra das Canavieiras (1970-2015)

Barra Velha
Barra Velha is the northernmost inlet that connects the Caravelas Estuary with the Atlantic Ocean. The tidal range is 1.6 m (Pentcheff, 2010) and the mean significant wave height is 1.4 m with a mean direction of 90°N (WaveWatch III, 2017), which means that the inlet is mixed energy according to classification of Davis & Hayes (1984). The inlet has a single channel which migrates in northerly direction with a rate of circa 13 m/year.

Coastal dunes are present on the island south of the Barra Velha. This dune system is expanding and the dunes closest to the inlet have a vegetation cover of 1/8. The maximum dune height could not be determined, because the available DEM mosaic from the NCEI (2016) was to coarse. The mean wind speed is m/s with a mean direction of 13.5° (INMET, 2017).

Figure 53: sand spit south of Barra Velha (1970-2017)

Itaúnas River Mouth
The Itaúnas River Mouth is located just north of Conceição da Barra in the state Espirito Santo and is the point where the Itaúnas River meets the Atlantic Ocean. The tidal range is circa 2.5 m (Pentcheff, 2010). The mean significant wave height is 1.6 m coming from 112°N (WaveWatch III, 2017). The inlet is mixed energy according to Davis & Hayes (1984). Satellite images from the period 1970-2016 show that the inlet migrates in southerly direction with a rate of circa 27 m/year. From the images it is also visible that the inlet has one channel.

Coastal dunes can be found on both sides of the Itaúnas River Mouth. The dunes at the north side are expanding and have a vegetation cover of 3/8. The dunes at the south side are retreating and have a vegetation cover of 7/8. The maximum dune height could not be determined, because of the low resolution of the global DEM mosaic produced by the NCEI (2016). The mean offshore wind speed is 6.1 m/s with a mean direction of 318°N (WaveWatch III, 2017).

Figure 54: Itaúnas River Mouth. The black line shows the location of the river in 1970.

Icapara Inlet

The Icapara Inlet connects the Cananéia-Iguape Lagoon system with the Atlantic Ocean. At the south side of the inlet lays the Ilha Comprida barrier. The mean tidal range at this area is 0.6 m and the mean wave height is 1.3 m with a mean direction of 90°N (Sawakuchi et al., 2008), which means that the inlet is wave-dominated (R. A. Davis & Hayes, 1984). Satellite imagery shows that the inlet has a single channel and that it migrated to the northeast with a rate of circa 25 m/year.

Coastal dunes were found on both sides of Icapara Inlet. The dunes on Ilha Comprida are expanding and have a vegetation cover of 7/8. The dunes at the other side of the inlet have retreated and had a cover of 6/8. The maximum dune height is circa 3 m. The mean wind speed is 4.5 m/s coming from 155°N (Sawakuchi et al., 2008).

Figure 55: Icapara Inlet (1984-2016)

Ararapira Channel

The Ararapira Channel connects to the Atlantic Ocean. The tidal range is 1.2 m (Pentcheff, 2010), and the mean wave height is 1.8 m coming from 127°N (Lessa, Angulo, Giannini, &

Araújo, 2000). The inlet is thus wave-dominated according to Davis & Hayes (1984). The inlet has two channels and migrates in to the southwest with a rate of 15 m/year.

There are dune systems on both sides of Ararapira Channel. The dune system in the northeast is expanding and has a vegetation cover of 7/8. The dune system at the other side of the inlet is retreating and has a vegetation cover of 5/8. The dunes have a maximum height of 5 m (Lessa et al., 2000). The mean wind speed is 5.7 m/s from 291°N (WaveWatch III, 2017).

Figure 56: Ararapira Channel (1984-2016)

Ibiraquera Channel

Ibiraquera Channel connects the Ibiquera Lagoon with the Atlantic Ocean. The tidal range is 0.4 m (Pentcheff, 2010) and the mean significant wave height is 2.0 m from 135°N (WaveWatch III, 2017). The inlet is thus wave-dominated according to Davis & Hayes (1984). The inlet is not permanently open, but when it is open it does not migrate a lot, so it is assumed to be on a fixed position. When the inlet is open, it has one channel.

Expanding dune systems are present on both sides of the inlet. The southern dunes are 2/8 vegetated, while the northern dunes are 7/8 vegetated. No maximum dune height for this area could be found or determined using DEMs. The offshore wind has a mean speed of 7.1 m/s from a 293° (WaveWatch III, 2017).

Figure 57: Ibiraquera Channel (2003-2007)

Australia

Six inlet systems on the Australian coast were assessed. Not all systems had recognizable dune systems. Three inlet systems are selected for further research (Table 21 and Figure 58). There are situated on the south and west coast of Australia. The coast of Australia faces the Indian Ocean in the southwest, west and north. The Coral Sea is in the east and the Tasman sea is on the southeast side. The north coast of Australia has a tropical climate (A). The east and south coast have a temperate climate (C). Large parts of the western coast experience an arid climate (B). The amount of precipitation and the temperature shows a lot of variation along the coast (Peel et al., 2007).

Table 21: Inlets in Australia

State	Inlet name
Victoria	Shallow Inlet
South Australia	Murray Mouth
Queensland	Jumpinpin Channel

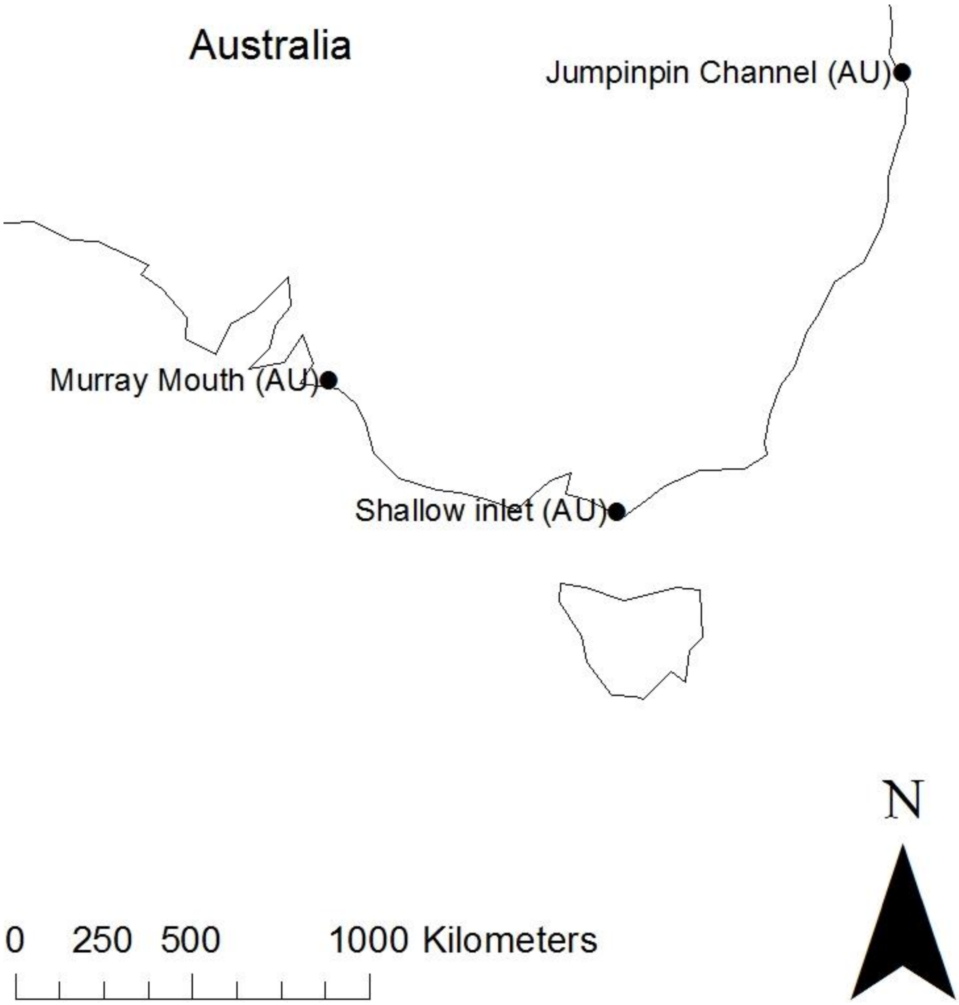

Figure 58: selected tidal inlet locations on the coast of Australia

Shallow Inlet

Shallow Inlet is opening into Waratah Bay at the south coast of Australia. The tidal range is 1.8 m (Pentcheff, 2010), the mean significant wave height is 1.7 m and the mean wave direction is 239°N (WaveWatch III, 2017). The inlet is mixed energy (R. A. Davis & Hayes, 1984). The inlet has one channel and migrates in easterly direction with a rate of circa 45 m/year as estimated from satellite imagery from the period 1984-2016.

Coastal dunes are present on both sides of Shallow Inlet. The dunes at the west side are expanding and have a vegetation cover of 1/8. The dunes at the east side are retreating and are fully vegetated (8/8). The maximum observed dune height is 12 m (NCEI, 2016). Weather statistics from Sandy Point show a mean wind speed of 2 m/s and a mean wind direction of 337°N (Windfinder, 2017).

Figure 59: Shallow Inlet (1984-2016)

Murray Mouth

Murray Mouth is the point where the Murray River flows into the Great Australian Bight. The mean tidal range at the inlet is circa 0.5 m (Pentcheff, 2010). The mean significant wave height is 2.6 m with a mean wave direction of 212°N (WaveWatch III, 2017). The inlet is thus wave-dominated according to Davis & Hayes (1984). The inlet has a single channel which displays dynamic behaviour. Migration speeds can be up to 80 m/year. The inlet is wave-dominated (Shuttleworth, Woidt, Paparella, Herbig, & Walker, 2005).

Expanding dune systems can be found on both sides of Murray Mouth. Both dune systems are sparsely vegetated (1/8 and 2/8) and the maximum observed dune height is only 2 m (NCEI, 2016). The prevailing wind direction is 180°N with a speed of 6 m/s as measured at Goolwa/Hindmarsh Island (Windfinder, 2017).

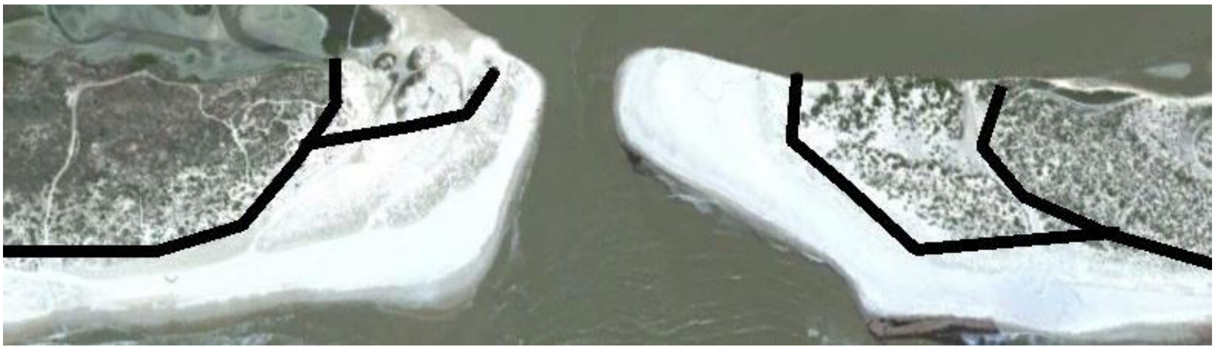

Figure 60: Murray Mouth (2003-2017)

Jumpinpin Channel

Jumpinpin Channel connects the Moreton Bay-Broadwater intracoastal system with the Pacific Ocean. The inlet separates North Stradbroke Island and South Stradbroke Island. The tidal range in the area is 1 m (Sedigh, Tomlinson, Cartwright, & Etemad-Shahidi, 2016). The mean significant wave height is 1.6 m (Shand & Carley, 2011). The mean wave direction is 131°N (WaveWatch III, 2017). The inlet is wave-dominated according to the classification of Davis & Hayes (1984). Most of the time the inlet has only one channel, but a secondary channel opens sometimes. The total inlet system does not migrate (Mccauley & Tomlinson, 2006).

Coastal dunes are present on both sides of Jumpinpin Channel. The dunes at North Stradbroke Island are retreating and have a vegetation cover of 7/8. The dunes at South Stradbroke Island are expanding and the youngest dunes have a vegetation cover of 1/8. The maximum dune height in the area is 7 m (NCEI, 2016). Weather statistics from the Gold Coast Seaway show a mean wind speed of 6 m/s with a mean direction of 157°N (Windfinder, 2017).

Figure 61: Jumpinpin Channel (1984-2016)

Africa

The western coast of Africa borders the Atlantic Ocean from the Morocco to the South Africa. Our study area is laying between Guinea (10°N) to South Africa (35°S). Fifteen inlets along the west coast of Africa were assessed. The northern part of this area (north of 7°S) has a tropical climate (A). The area between 7°S and 32°S has an arid climate (B). The southern part of South Africa has a temperate climate (C) (Peel et al., 2007). Three inlets were found that were suitable for further research (Table 22). The other inlet systems did not have a recognizable dune system or there was simple no information to be found. The Cunene River Mouth is situated on the border of Namibia and Angola (Figure 62), but for this research it is assumed to be fully in Namibia.

Table 22: Inlets in Africa

Country	Inlet name
Congo	Conkouati Inlet
Namibia	Cunene River Mouth
	Sandwich Bay

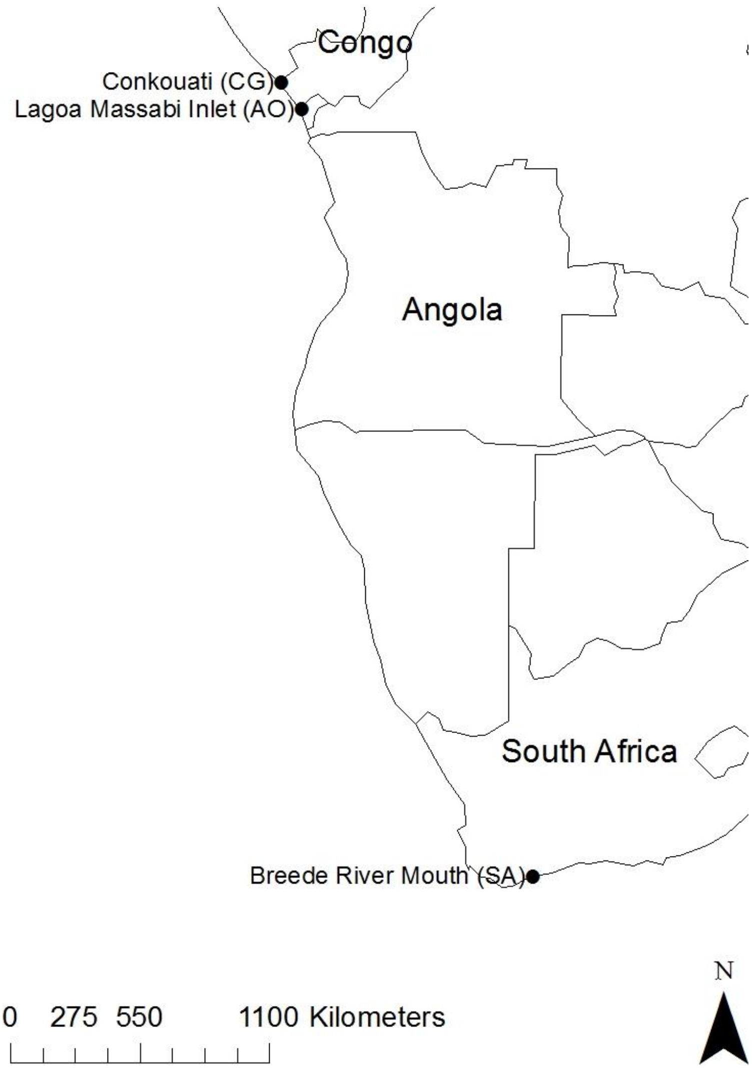

Figure 62: selected tidal inlet locations on the coast of Africa.

Conkouati

Conkouati is the name of the connection between the Conkouati Lagoon and the Atlantic Ocean. The inlet is part of the Conkouati-Douli National Park in the Republic of the Congo. The nearby Mussolo Lagoon experiences a tidal range of 1.1 m (Dronkers, 2016). The mean significant wave height is 1.4 m with a mean direction of 206°N (WaveWatch III, 2017). The Conkouati is wave-dominated when using the parameters as given above (R. A. Davis & Hayes, 1984). From low-resolution satellite images it can be seen that the inlet migrates in northerly direction with an average rate of 33 m/year. The number of channels cannot be clearly seen, but there is no reason to assume that there is more than one channel.

Bird (2010) states that coastal dunes are present near Conkouati Inlet. From the satellite images it is not possible to distinguish the dune areas, so it is not possible to see if they are expanding or retreating. The global DEM mosaic produced by the NCEI (2016) was too coarse to even recognize the inlet, let alone determine maximum dune heights. The nearest weather station is at Pointe Noire Airport. This station shows a mean wind speed of 4 m/s with a mean direction of 202°N (Windfinder, 2017).

Figure 63: Conkouati, the line shows the location of the river in 1984.

Lagoa Massabi Inlet

The Lagoa Massabi Inlet connects Lagoa Massabi to the Atlantic Ocean. The inlet is situated in Cabinda, an enclave that belongs to Angola. The tidal range is assumed to be the same as at the Mussolo Lagoon, thus 1.1 m (Dronkers, 2016). The mean significant wave height is 1.4 m with a mean direction of 206°N (WaveWatch III, 2017). This values lead to the inlet being wave-dominated (R. A. Davis & Hayes, 1984). Satellite images show no displacement in the period 1984-2016, so the inlet is assumed stable. The number of channels cannot be clearly seen, but there is no reason to assume that there is more than one channel.

Bird (2010) states that there are coastal dunes near Lagoa Massabi Inlet, but they cannot be distinguished from satellite imagery. It was thus impossible to determine whether they are expanding or retreating. The maximum dune heights could also not be determined, because the global DEM mosaic produced by the NCEI (2016) was to coarse to recognize the inlet. The weather station at Pointe Noire Airport shows a mean wind speed of 4 m/s with a mean direction of 202°N (Windfinder, 2017).

Figure 64: Lagoa Massabi Inlet

Breede River Mouth

The Breede River Mouth is the point in South Africa where the Breede River flows into the Indian Ocean. The cape at its south border is called Cape Infanta and on the north shore is the town Witsand. The tidal range is assumed to be the same as the tidal range at Mossel Bay, namely 1.2 m. Hindcast data produced by WaveWatch III (2017) show a mean significant wave height of 2.8 m and a mean wave direction of 213°N. This direction means that the waves are going away from the inlet, so this value is not reliable. Wave direction is very much influenced by the local shape of the coastline. The inlet is wave-dominated according to Davis & Hayes (1984). The inlet has a single channel and the inlet stays on a fixed location, because the south shore is fixed by bedrock.

Coastal dunes are present in the Witsand area. A retreat of this dune system is visible on satellite images from 1984-2016. The dunes are sparsely vegetated (1/8). The global DEM mosaic from the NCEI (2016) was to coarse to determine dune heights. Weather station Still Bay shows that the mean wind speed is 4 m/s with a mean direction of 23°N (Windfinder, 2017).

Figure 65: North side of the Breede River Mouth (2003-2017)

E. Raw and categorical data

Name	Country	Climate	TR	Hs	Dom	Dwave	Mig_style	Mig_rate	Nr_Ch	Vwind	Dwind	Dev_UD	Dev_DD	A_UD	A_DD	Veg_UD	Veg_DD	H_dune
Texel Inlet	NL	C	1,4	1,3	mixed	345	fixed	0	1	5,8	340	expanding		partly		2		15
Eierlandse Gat	NL	C	1,7	1,3	mixed	315	fixed	0	2	8	295	fixed	expanding	partly	fully	3	7	20
Vlie Inlet	NL	C	1,9	0,7	mixed	310	fixed	0	2	8	265	fixed	retreating	partly	partly	1	1	30
Ameland Inlet	NL	C	2,1	1,2	mixed	275	fixed	0	2	7	230	retreating	fixed	partly	partly	1	5	20
Frisian Inlet	NL	C	2,3	0,8	mixed	280	fixed	0	2	8	212	expanding	expanding	partly	partly	4	8	20
Eems-Dollard Inlet	NL	C	2,2	1,1	mixed	295	fixed	0	1	8	227	retreating	expanding	fully	partly	7	1	13
Osterems	DE	C	2,2	1,1	mixed	310	fixed	0	1	6	242	expanding	retreating	partly	partly	3	7	11
Norderneyer Seegat	DE	C	2,4	1,6	mixed	285	fixed	0	2	7	265	expanding		partly		3		19
Listerdyb	DE	C	1,8	1,3	mixed	288	fixed	0	1	9	275	expanding	expanding	partly	partly	1	1	21
Graadyb	DK	C	1,7	1,3	mixed	8	fixed	0	2	7	40	expanding	fixed	partly	partly	1	2	12
Exmouth Inlet	GB	C	2,6	0,6	tide	33	fixed	0	1	8	95	retreating		partly		7		6
Maumusson Inlet	FR	C	4,0	1,5	tide	23	fixed	0	1	5	27	retreating	retreating	partly	partly	1	6	55
Cávado Estuary Inlet	PT	C	3,7	2,1	mixed	75	fixed	0	1	3	75	expanding		partly		1		21
Sado River Inlet	PT	C	1,1	2,4	wave	0	fixed	0	1	3	90	expanding		partly		2		27
Armona Inlet	PT	C	2,0	1,2	mixed	5	one_direction	20	1	4	320	expanding	expanding	fully	partly	1	1	9
Piedras River Mouth	ES	C	2,0	0,4	tide	35	one_direction	30	1	3	35	expanding	fixed	partly	partly	1	1	4
Fire Island Inlet	US	D	1,4	1,3	wave	340	fixed	0	1	5	22	expanding	retreating	partly	partly	2	3	9
Little Egg Inlet	US	D	1,1	1,2	wave	16	fixed	0	1	5	172	expanding	expanding	partly	fully	6	2	6
Brigantine Inlet	US	D	1,1	1,2	wave	51	one_direction	12	1	3	207	expanding	retreating	partly	partly	1	7	5
Chincoteague Inlet	US	C	0,7	1,2	wave	316	fixed	0	1	4	45	expanding	expanding	partly	partly	6	4	5
Oregon Inlet	US	C	0,6	1,5	wave	78	fixed	0	1	5	342	expanding	retreating	partly	fully	3	1	9
Ocracoke Inlet	US	C	0,3	1,5	wave	329	fixed	0	2	4	245	expanding	retreating	partly	partly	6	6	7
New Topsail Inlet	US	C	1,2	0,9	mixed	337	one_direction	10	1	3	190	expanding	retreating	partly	fully	5	1	2
North Inlet	US	C	1,5	1,3	mixed	36	fixed	0	1	4	332	expanding	retreating	partly	partly	1	6	1
Matanzas Inlet	US	C	1,2	1,2	wave	32	fixed	0	1	3	307		expanding		partly		6	7
Big Carlos Pass	US	A	0,6	0,9	wave	298	fixed	0	1	3	197	expanding		partly		6		2
Hurricane Pass	US	C	0,6	0,9	wave	273	fixed	0	1	5	217	expanding	expanding	fully	partly	5	6	4
Pensacola Pass	US	C	0,3	0,5	wave	3	fixed	0	1	4	172	retreating	retreating	partly	partly	1	5	7
Pelican Inlet	US	C	0,3	0,9	wave	20	one_direction	14	1	6	27	expanding	expanding	fully	partly	3	5	4
Netarts Bay Inlet	US	C	1,5	2,3	wave	0	fixed	0	1	2	17	expanding		partly		3		26
Tomales Bay Inlet	US	C	1,1	2,2	wave	320	fixed	0	1	6	345		fixed		partly		5	17
Pajaro River Mouth	US	C	1,1	2,2	wave	38	one_direction	65	1	5	42	expanding	retreating	fully	partly	1	4	14
Galinhos Inlet	BR	B	1,9	1,7	mixed	82	fixed	0	1	8,8	138	expanding	retreating	fully	partly	4	1	6
Barra das Canavieiras	BR	A	1,4	1,8	wave	78	one_direction	20	1	6,2	234	expanding	retreating	partly	partly	2	7	
Barra Velha	BR	A	1,6	1,4	mixed	35	one_direction	13	1	2	318	expanding	<undefined>	partly		1		
Itaúnas River Mouth	BR	A	2,5	1,6	mixed	22	one_direction	27	1	6,1	228	expanding	retreating	fully	partly	3	7	
Icapara Inlet	BR	C	0,6	1,3	wave	315	one_direction	25	1	4,5	20	expanding	retreating	partly	fully	7	6	3
Ararapira Channel	BR	C	1,2	1,8	wave	2	one_direction	15	2	5,7	166	expanding	retreating	partly	partly	7	5	5
Ibiraquera	BR	C	0,4	2,0	wave	15	fixed	0	1	7,1	173	expanding	expanding	fully	partly	2	7	
Shallow Inlet	AU	C	1,8	1,7	mixed	14	one_direction	45	1	2	112	expanding	retreating	fully	partly	1	8	12
Murray Mouth	AU	B	0,5	2,6	wave	7	back_and_forth	80	1	6	213	expanding	expanding	partly	partly	1	2	2
Jumpinpin Channel	AU	C	1,0	1,6	wave	36	fixed	0	1	6	62	expanding	retreating	partly	partly	1	7	7
Conkouati	CG	A	1,1	1,4	wave	341	one_direction	33	1	4	337							
Lagoa Massabi Inlet	AO	A	1,1	1,4	wave	321	fixed	0	1	4	317							
Breede River Mouth	SA	C	1,2	2,8	wave	118	fixed	0	1	4	288	retreating		fully		1		

Name	Country	Climate	Mean tidal Range	Mean significant wave height	Dominant forcing	Mean wave Direction	Migration style	Migration rate	Nr. of channels	Mean wind speed	Mean wind direction	Development updrift dune system	Development downdrift dune system	Active part updrift dune system	Active part downdrift dune system	Vegetation cover updrift dune system	Vegetation cover downdrift dune system	Dune height
Texel Inlet	NL	C	micro	low	mixed	Dir_315-360	fixed	none	single	moderate	Dir_270-360	expanding		partly		2		medium
Eierlandse Gat	NL	C	micro	low	mixed	Dir_315-360	fixed	none	multiple	heavy	Dir_270-360	fixed	expanding	partly	fully	3	7	medium
Vlie Inlet	NL	C	micro	low	mixed	Dir_270-315	fixed	none	multiple	heavy	Dir_180-270	fixed	retreating	partly	partly	1	1	high
Ameland Inlet	NL	C	meso	low	mixed	Dir_270-315	fixed	none	multiple	moderate	Dir_180-270	retreating	fixed	partly	partly	1	5	medium
Frisian Inlet	NL	C	meso	low	mixed	Dir_270-315	fixed	none	multiple	heavy	Dir_180-270	expanding	expanding	partly	partly	4	8	medium
Eems-Dollard Inlet	NL	C	meso	low	mixed	Dir_270-315	fixed	none	single	heavy	Dir_180-270	retreating	expanding	fully	partly	7	1	medium
Osterems	DE	C	meso	low	mixed	Dir_270-315	fixed	none	single	moderate	Dir_180-270	expanding	retreating	partly	partly	3	7	medium
Norderneyer Seegat	DE	C	meso	medium	mixed	Dir_270-315	fixed	none	multiple	moderate	Dir_180-270	expanding		partly		3		medium
Listerdyb	DE	C	micro	low	mixed	Dir_270-315	fixed	none	single	heavy	Dir_270-360	expanding	expanding	partly	partly	1	1	medium
Graadyb	DK	C	micro	low	mixed	Dir_0-45	fixed	none	multiple	moderate	Dir_0-90	expanding	fixed	partly	partly	1	2	medium
Exmouth Inlet	GB	C	meso	low	tide	Dir_0-45	fixed	none	single	heavy	Dir_90-180	retreating		partly		7		low
Maumusson Inlet	FR	C	macro	medium	tide	Dir_0-45	fixed	none	single	moderate	Dir_0-90	retreating	retreating	partly	partly	1	6	high
Cávado Estuary Inlet	PT	C	meso	medium	mixed	Dir_45-90	fixed	none	single	light	Dir_0-90	expanding		partly		1		medium
Sado River Inlet	PT	C	micro	medium	wave	Dir_0-45	fixed	none	single	light	Dir_90-180	expanding		partly		2		high
Armona Inlet	PT	C	meso	low	mixed	Dir_0-45	one_direction	fast	single	light	Dir_270-360	expanding	expanding	fully	partly	1	1	medium
Piedras River Mouth	ES	C	meso	low	tide	Dir_0-45	one_direction	fast	single	light	Dir_0-90	expanding	fixed	partly	partly	1	1	low
Fire Island Inlet	US	D	micro	low	wave	Dir_315-360	fixed	none	single	moderate	Dir_0-90	expanding	retreating	partly	partly	2	3	medium
Little Egg Inlet	US	D	micro	low	wave	Dir_0-45	fixed	none	single	moderate	Dir_90-180	expanding	expanding	partly	fully	6	2	low
Brigantine Inlet	US	D	micro	low	wave	Dir_45-90	one_direction	moderate	single	light	Dir_180-270	expanding	retreating	partly	partly	1	7	low
Chincoteague Inlet	US	C	micro	low	wave	Dir_315-360	fixed	none	single	light	Dir_0-90	expanding	expanding	partly	partly	6	4	low
Oregon Inlet	US	C	micro	medium	wave	Dir_45-90	fixed	none	single	moderate	Dir_270-360	expanding	retreating	partly	fully	3	1	medium
Ocracoke Inlet	US	C	micro	medium	wave	Dir_315-360	fixed	none	multiple	light	Dir_180-270	expanding	retreating	partly	partly	6	6	medium
New Topsail Inlet	US	C	micro	low	mixed	Dir_315-360	one_direction	moderate	single	light	Dir_180-270	expanding	retreating	partly	fully	5	1	low
North Inlet	US	C	micro	low	mixed	Dir_0-45	fixed	none	single	light	Dir_270-360	expanding	retreating	partly	partly	1	6	low
Matanzas Inlet	US	C	micro	low	wave	Dir_0-45	fixed	none	single	light	Dir_270-360		expanding		partly		6	medium
Big Carlos Pass	US	A	micro	low	wave	Dir_270-315	fixed	none	single	light	Dir_180-270	expanding		partly		6		low
Hurricane Pass	US	C	micro	low	wave	Dir_270-315	fixed	none	single	moderate	Dir_180-270	expanding	expanding	fully	partly	5	6	low
Pensacola Pass	US	C	micro	low	wave	Dir_0-45	fixed	none	single	light	Dir_90-180	retreating	retreating	partly	partly	1	5	medium
Pelican Inlet	US	C	micro	low	wave	Dir_0-45	one_direction	moderate	single	moderate	Dir_0-90	expanding	expanding	fully	partly	3	5	low
Netarts Bay Inlet	US	C	micro	medium	wave	Dir_0-45	fixed	none	single	light	Dir_0-90	expanding		partly		3		high
Tomales Bay Inlet	US	C	micro	medium	wave	Dir_315-360	fixed	none	single	moderate	Dir_270-360		fixed		partly		5	medium
Pajaro River Mouth	US	C	micro	medium	wave	Dir_0-45	one_direction	fast	single	moderate	Dir_0-90	expanding	retreating	fully	partly	1	4	medium
Galinhos Inlet	BR	B	micro	medium	mixed	Dir_45-90	fixed	none	single	heavy	Dir_90-180	expanding	retreating	fully	partly	4	1	low
Barra das Canavieiras	BR	A	micro	medium	wave	Dir_45-90	one_direction	fast	single	moderate	Dir_180-270	expanding	retreating	partly	partly	2	7	
Barra Velha	BR	A	micro	low	mixed	Dir_0-45	one_direction	moderate	single	light	Dir_270-360	expanding		partly		1		
Itaúnas River Mouth	BR	A	meso	medium	mixed	Dir_0-45	one_direction	fast	single	moderate	Dir_180-270	expanding	retreating	fully	partly	3	7	
Icapara Inlet	BR	C	micro	low	wave	Dir_315-360	one_direction	fast	single	light	Dir_0-90	expanding	retreating	partly	fully	7	6	low
Ararapira Channel	BR	C	micro	medium	wave	Dir_0-45	one_direction	moderate	multiple	moderate	Dir_90-180	expanding	retreating	partly	partly	7	5	low
Ibiraquera	BR	C	micro	medium	wave	Dir_0-45	fixed	none	single	moderate	Dir_90-180	expanding	expanding	fully	partly	2	7	
Shallow Inlet	AU	C	micro	medium	mixed	Dir_0-45	one_direction	fast	single	light	Dir_90-180	expanding	retreating	fully	partly	1	8	medium
Murray Mouth	AU	B	micro	high	wave	Dir_0-45	back_and_forth	fast	single	moderate	Dir_180-270	expanding	expanding	partly	partly	1	2	low
Jumpinpin Channel	AU	C	micro	medium	wave	Dir_0-45	fixed	none	single	moderate	Dir_0-90	expanding	retreating	partly	partly	1	7	medium
Conkouati	CG	A	micro	low	wave	Dir_315-360	one_direction	fast	single	light	Dir_270-360							
Lagoa Massabi Inlet	AO	A	micro	low	wave	Dir_315-360	fixed	none	single	light	Dir_270-360							
Breede River Mouth	SA	C	micro	high	wave		fixed	none	single	light	Dir_270-360	retreating		fully		1		

F. Transformation plots

This appendix shows the transformation plots as generated by the CATREG algorithm. For each variable, the category quantifications (vertical axis) are plotted against the original category values (horizontal axis). The meaning of the numbers on the horizontal axis are given above the figures. Larger positive or negative quantifications mean that the category has more impact on the regression.

F.1. Development of the updrift dune system

Figure 66: 1=retreating, 2=stable, 3=expanding

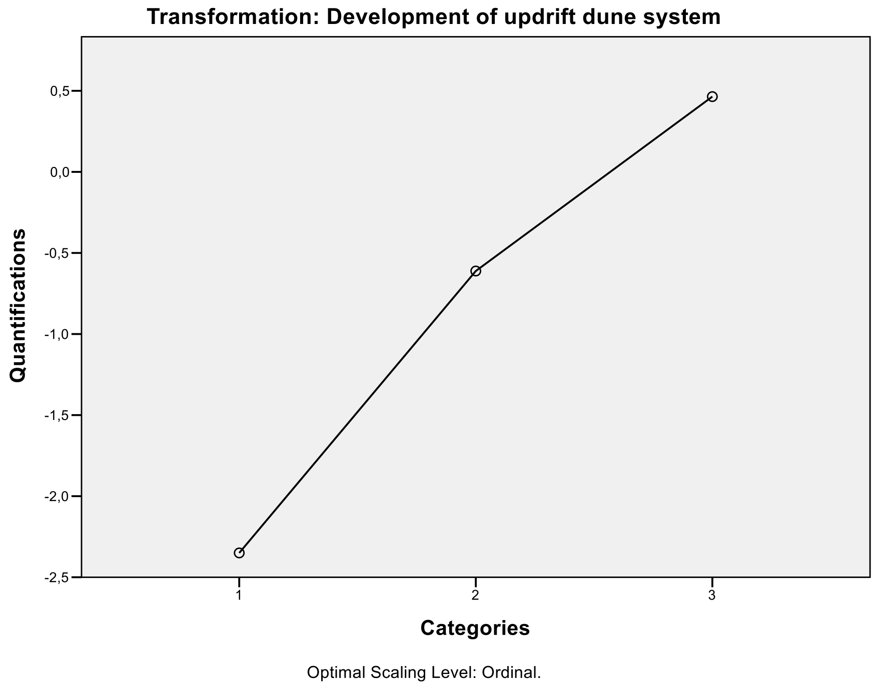

Figure 67: 1=fixed, 2=back-and-forth, 3=one direction

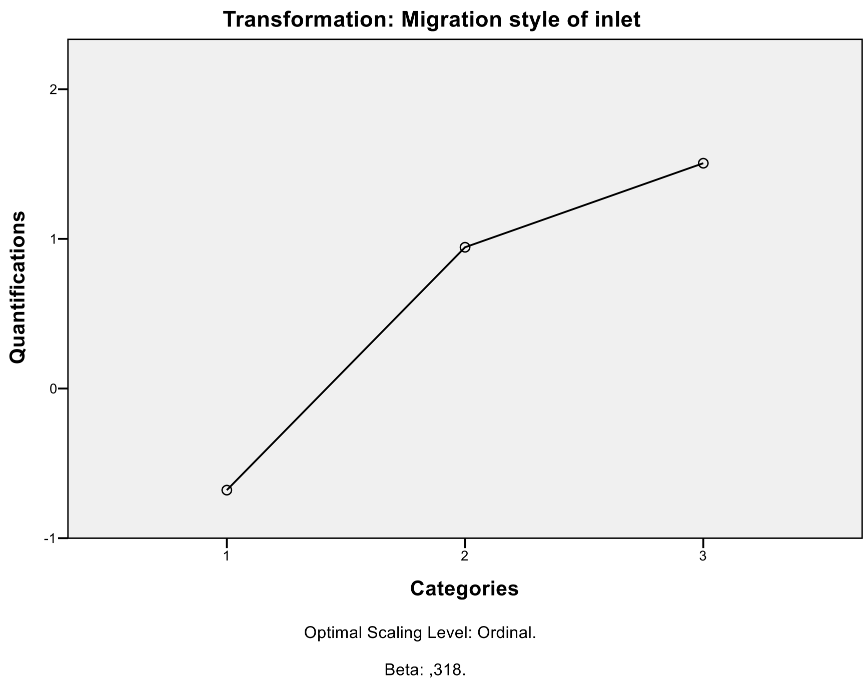

Figure 68: 1=wave-dominated, 2=mixed energy, 3=tide-dominated

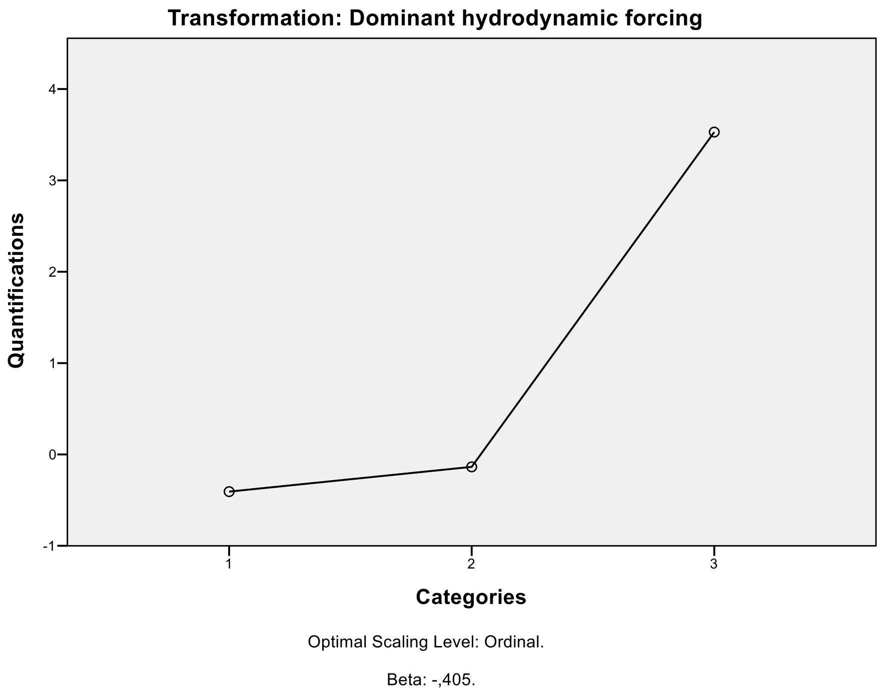

F.2. Development of the downdrift dune system

Figure 69: 1=retreating, 2=stable, 3=expanding

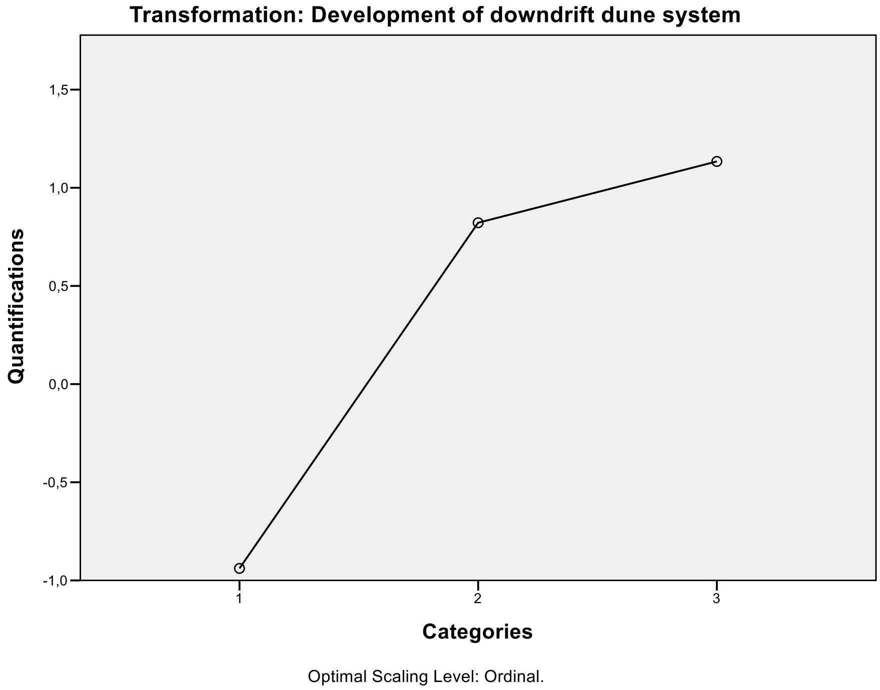

Figure 70: 1=0°-45°, 2=45°-90°, 3=207°-315°, 4=315°-360°

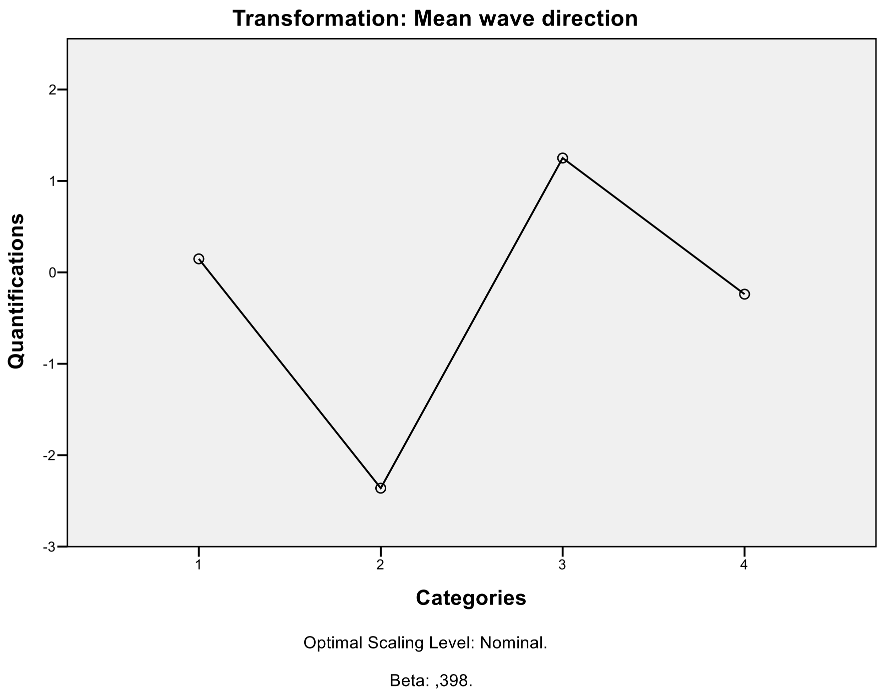

F.3. Extent of the active part of the updrift dune system

Figure 71: 1=partly, 2=fully

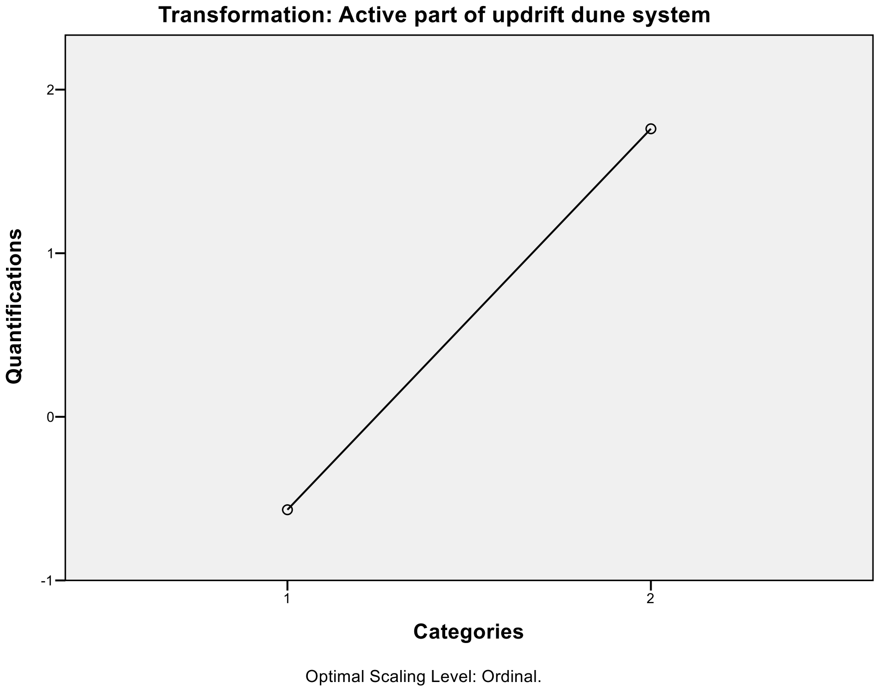

Figure 72: 1=A, 2=B, 3=C, 4=D

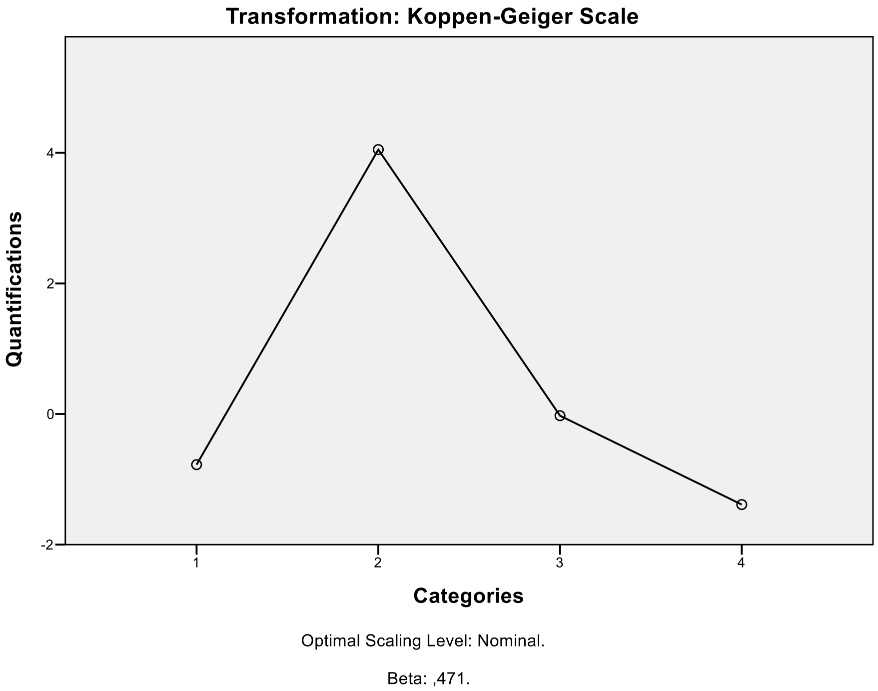

Figure 73: 1=fixed, 2=back-and-forth, 3=one direction

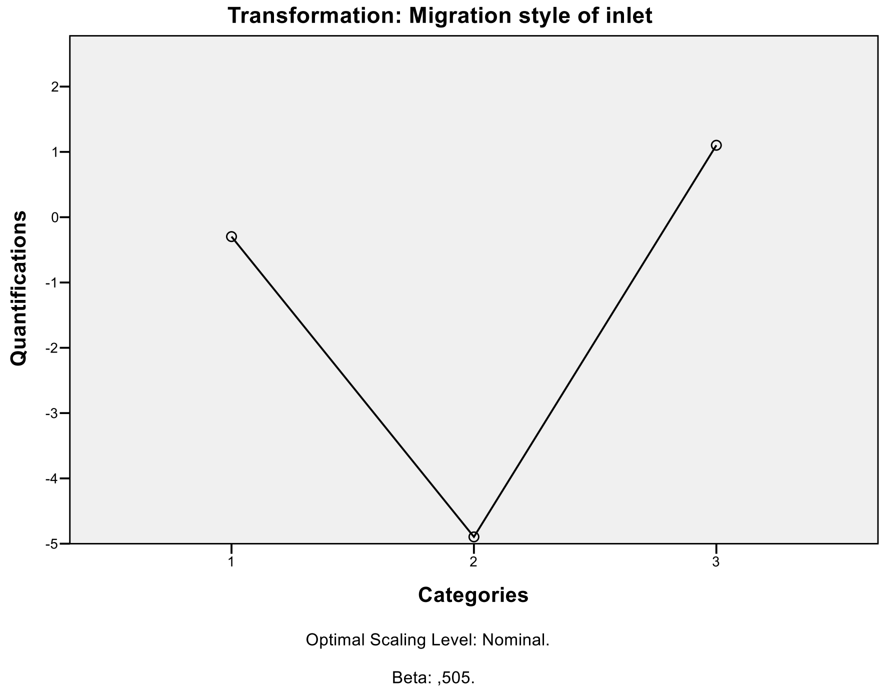

F.4. Extent of the active part of the downdrift dune system

Figure 74: 1=partly, 2=fully

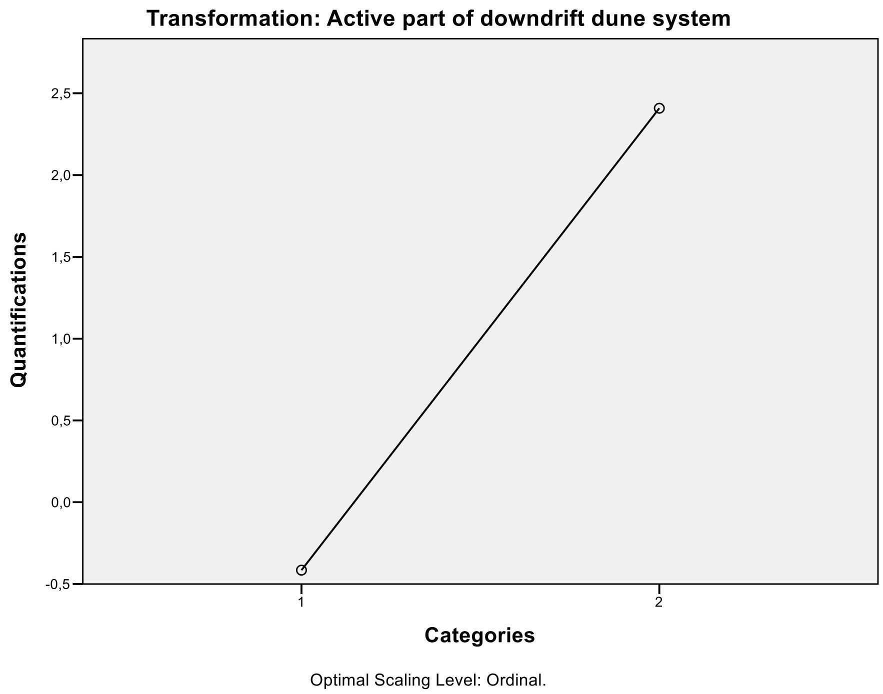

Figure 75: 1=0°-90°, 2=90°-180°, 3=180°-270°, 4=270°-360°

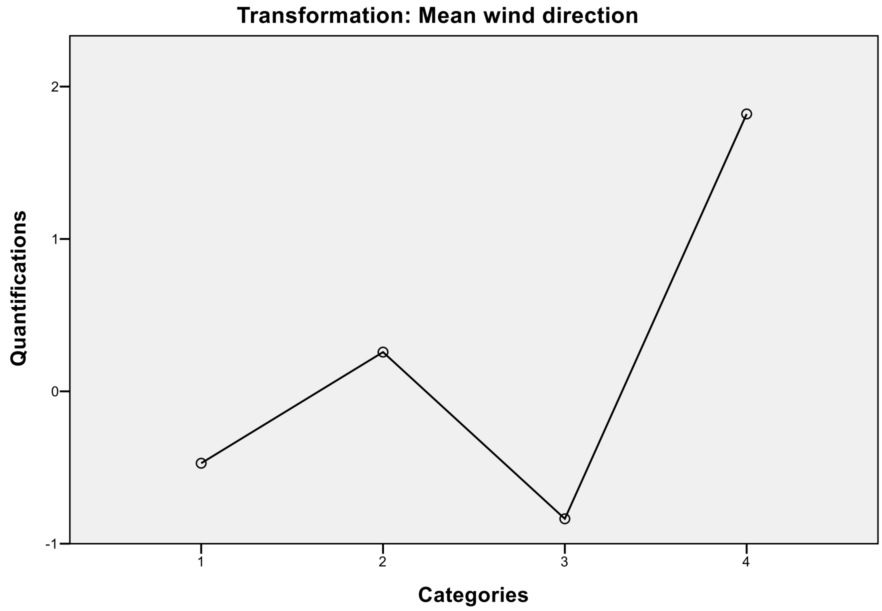

Optimal Scaling Level: Nominal.

Beta: ,215.

F.5. Maximum dune height

Figure 76: 1=low, 2=medium, 3=high

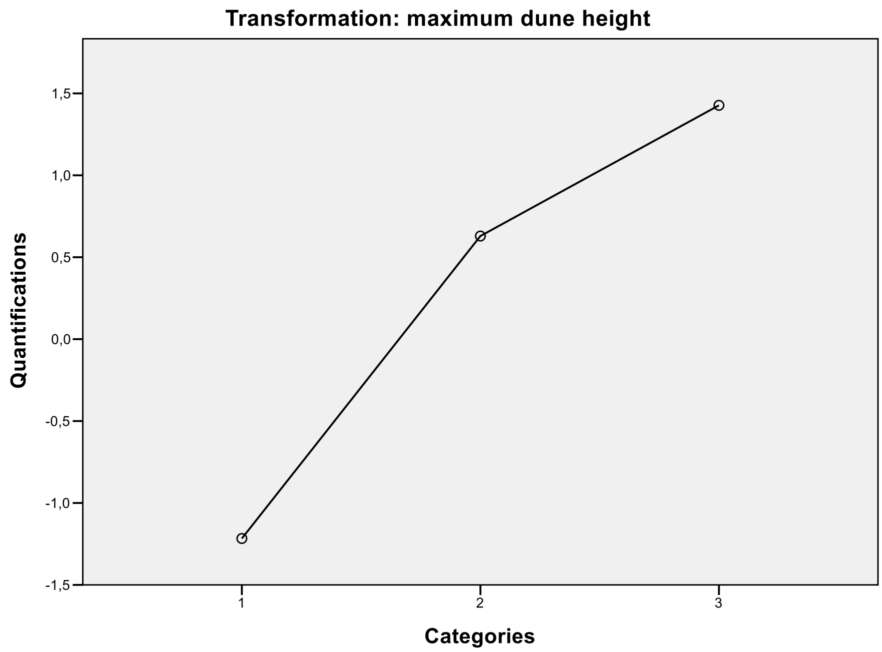

Optimal Scaling Level: Ordinal.

Figure 77: 1=fixed, 2=back-and-forth, 3=one direction

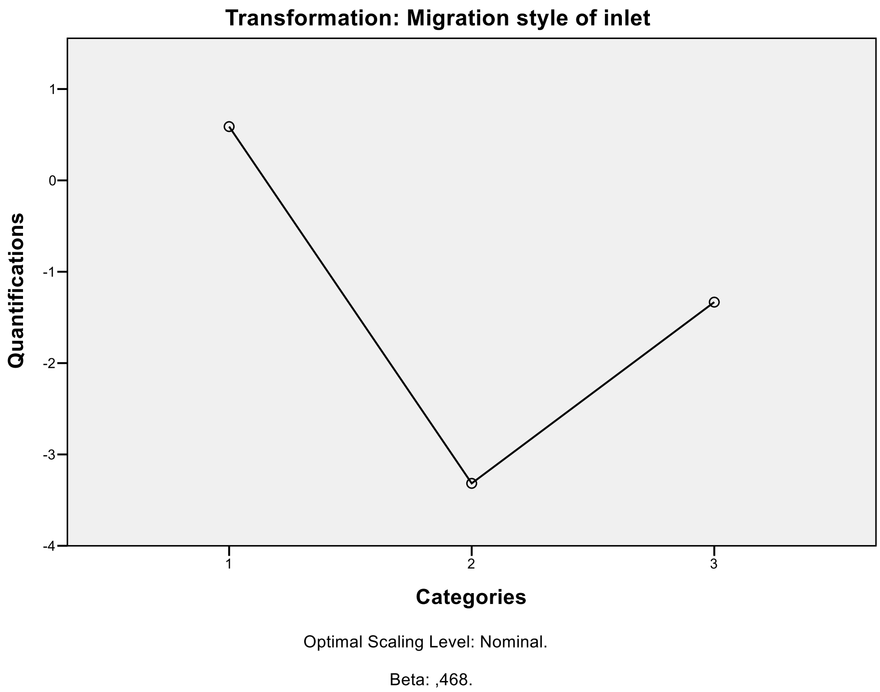

Figure 78: 1=A, 2=B, 3=C, 4=D

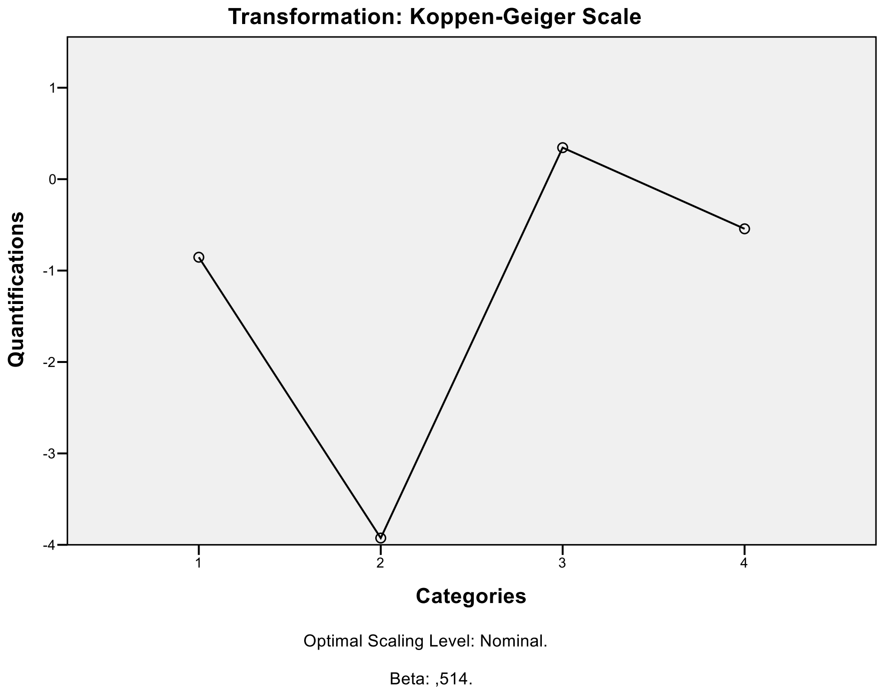

Figure 79: 1=low, 2=moderate, 3=high

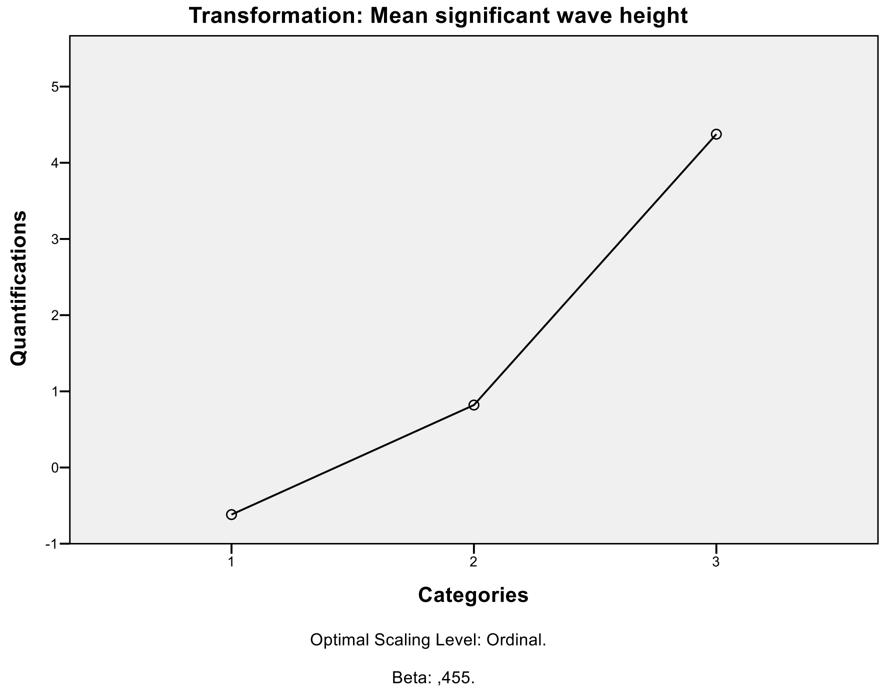

Figure 80: categories are vegetation cover in octas

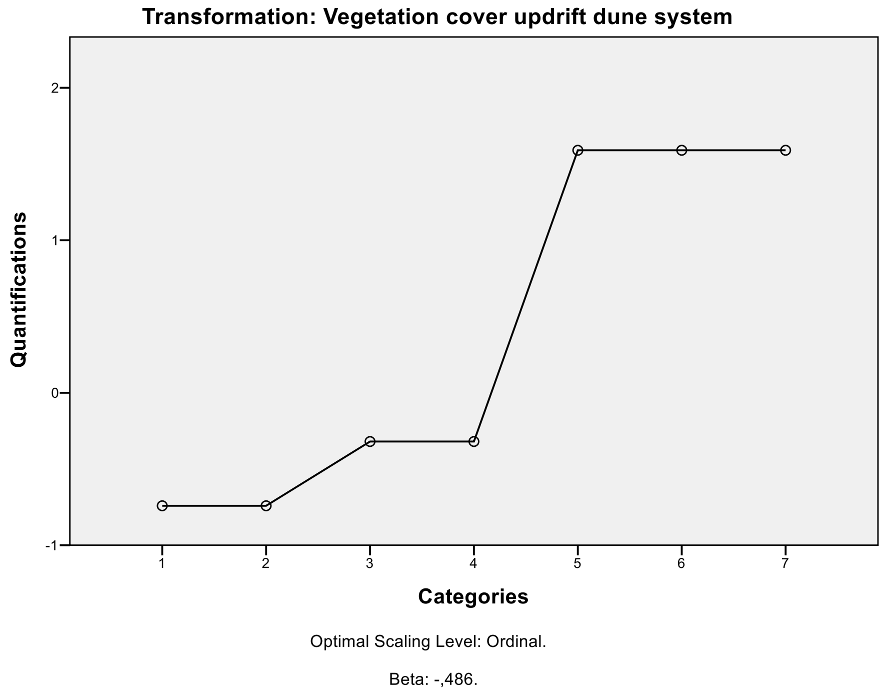

F.6. Vegetation cover of the updrift dune system

Figure 81: categories are vegetation cover in octas

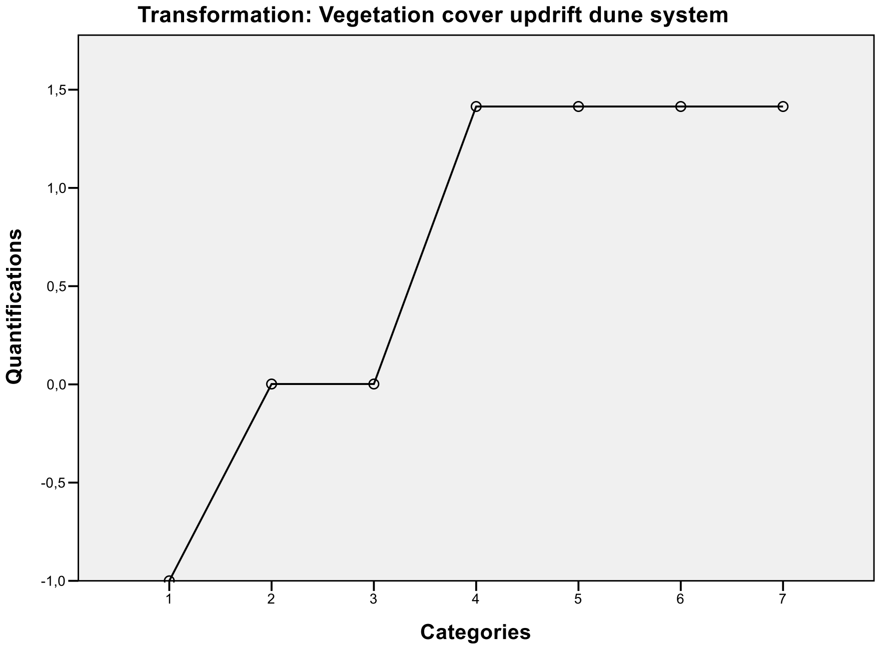

Optimal Scaling Level: Ordinal.

Figure 82: 1=fixed, 2=back-and-forth, 3=one direction

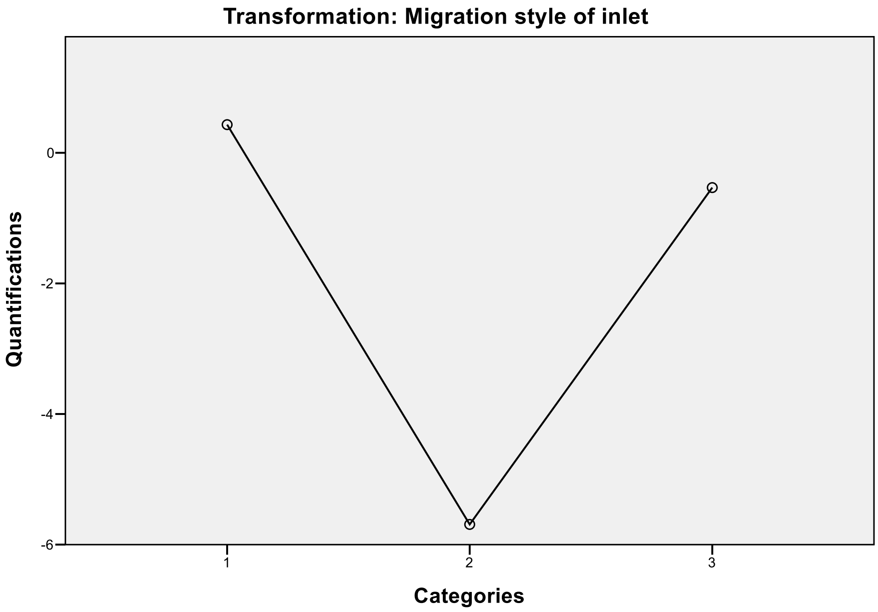

Optimal Scaling Level: Nominal.

Beta: ,244.

Figure 83: 1=0°-90°, 2=90°-180°, 3=180°-270°, 4=270°-360°

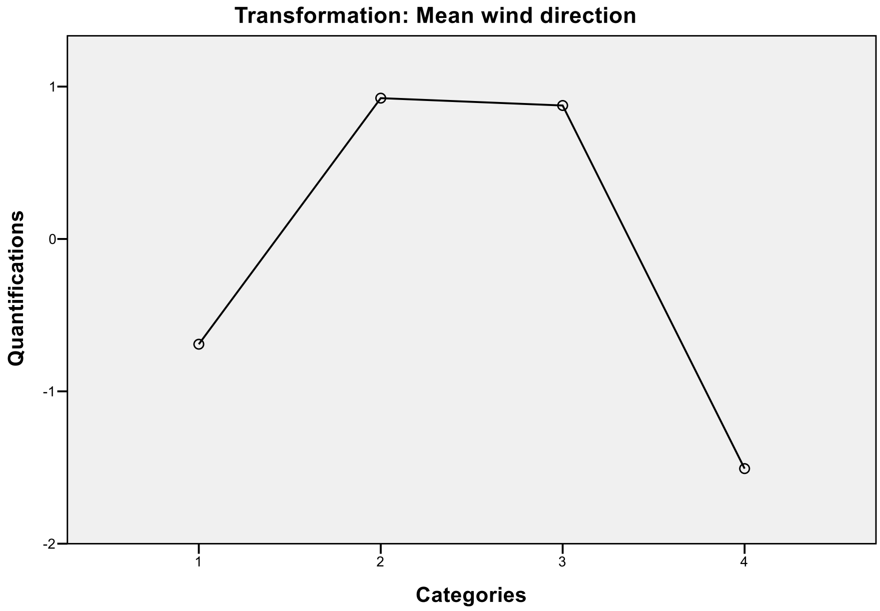

Optimal Scaling Level: Nominal.

Beta: ,445.

F.7. Vegetation cover of the downdrift dune system

Figure 84: categories are vegetation cover in octas

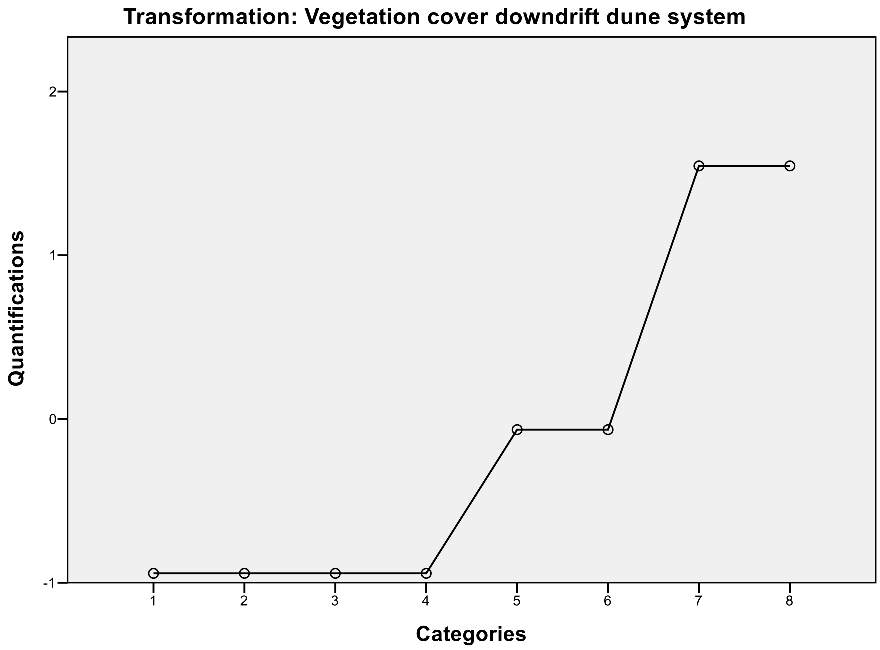

Optimal Scaling Level: Ordinal.

Figure 85: 1=A, 2=B, 3=C, 4=D

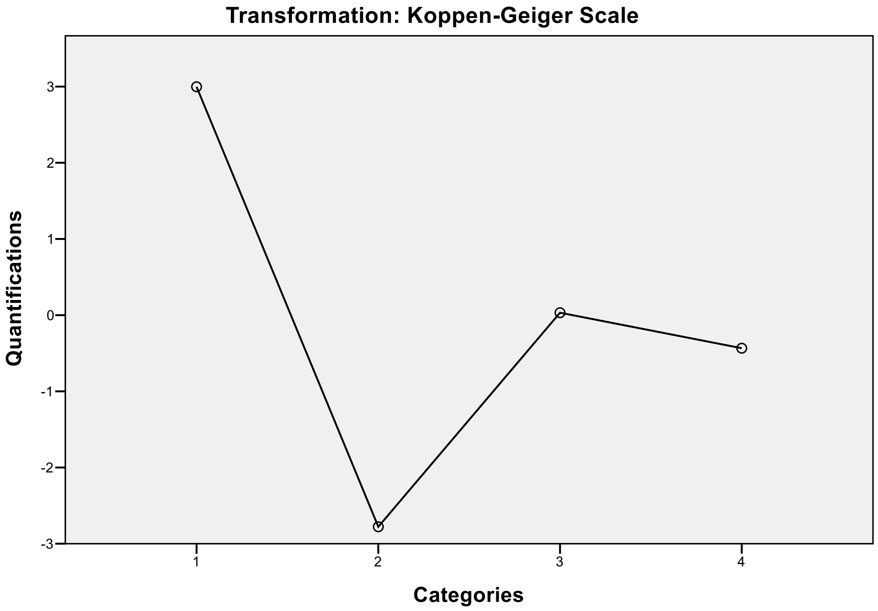

Optimal Scaling Level: Nominal.

Beta: ,449.

Figure 86: 1=0°-90°, 2=90°-180°, 3=180°-270°, 4=270°-360°

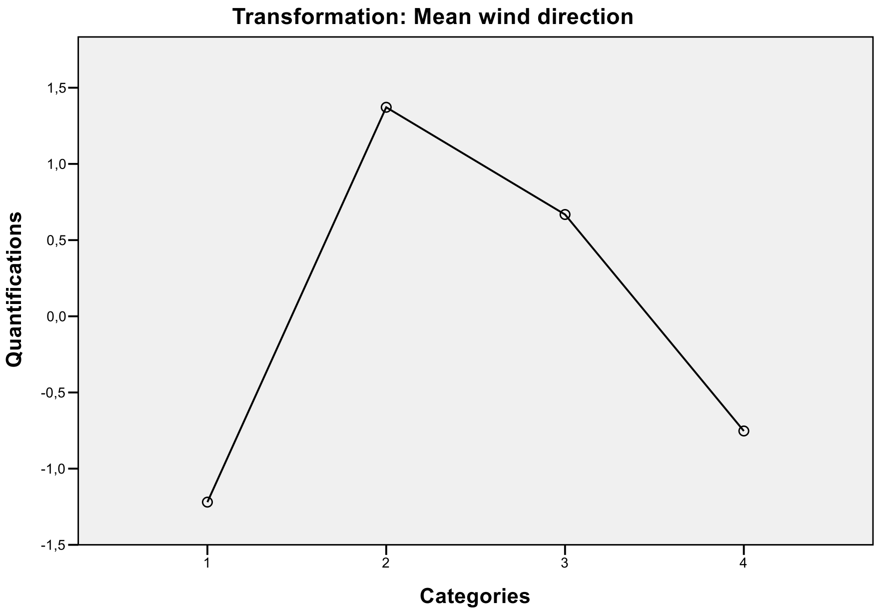

Optimal Scaling Level: Nominal.

Beta: ,299.